USGS
science for a changing world

Summary of Hydrologic Modeling for the Delaware River Basin Using the Water Availability Tool for Environmental Resources (WATER)

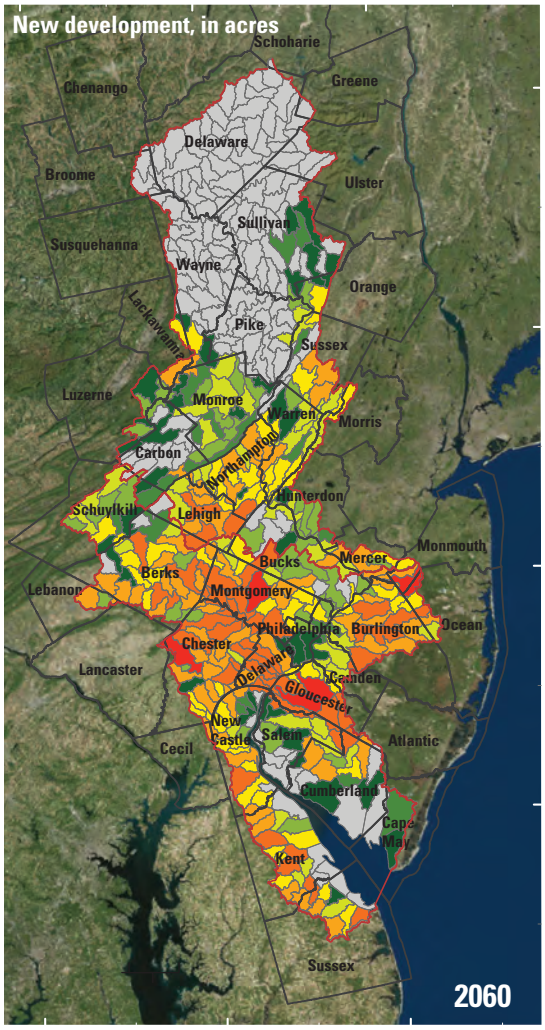

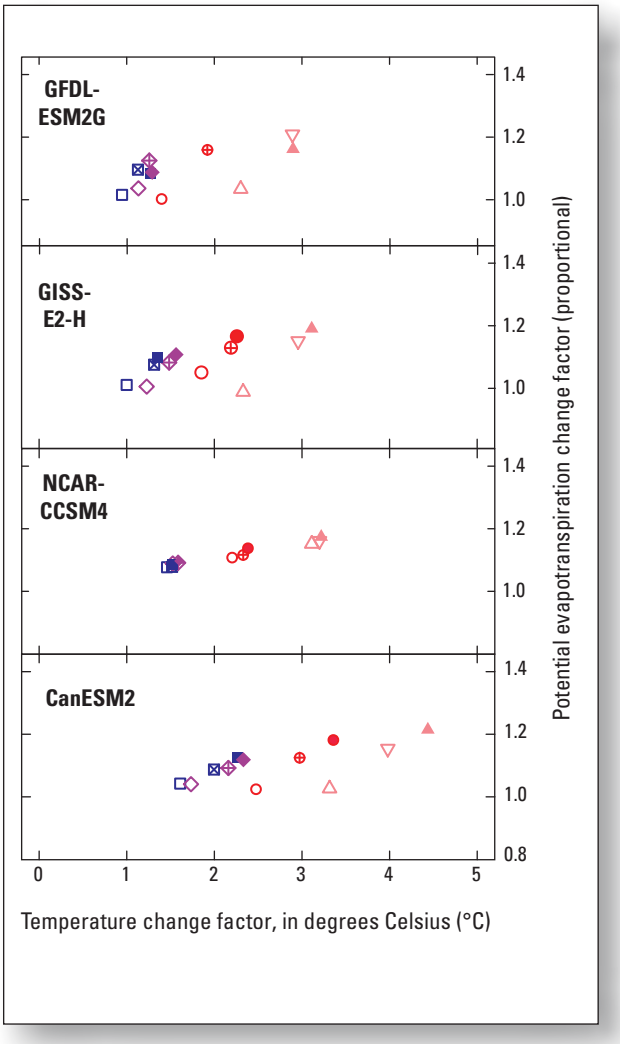

Scientific Investigations Report 2015–5143

U.S. Department of the Interior
U.S. Geological Survey

Cover: Left image shows forecasted development for 2060 in the Delaware River Basin (from figure 6*B*).
Right image shows range of forecasted annual change in temperature and potential evapotranspiration for 2030 and 2060, (from figure 7*B*).

Summary of Hydrologic Modeling for the Delaware River Basin Using the Water Availability Tool for Environmental Resources (WATER)

By Tanja N. Williamson, Jeremiah G. Lant, Peter R. Claggett, Elizabeth A. Nystrom, Paul C.D. Milly, Hugh L. Nelson, Scott A. Hoffman, Susan J. Colarullo, and Jeffrey M. Fischer

Scientific Investigations Report 2015–5143

U.S. Department of the Interior
U.S. Geological Survey

U.S. Department of the Interior
SALLY JEWELL, Secretary

U.S. Geological Survey
Suzette M. Kimball, Acting Director

U.S. Geological Survey, Reston, Virginia: 2015

Suggested citation:
Williamson, T.N., Lant, J.G., Claggett, P.R., Nystrom, E.A., Milly, P.C.D., Nelson, H.L., Hoffman, S.A., Colarullo, S.J., and Fischer, J.M., 2015, Summary of hydrologic modeling for the Delaware River Basin using the Water Availability Tool for Environmental Resources (WATER): U.S. Geological Survey Scientific Investigations Report 2015–5143, 68 p., http://dx.doi.org/10.3133/sir20155143.

ISSN 2328-0328 (online)

Preface

Development of the Water Availability Tool for Environmental Resources (WATER) for the Delaware River Basin (DRB) was done as part of a U.S. Geological Survey National Water Census Focus Area Study. The DRB Focus Area Study is part of implementation of the U.S. Department of Interior's Secure Water Act to Sustain and Manage America's Resources for Tomorrow (WaterSMART). WATER–DRB addresses multiple aspects of this WaterSMART work by providing a foundation on which to better understand streamflow, water use, and ecological water needs under current conditions and those associated with forecasted climate change and population expansion. This report documents data used to develop and inform the model, those hydrologic and hydroclimatic models encapsulated within WATER–DRB, and how this decision support system has been integrated with general circulation models and urbanization forecasts to provide resource managers with a way to objectively and consistently investigate water management strategies.

Acknowledgments

Development of the Water Availability Tool for Environmental Resources (WATER) for the Delaware River Basin (DRB) has benefitted from interaction with a large group of stakeholders who helped U.S. Geological Survey (USGS) identify critical questions in the basin. Among those stakeholders are the Delaware River Basin Commission and the five states included in the DRB.

The WATER decision support system (DSS) was developed in parallel with other DRB efforts. The Water-Census team was welcoming in helping to incorporate the needs of the WATER DSS into their data preparation and output, and they enabled the seasonal approach incorporated in the DSS. In addition, Natural Resources Conservation Service soil scientists in Pennsylvania (Yuri Plowden) and New Jersey (Richard Shaw and Edwin Muñiz) were integral to our obtaining an updated set of soils data while the newer Soil Survey Geographic dataset was still being processed. Kenneth Clark of the U.S. Department of Agriculture (USDA) Forest Service graciously helped us access evapotranspiration data from the New Jersey pineland sites, and Mathieu Gerbush, assistant State climatologist, helped us access data from the New Jersey Mesonet of climate sites. Finally, Amy Shallcross and Hernán Quinodoz, from the Delaware River Basin Commission, patiently helped us access and incorporate the subbasins needed to integrate WATER output with their Planning Support Tool format. Several universities have shown interest in incorporating WATER into future research, including Drexel University, The Pennsylvania State University, and the State University of New York, where Theodore Endreny and Yong Seuk Kwon provided a test of the DSS during its developmental stages

Contents

Figures

Tables

Conversion Factors

[International System of Units to Inch/Pound]

Multiply	By	To obtain
	Length	
millimeter (mm)	0.03937	inch (in.)
meter (m)	3.281	foot (ft)
kilometer (km)	0.6214	mile (mi)
	Area	
square kilometer (km^2)	247.1	acre
square kilometer (km^2)	0.3861	square mile (mi^2)
	Flow rate	
cubic meter per second (m^3/s)	35.31	cubic foot per second (ft^3/s)
cubic meter per second (m^3/s)	22.83	million gallons per day (Mgal/d)
millimeter per year (mm/yr)	0.03937	inch per year (in/yr)
	Radiative forcing	
watt per square meter (W/m^2)	0.3170	British thermal unit per hour per square foot

Temperature in degrees Celsius (°C) may be converted to degrees Fahrenheit (°F) as:

$°F = (1.8 \times °C) + 32.$

Temperature in degrees Fahrenheit (°F) may be converted to degrees Celsius (°C) as:

$°C = (°F - 32) / 1.8.$

Datum

Vertical coordinate information is referenced to the North American Vertical Datum of 1988 (NAVD 88).

Horizontal coordinate information is referenced to the North American Datum of 1983 (NAD 83).

Elevation, as used in this report, refers to distance above the vertical datum.

Supplemental Information

1 micrometer (µm) is 10^{-6} meter.

Carbon dioxide concentrations are given in parts per million (ppm).

Abbreviations

AET	actual evapotranspiration
awc	available water-holding capacity
CBLCM	Chesapeake Bay Land Change Model
CMIP5	Coupled Model Intercomparison Project Phase 5
conmult	conductivity multiplier
δ	change factor or delta
DEM	digital elevation model
DRB	Delaware River Basin
DSS	decision support system
E_f	Nash-Sutcliffe efficiency
EPA	U.S. Environmental Protection Agency
ET	evapotranspiration
fc	field capacity
FDC	flow-duration curve
GCM	general circulation model
gSSURGO	gridded Soil Survey Geographic dataset
GUI	graphical user interface
HRU	hydrologic response unit
HUC–12	12-digit hydrologic unit code
ICLUS	EPA Integrated Climate and Land Use Scenarios
K_{sat}	saturated hydraulic conductivity
m	scaling parameter
NED	National Elevation Dataset
NLCD	National Land Cover Database
NRCS	Natural Resources Conservation Service
NWIS	National Water Information System
NWS	National Weather Service
PET	potential evapotranspiration
PST	Planning Support Tool
rho	Spearman rank correlation coefficient

RMSEn	normalized root mean squared error
$RMSEn_{57}$	average RMSEn for daily streamflow at 57 sites used for statistical evaluation of WATER
$RMSEn_{45\text{-}mon}$	average RMSEn for mean monthly streamflow at 45 sites that had a 9-year period of record for statistical evaluation
$RMSEn_{57mon\text{-}PORnorm}$	average RMSEn for mean monthly streamflow at 57 sites normalized over the period of record for each site
RSR	ratio of the root mean squared error to the standard deviation of the observed record
SpCf	spatial coefficient
SSEB	Simplified Surface Energy Balance
SSURGO	Soil Survey Geographic dataset
TR–55	USDA Technical Release 55 (an urban hydrology model)
TWI	topographic wetness index
USACE	U.S. Army Corps of Engineers
USDA	U.S. Department of Agriculture
USGS	U.S. Geological Survey
WATER	Water Availability Tool for Environmental Resources
WaterSMART	Secure Water Act to Sustain and Manage America's Resources for Tomorrow

Summary of Hydrologic Modeling for the Delaware River Basin Using the Water Availability Tool for Environmental Resources (WATER)

By Tanja N. Williamson, Jeremiah G. Lant, Peter R. Claggett, Elizabeth A. Nystrom, Paul C.D. Milly, Hugh L. Nelson, Scott A. Hoffman, Susan J. Colarullo, and Jeffrey M. Fischer

Abstract

The Water Availability Tool for Environmental Resources (WATER) is a decision support system for the nontidal part of the Delaware River Basin that provides a consistent and objective method of simulating streamflow under historical, forecasted, and managed conditions. In order to quantify the uncertainty associated with these simulations, however, streamflow and the associated hydroclimatic variables of potential evapotranspiration, actual evapotranspiration, and snow accumulation and snowmelt must be simulated and compared to long-term, daily observations from sites. This report details model development and optimization, statistical evaluation of simulations for 57 basins ranging from 2 to 930 km^2 and 11.0 to 99.5 percent forested cover, and how this statistical evaluation of daily streamflow relates to simulating environmental changes and management decisions that are best examined at monthly time steps normalized over multiple decades. The decision support system provides a database of historical spatial and climatic data for simulating streamflow for 2001–11, in addition to land-cover and general circulation model forecasts that focus on 2030 and 2060. WATER integrates geospatial sampling of landscape characteristics, including topographic and soil properties, with a regionally calibrated hillslope-hydrology model, an impervious-surface model, and hydroclimatic models that were parameterized by using three hydrologic response units: forested, agricultural, and developed land cover. This integration enables the regional hydrologic modeling approach used in WATER without requiring site-specific optimization or those stationary conditions inferred when using a statistical model.

Introduction

The Water Availability Tool for Environmental Resources (WATER) was constructed for the Delaware River Basin (DRB; fig. 1) to provide a decision support system (DSS) that could be used by regulators, managers, and other interested parties. The DRB WATER DSS (hereafter called WATER) employs a process-based hydrologic model that was implemented with a spatial dataset that catalogues the spatial variability in topography, climate, soil properties, and anthropogenic features that affect water movement in this five-state area (fig. 1).

WATER was developed and implemented by using historical data; however, the ultimate goal was to provide a DSS that could simulate streamflow under a range of forecasted climatic and land-use scenarios. Initial work in the DRB focused on modeling of minimally impacted streams that were upstream of the reservoir system that provides public-supply water for the basin as well as New York City, New York. Streamflow was simulated for the period 2001–11, using the National Land Cover Database (NLCD), data from the Soil Survey Geographic (SSURGO) database, Daymet precipitation and temperature data, and water-use data provided by the U.S. Geological Survey (USGS) National Water Census program; sources and details of these data are provided in the section "Framework of the WATER Decision Support System." Because WATER was designed to use a standard set of data sources that are available for the entire study area, temperature-indexed equations were used to simulate snowpack and potential evapotranspiration (PET). To provide for reservoir management planning, streamflow simulations can be completed for inflow points to the reservoirs and formatted in the output required by the Delaware River Basin Commission's DRB-Planning Support Tool (PST; DRBC [2015]), formerly the DRB-OASIS model (Hydrologics, 2002).

WATER also interacts with a scenario-building tool (WATER Application Utilities) that provides a range of general circulation model (also known as global circulation model or global climate model; GCM) datasets that use the change-factor (delta [δ]) approach to synthesize a climate record for future conditions. This approach quantifies the difference for each GCM between historical and forecasted conditions for hydroclimatic variables; this difference is then applied to those historical data provided with WATER in order to create a new hydroclimatic record for the desired time period. The scenario builder also incorporates water-use data and reformats the simulated flow record into the desired output structure.

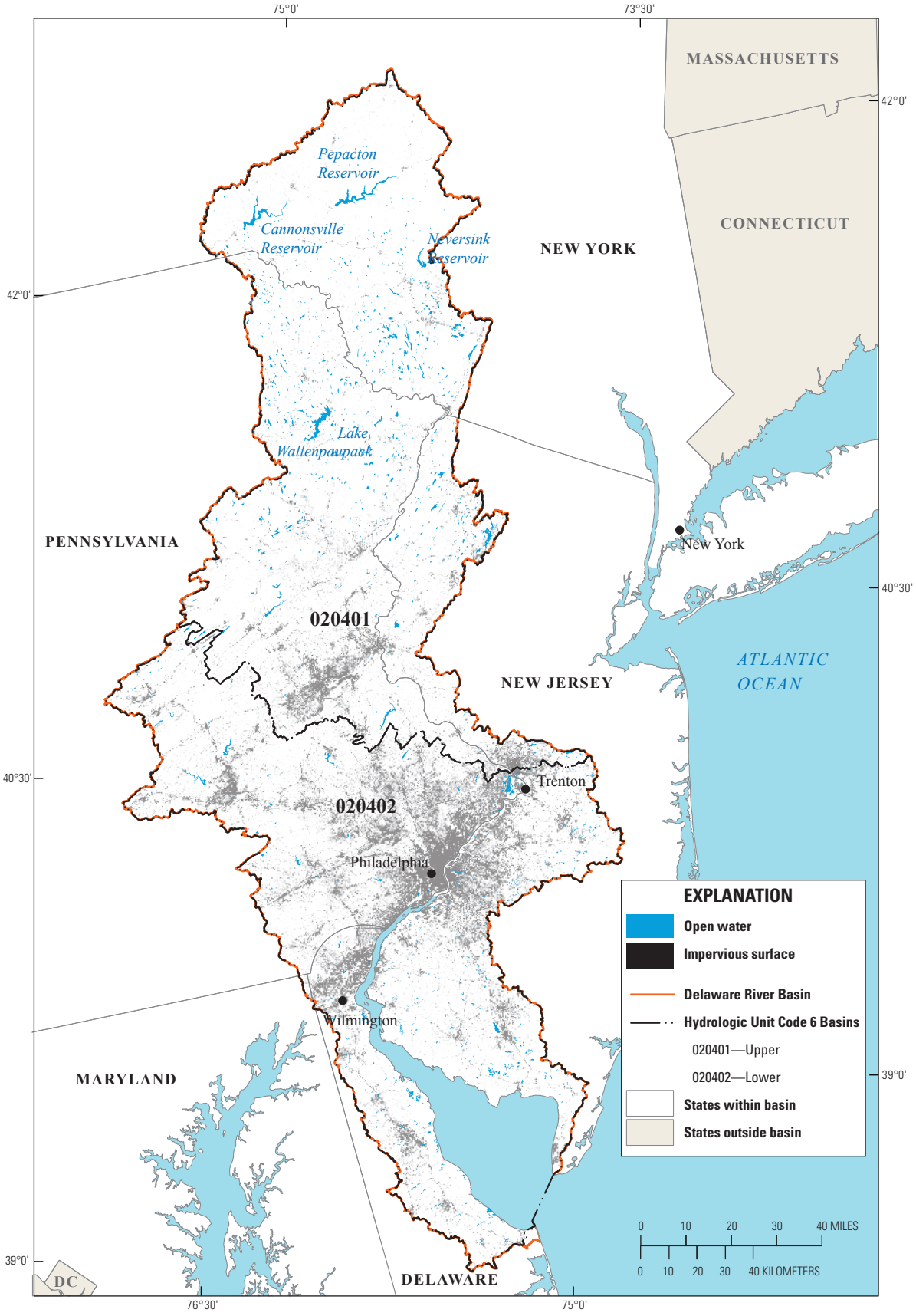

Figure 1. The Delaware River Basin (DRB), including parts of Delaware, New Jersey, New York, and Pennsylvania, as well as a small part of Maryland. Also shown are major population centers and upper-basin reservoirs.

Purpose and Scope

This report focuses on the aggregation and sampling of geospatial data, the hydrologic model approach, and the ability of WATER to simulate streamflow for historical conditions in the DRB. The uncertainty of historical simulations can be used to understand the uncertainty related to streamflow simulation for forecasted conditions and scenario testing. However, although uncertainty associated with scenario testing is discussed in this report, results from scenario testing are intended to be discussed in separate publications.

Focus Area and Overall Approach of WATER

The DRB encompasses 35,075 square kilometers (km^2; 13,539 square miles [mi^2]) and includes parts of Delaware, Maryland, New Jersey, New York, and Pennsylvania, including the population centers of Wilmington, Delaware, Philadelphia, Pennsylvania, and Trenton, New Jersey, and a total population in 2010 of approximately 8.2 million people (fig. 1). In addition, the basin supplies drinking water to New York City, N.Y. (essentially doubling the effective population), via an interbasin transfer that is supplied by a series of reservoirs in the northern part of the DRB. This interbasin transfer is managed in accordance with the 1954 Supreme Court decree that specifies a minimum flow requirement of 1,750 cubic feet per second (ft^3/s) at Montague, NJ (U.S. Supreme Court, 1954, 1982). A 1983 agreement later established a minimum flow requirement of 3,000 ft^3/s at Trenton, NJ (DRBC, 2013). Because the DRB reservoir system is strictly managed on a daily basis, evaluation of WATER and the associated hydroclimatic variables focused on basins upstream of this reservoir system.

Uses and Objectives of WATER

WATER was developed for users with the range of hydrologic understanding, geographic interest, and management responsibility included in the DRB stakeholder group. Potential users include but are not limited to the following:

- university researchers focused on small subbasins where a historical streamflow record is not available;
- local water-resource managers tasked with determining the effect of new water-use permits;
- conservation managers working to establish streamflow-restoration goals;
- regional planners who need an objective and informed method for assessing expansion of developed areas in the coming decades; and
- those needing local or regional quantifications related to forecasted climate, including snowpack, growing season and presence of plant-available water for evapotranspiration (ET), and seasonal streamflow changes.

Consequently, the explanation of the hydrologic modeling approach, data sources, and uncertainty (or error) of streamflow simulations are presented at multiple time steps and with different organizational approaches (for example, streamflow simulations can be compared as a function of land cover or organized by streamflow percentiles). Depending on the question being asked, WATER output should be used differently and with a different approach to uncertainty, as in the following examples:

- Those simulating historical streamflow can use WATER output in its original form as daily streamflow because the original precipitation and temperature data were reported at a daily time step.
- Those asking questions involving forecasted climate (GCMs) are strongly discouraged from examining the daily WATER output. Instead, these users should focus on aggregated streamflow metrics, for example the flow-duration curve (FDC) or monthly averages across the entire period of record, because climate data are adjusted according to a forecasted, long-term, monthly change in climatic conditions.

The objectives of this report were to:

1. detail the spatial layers used by WATER to delineate basins and inform the hydrologic models;
2. document the incorporation of a 2010 snapshot of water use for the DRB;
3. explain how GCM data were processed and incorporated and how WATER simulates potential evapotranspiration (PET) and actual evapotranspiration (AET) for 2030 and 2060 target conditions;
4. document the development and incorporation of land-cover projections used to characterize 2030 and 2060 target conditions;
5. compare hydroclimatic observations that affect the water budget of the landscape (snow accumulation and snowmelt, PET, and AET) to those simulated by WATER;
6. quantify the uncertainty in daily streamflow simulations for the 2001–10 time period and how this uncertainty varies with land cover, basin size, and flow regime;
7. quantify the uncertainty in aggregated simulation results, including FDCs and monthly flow normals; and
8. explain how uncertainty in streamflow simulations can be incorporated into scenario testing.

Framework of the WATER Decision Support System

WATER integrates geospatial sampling of landscape characteristics with a hillslope-hydrology model and an impervious-surface model in order to simulate water movement to streams in the DRB. The hillslope-hydrology model underlying WATER, TOPMODEL (Beven and Kirkby, 1979), is a rainfall-runoff model that is based on a water-budget approach and simulates hillslope water movement as a function of topographically defined landscape positions. TOPMODEL is process based and simulates the variable-source-area concept of streamflow generation from pervious areas (in other words, areas where precipitation infiltrates into the soil) by combining these topographic landscape positions with basin soil characteristics (Wolock, 1993). TOPMODEL assumes three conditions:

- steady-state recharge to the groundwater,
- a hydraulic gradient of the water table that approximates that of the surface slope, and
- soil-water movement that decreases exponentially with depth.

WATER combines streamflow simulation from TOPMODEL for pervious areas with an estimation of runoff from impervious surfaces derived by using the curve number approach described in U.S. Department of Agriculture (USDA) Technical Release 55 (TR–55; USDA, 1986). To inform these models and differentiate pervious from impervious areas, WATER geospatially samples climatic, land-cover, topographic, and soils data for the basin of interest (table 1 and fig. 2; details of different DSS processes are discussed in the sections "Data Sources and Processing of Data for WATER" and "Model Development, Statistical Evaluation, and Validation of Hydroclimatic Components of WATER"). The hydrologic models are driven by a daily precipitation and temperature record, and WATER provides mean daily streamflow. Hydroclimatic variables, including PET and snow accumulation and snowmelt, are simulated within DRB WATER through the use of temperature-indexed equations (Hamon, 1963; U. S. Army Corps of Engineers [USACE], 1998); AET is calculated by TOPMODEL on a daily time step on the basis of a combination of PET and soil-water storage. Disposition of precipitation as infiltration, overland flow, and soil-water storage and movement are simulated by TOPMODEL as a function of soil characteristics, including soil thickness, pore-size distribution, and saturated hydraulic conductivity (K_{sat}). Any remaining precipitation infiltrates into the soil, and the soil-water storage is then equilibrated with the rest of the soil thickness before gravity drainage delivers water to either a downslope landscape position or to streamflow. This streamflow is then combined with runoff generated from impervious surfaces in the basin (TR–55). Soil-water storage is then averaged for the entire basin as a mass balance (equation 2). Simulated streamflow generated from forested, agricultural, and developed areas are then added to obtain daily streamflow.

WATER is a DSS that is based on a regional modeling approach, meaning that the model works with the same parameterization in all areas of the basin. WATER is able to model areas with specificity because it uses geospatial data layers that catalog differences in land use, soil conditions, and topography on a cell size less than or equal to (≤) 30 meters (m), with no site-specific optimization (Williamson and others, 2009, 2013); instead, parameters were optimized as a function of land cover. **By using this regional approach, with no site-specific optimization, this process-based simulation of streamflow and the water budget can be used to examine management scenarios that involve forecasted climate change, expansion of urban and suburban areas, and restoration goals of minimally impacted flow environments.** In contrast, statistical models cannot be used to model nonstationary conditions like those associated with land-cover and climate change (Farmer and others, 2015).

Table 1. Data sources and citations for the Delaware River Basin Water Availability Tool for Environmental Resources.

[WATER, Water Availability Tool for Environmental Resources; SSURGO, Soil Survey Geographic; NRCS, Natural Resources Conservation Service; DEM, digital elevation model; TWI, topographic wetness index; HRU, hydrologic response unit]

Data source	Contribution to WATER
Daymet (Thornton and others, 2012) http://daymet.ornl.gov/index.html	Daily temperature and precipitation data for 1980–2011
National Elevation Dataset (Gesch and others, 2002) http://ned.usgs.gov/	Elevation data (as DEM) used for basin delineation and TWI calculations
2011 National Land Cover Database (Jin and others, 2013) http://www.mrlc.gov/	HRUs and impervious area
Soil Survey Geographic (SSURGO) database (SSURGO; NRCS, 2014) http://datagateway.nrcs.usda.gov/	Hydrologic soil characteristics and TOPMODEL specific parameters

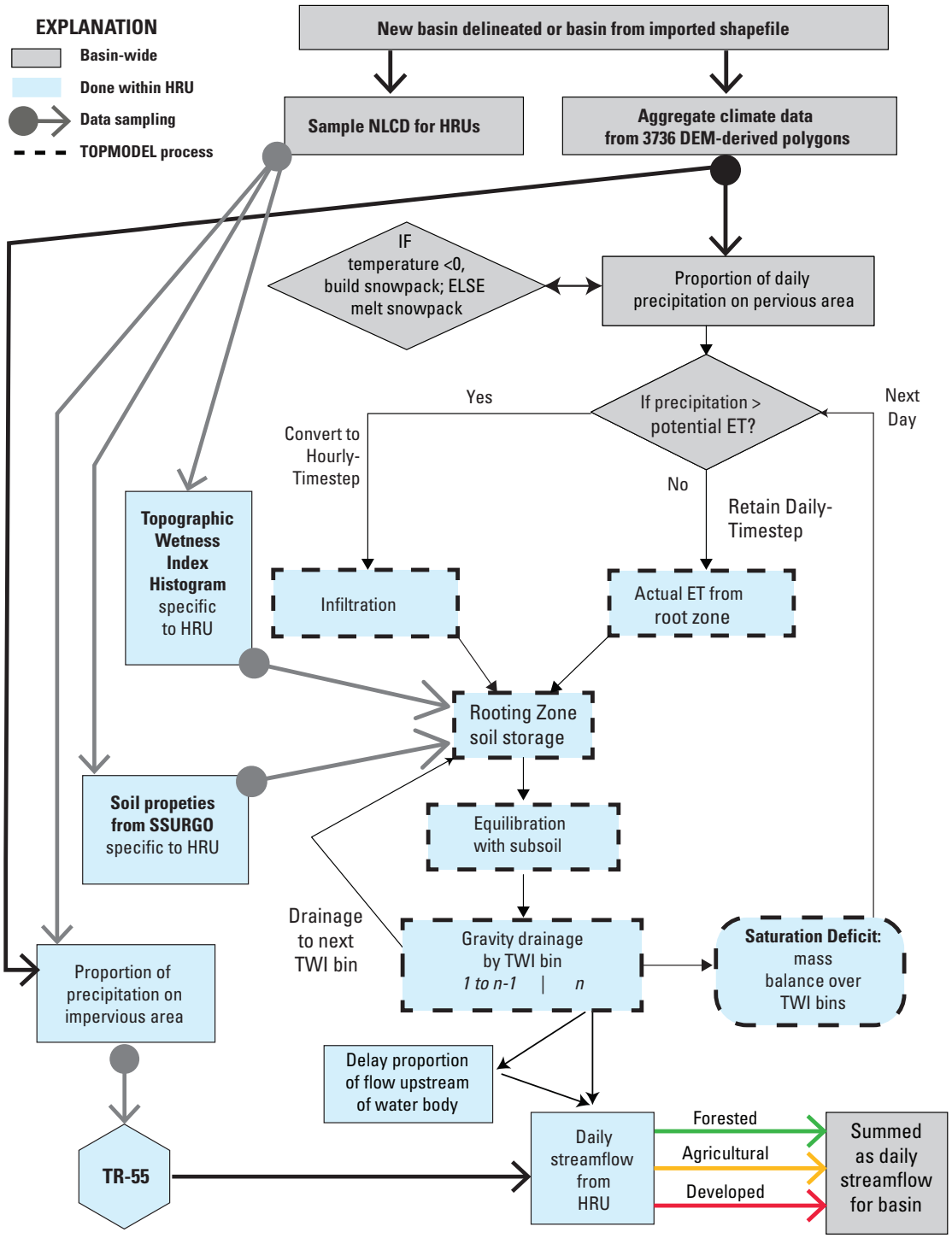

Figure 2. How the Water Availability Tool for Environmental Resources samples geospatial data and feeds it to the two hydrologic models (TOPMODEL and the U.S. Department of Agriculture urban hydrology model [TR–55]). The basin is apportioned into three hydrologic response units (HRUs). Daily precipitation is sampled from Daymet and proportionally distributed between pervious and impervious areas. Potential evapotranspiration (PET) is estimated from Hamon (1963). Actual evapotranspiration (AET) is removed from soil-water storage in the root zone (table 2), and the remainder infiltrates into the soil. The soil-water storage is then equilibrated with the rest of the soil thickness before gravity drainage delivers water either to the next topographic-wetness-index (TWI) bin (bins 1 to *n*–1; *n*=30) or to streamflow. Soil-water storage for the entire basin is then averaged using a mass balance (equation 2). Simulated streamflow generated from three separate HRUs is then summed to obtain daily streamflow. DEM, digital elevation model; ET, evapotranspiration; NLCD, National Land Cover Database; SSURGO, Soil Survey Geographic database; >, greater than; <, less than.

The WATER developed for the DRB includes the entire basin. For some areas, streamflow simulations derived with WATER should be used cautiously. For example, WATER provides no method of simulating the influence of tides on streamflow that would be expected in stream reaches south of Trenton, N.J., along the Delaware River, and in tributaries along Delaware Bay (fig. 3). In addition, WATER does not take into account the daily controlled releases from dams and reservoirs in the basin, so it will not accurately simulate flows on large rivers affected by these releases. These rivers include, in particular, the entire length of the main-stem Delaware River, but also parts of the Neversink, Lackawaxen, Mongaup, Lehigh, Schuylkill Rivers and Brandywine Creek, as well as other locations (fig. 3). In anticipation of this constraint, WATER was designed to output data at river locations (nodes) known to be inflow points for the DRB-PST (DRBC, 2015) and is compatible with this reservoir operation support tool. If WATER is used to simulate streamflow for areas that include reservoirs, they will be treated as areas with any other water bodies. Consequently, users should be familiar enough with their area of interest to understand whether streamflow is controlled by reservoir management.

Relation of Delaware River Basin WATER to Previous Studies

WATER is built upon a physically based hydrologic model that simulates the variable-source-area concept of streamflow and is an extension of the TOPMODEL code described in Wolock (1993). The TOPMODEL code was originally developed by Beven and Kirkby (1979); however, many researchers have extensively modified the code, and numerous versions of TOPMODEL now exist in several programming languages (e.g. Robson and others, 1992; Romanowicz, 1997; Metcalfe and others, 2014). TOPMODEL has been used to study a variety of hydrologic research topics, including topographic effects on water quality (Wolock, 1988; Wolock and others, 1990; Wolock and McCabe, 1999), topographic effects on streamflow (Beven and Wood, 1983; Beven and others, 1984; Kirkby, 1986), spatial-scale effects on hydrologic processes (Sivapalan and others, 1987; Beven and others, 1988; Wood and others, 1988; Sivapalan and others, 1990; Wood and others, 1990; Famiglietti and Wood, 1991; Famiglietti, 1992), and the geomorphic evolution of basins (Ijjász-Vásquez and others, 1992). TOPMODEL has also been used for estimating regional-scale variability in hydrologic properties in the United States (Wolock, 2003), flood frequency (Beven, 1986a, b), effects of climate change on hydrologic processes (Wolock and Hornberger, 1991), soil-water storage (Williamson and others, 2014), carbon budgets (Band and others, 1991), base-flow residence times (Vitvar and others, 2002), and ecological-flow factors (Kennen and others, 2008). Finally, TOPMODEL has been used to reveal interactions among variables in model-parameter calibration (Hornberger and others, 1985; Wolock, 1988; Wolock and McCabe, 1995; Williamson and others, 2013), including how input data must change with a change in digital-data resolution (Brasington and Richards, 1998).

WATER for the DRB builds on previous hydrologic modeling in New Jersey (Kennen and others, 2008) and is an updated version of the DSS developed in Kentucky (Williamson and others, 2009, 2013). New functionality in WATER for the DRB includes estimates of snow accumulation and melting as well as implementation of a hydrologic response unit (HRU) approach that is based on three general land-cover categories: forested, agricultural, and developed areas. This HRU refinement enabled multiple aspects of the WATER approach by differentiating the interaction among the topography, soil characteristics, and hydroclimatic variables critical to TOPMODEL and how it simulates the water-budget and hillslope processes among the HRUs. Consequently, data sources and parameterization discussed in the following section are unique to WATER for the DRB.

Data Sources and Processing of Data for WATER

WATER is provided with a database of model inputs for the 2001–11 period because this is the temporal overlap of the many data layers required to inform the model. Limitations leading to the selection of this time period are the intersection of the historical climate record (1980–2011), the generation of land-cover data (2011), and the water-use snapshot (2010). Other data (for example, topography and soil data) are not time sensitive. Each of these data sources is encapsulated within WATER to provide all of those data required to simulate streamflow and water availability. Unless otherwise stated, all geospatial data are at a 10-m resolution in the North American Datum of 1983 Albers Equal Area Projection using the Geodetic Reference System 1980 spheroid. All geoprocessing was done with ArcMap 10.0 (https://www.arcgis.com). Output of the hydrologic simulations is provided on daily (WATER.txt), monthly (WATERMonth.txt), and annual (WATERAnnual.txt) time steps and can be imported by the user into a spreadsheet or statistical program for analysis.

As described in the section "Framework of the WATER Decision Support System," WATER uses a hydrologic modeling approach that depends on the accompanying spatial layers of topography, soil properties, and climatic data to simulate precipitation disposition throughout the DRB (fig. 2). HRUs are delineated by intersecting an individual basin (either delineated by WATER or provided by the user) with the land cover in order to separate forested, agricultural, and developed areas; each HRU may include multiple, discontinuous areas with similar land cover. WATER then calculates an arithmetic mean for each spatial layer for each HRU; currently, this process uses the Spatial Analyst extension in ArcGIS 10.0. To optimize the incorporation of these geospatial data with the hydrologic modeling, a subset of ten parameters (table 2) that control the

Table 2. Parameters optimized for regional hydrologic simulations with the Water Availability Tool for Environmental Resources. These parameters control the soil-plant-water interactions and how they differ among hydrologic response units. These parameters also equip the model for scenario testing in terms of both land-cover and climate forecasts.

[Color coding is included to highlight the parameters related to TOPMODEL (white), interaction with water bodies (grey), impervious-surface runoff (blue), snow accumulation (purple), and evapotranspiration (green). AET, actual evapotranspiration; ET, evapotranspiration; >, greater than; km², square kilometers; NLCD, National Land Cover Database; TR–55, U.S. Department of Agriculture Technical Release 55; USDA, U.S. Department of Agriculture; mm/d/°C, millimeters per day per degree Celsius; USACE, U.S. Army Corps of Engineers; PET, potential evapotranspiration; HRU, hydrologic response unit]

Parameter	Parameter alias	Application and unit	Hydrologic response unit		
			Forested	Agricultural	Developed
Spatial coefficient	spatialcoeff	Used to calculate scaling parameter (m) for TOPMODEL	0.4	0.3	0.25
Topographic adjustment	wiadjustment	Adjusts topographic-wetness-index values in histogram for TOPMODEL	1	1	0.5
Rooting depth factor	rootdepthfactor	Proportion of soil thickness used for ET in TOPMODEL	0.75	0.25	0.75
Travel through macropores	percentmacropore	Proportion of precipitation that bypasses ET soil thickness in TOPMODEL	0.15	0.15	0.2
Water-body delay	lakedelay	days—proportional increase in days that water is delayed if upstream of a water body; water bodies >10 acre (0.04 km²)	15	1.5	1.5
Effective impervious	effimpervious	Multiplied by NLCD value to change total impervious surface for study area	0.7	1	1
Impervious runoff delay	imperviousrunoff	Proportion of precipitation delayed to next day from impervious surface and TR–55 calculations	0.1	0.5	0.1
Impervious curve number	imperviouscurve	TR–55 parameter that characterized type of impervious surface (USDA, 1986)	90	90	100
Snowmelt coefficient	snowcoeff	mm/d/°C above 0 (USACE, 1998) for snowmelt	2	2	4
Rain-on-snowmelt coefficient	rainonsnowcoeff	mm/d/°C above 0 (USACE, 1998) for snowmelt	3	4	6
Exponent for seasonal AET	etexponent	$AET = PET_{calculated} \times \left(\frac{soil\ storage}{maximum\ soil\ storage} \right)^{Exponent}$		0.5 (growth)	
				5 (dormant)	
Growing season trigger	growtemp	°C—transitions to/from growing season exponent for AET calculation		15	

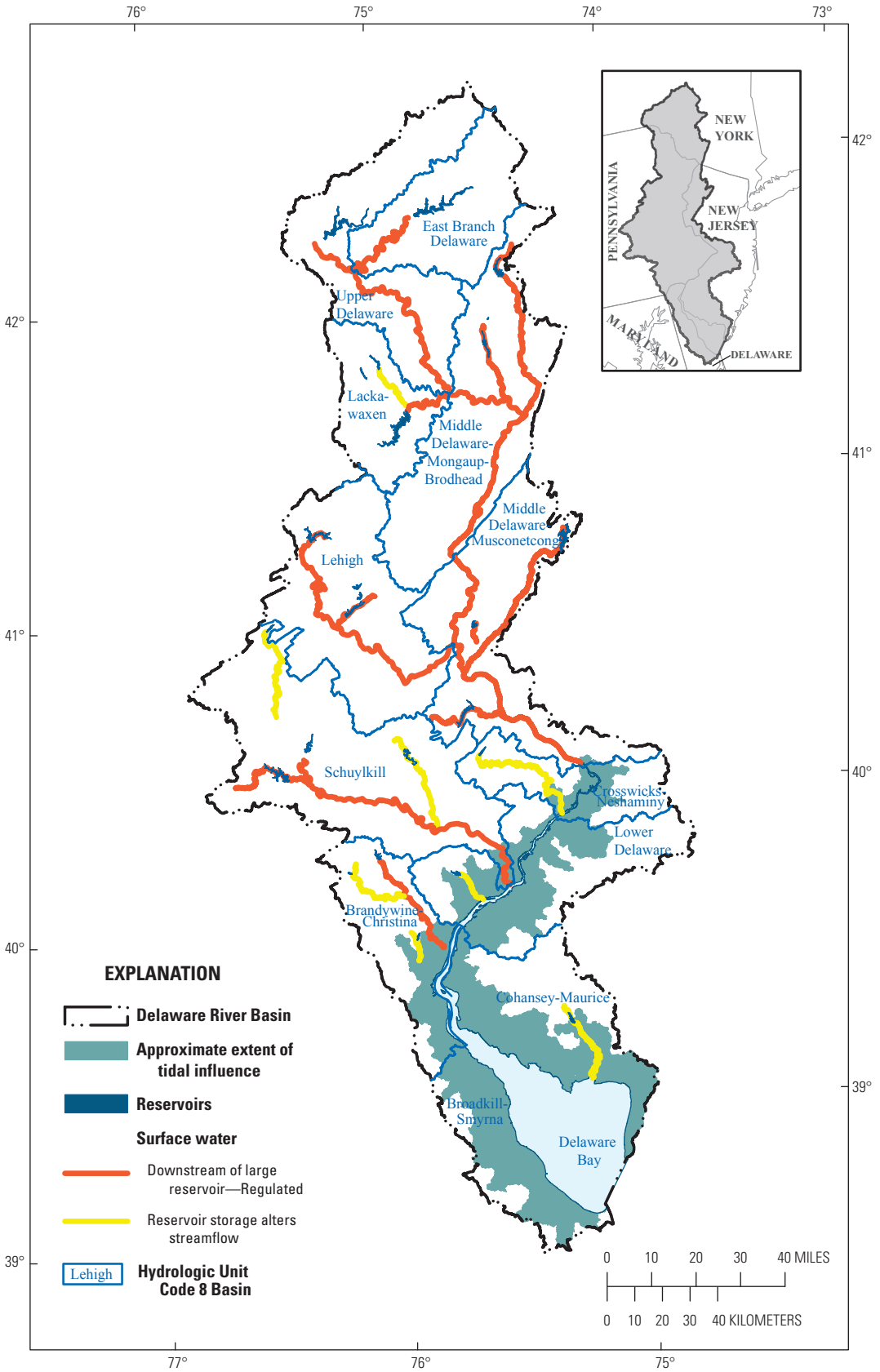

Figure 3. Parts of the Delaware River system for which streamflow information from the Water Availability Tool for Environmental Resources should be used cautiously because of stream regulation and tidal influences.

interaction of topography and vegetation with precipitation disposition was regionally optimized for the individual DRB HRUs (forested, agricultural, and developed land cover) to create the best fit for streamflow observations in basins with relatively homogeneous land cover. This regional approach to HRU optimization followed Williamson and others (2009) and incorporated parameter exploration (Doherty, 2008); this approach was used instead of site-specific optimization to identify a single set of HRU parameters that work throughout the DRB. An additional four parameters were optimized for simulation of snowmelt and accumulation as well as ET.

Data sources can be separated into those that inform the hydrologic models, those used for optimization and statistical validation of WATER simulations, and those that enable scenario testing. Data that inform the hydrologic models and those that enable scenario testing are included in the WATER database and WATER Application Utilities. The optimization and statistical validation discussed in the section "Model Development, Statistical Evaluation, and Validation of Hydroclimatic Components of WATER" provides a reference for understanding the potential error and uncertainty associated with hydrologic simulation (1) where no observations exist and (2) for forecasted or proposed scenarios in basin management or environmental change.

Data That Inform the Models

Data required for the hydrologic models (TOPMODEL and TR–55) to run include daily precipitation and temperature as well as basin characteristics that quantify topography and the potential to store water in the soil. In addition, parameters that describe how these basin characteristics interact and how water moves through the soil to the stream are derived with these same data.

Topography

Topographic data are from the 10-m resolution National Elevation Dataset (NED; Gesch and others, 2002). These data are used for three purposes: (1) basin delineation, (2) development of a digital elevation model (DEM)-derived stream network, and (3) development of the topographic wetness index (TWI). Because WATER was developed to analyze basins from physiographically diverse terranes, hydrologic parameters such as stream-channel width and the drainage area required to initiate channelized streamflow had to be uniformly defined. To estimate stream-cell area, the stream network raster was developed by applying the following criteria:

1. Streams were defined as 1 cell wide for the entire network.

2. Streams were initiated after accumulating a total of 0.3 km^2 (3,000 10-m cells) upstream area by using the Arc Hydro Flow Accumulation tool (with a single-flow-direction algorithm; https://www.arcgis.com).

These two flow-accumulation criteria area were established to include first-order, perennial, channelized drainages while excluding small, ephemeral, hillslope systems.

Basins are delineated within WATER by using a combination of flow-direction and flow-accumulation rasters, combined with 3,736 predelineated, DEM-derived polygons that range in size from 0.0001 to 132.4 km^2, with a mean area of 9.4 km^2 and median of 7.6 km^2. These predelineated basins were produced by using Arc Hydro (https://www.arcgis.com) and make the basin delineation process faster by providing a sequenced network of basins that can be aggregated into the site-specific basin delineation. Although the USGS National Hydrography Dataset (http://nhd.usgs.gov; U.S. Geological Survey and others, 2009) is used to help orient the user in the WATER graphical user interface (GUI), WATER uses the DEM-derived stream network to delineate basins and calculate stream area. The result is that WATER can be used to delineate a new basin from a pour-point (basin outlet) that is anywhere on the DEM-derived stream network.

The TWI raster used by TOPMODEL (discussed below) was developed from these same flow-direction and flow-accumulation rasters. Because TWI values along stream channels do not reflect hillslope processes (Quinn and others, 1997), these high values were removed. This prevents cells with high TWI values from altering the TWI distribution for a given basin while still maintaining a representative riparian zone to serve as a variable source area for streamflow.

Climate Data

The Daymet historical climate record was originally at a resolution of 1 km^2 (Thornton and others, 2012), and a geospatial mean was sampled by using the 3,736 DEM-derived polygons and processed by the USGS Geo Data Portal (http://cida.usgs.gov/gdp/). These Daymet data were geospatially sampled and supplied as part of the database in order to provide a long period of record with a minimum of processing time, and they include a historical record from January 1, 1980, through December 11, 2011. These data include maximum daily temperature and total daily precipitation. Total daily precipitation is randomly distributed during each day by WATER using a set seed, or starting point, so that the randomization is the same every time the model is run—this insures reproducibility of results and comparability of results among historical and forecasted conditions. This randomization distributes the daily total of precipitation to individual hours in the day; TOPMODEL functions on an hourly time step on days with precipitation. WATER uses maximum daily temperature to estimate daily PET (Hamon, 1963), and the accumulation and melt of snow (USACE, 1998), by using temperature-indexed equations; this is discussed in "Hydroclimatic Water-Budget Components" in more detail. Precipitation and temperature data are stored in the WATER database as text files for those 3,736 DEM-derived polygons.

Land Cover

The land-cover raster in the WATER database is NLCD 2011 (Jin and others, 2013), although initial development of WATER proceeded with NLCD 2006 until more recent data were published. The NLCD 2011 dataset has a 30-m resolution and is used for two purposes: (1) delineation of the forested, agricultural, and developed HRUs and (2) calculation of basin averages of impervious area.

These HRUs are a simplification of land cover into three categories: forested (deciduous, evergreen, mixed, shrubland, and wetland areas; NLCD classes 41–43, 51–52, and 90–95), agricultural (pasture and cropland; NLCD classes 81 and 82), and developed (all remaining categories; NLCD classes 21–24, 31, and 71). The DSS initially classifies open water (NLCD class 10) as developed because it does not match either the forested or agricultural land-cover categories, but the DSS later reassigns it as water.

The proportion of impervious surface area in the basin is estimated from a combination of the 2011 NLCD and a road layer (10-m resolution 2010 NAVTEQ; Homeland Security Infrastructure Program [2012]). WATER allocates a proportion of precipitation to the TR–55 impervious flow model on the basis of the proportion of impervious surface in the basin. The remaining precipitation is distributed for the pervious portion of the basin as a function of hillslope hydrology by TOPMODEL.

Soils Data

Representative values of soil parameters were aggregated from the SSURGO database by using a series of queries in Microsoft Access; these parameters include K_{sat}, soil thickness, field capacity (fc), total porosity, and available water-holding capacity (awc). Similarly to the case with NLCD, development of WATER originally proceeded with data downloaded in 2012 (Natural Resources Conservation Service [Soil Survey Staff [NRCS], 2012]), but the newer SSURGO (Soil Survey Staff [NRCS], 2014) product was used to replace these 2012 data during the validation process, and are provided in the WATER database; this was done to incorporate recent correlations among counties on the basis of discussion with NRCS. Soil-property data were upscaled from soil-layer data (corresponding to one or more horizons) to component-weighted means (corresponding to one or more soil series) for each soil-mapping unit after Williamson and others (2014) and were joined to spatial data by using the unique identifiers of soil-mapping-unit polygons. These polygons, attributed with individual soil parameters, were then converted to a 10-m raster to match that of the DEM and used for geospatial statistics.

For compilation of this database, soil thickness was defined as the sum of the soil layers for which the representative K_{sat} reported in the SSURGO database was greater than (>) 1 micrometer per second (µm/s)—approximately the conductivity of a silty sand (Dingman, 2002). This is equivalent to choosing all soil layers for which K_{sat} is "moderately high or higher" as defined by the Natural Resources Conservation Service (Soil Survey Staff [NRCS], 1993). The elimination of layers with $K_{sat} \leq 1$ µm/s is based on previous work that showed that these subsoil layers are not involved in the daily hydrologic processes simulated by TOPMODEL (Williamson and others, 2009). Consequently, the first query run on SSURGO data eliminated all soil layers that did not meet this criterion. The remaining soil layers were used to determine the soil thickness. Other soil properties, including fc, total porosity, and awc were upscaled by using the same soil layers.

Linking Topographic and Soil Data for Hydrologic Models

In addition to the soil properties listed above, two other hydrologic properties—the conductivity multiplier (*conmult*) and the scaling parameter—were calculated for each mapping unit. The *conmult* estimates the relative change in K_{sat} with depth:

$$conmult = \frac{K_{sat}\text{-}high}{K_{sat}\text{-}low}, \quad (1)$$

where

K_{sat}-*high* is maximum K_{sat} value for the soil map unit and

K_{sat}-*low* is minimum K_{sat} value for the soil map unit for which the representative K_{sat} is >1µm/s in the SSURGO database.

A smaller *conmult* indicates less change in K_{sat} with depth. Within the WATER database, the minimum *conmult* is 2, indicating that the K_{sat} at the surface is twice that at the base of the soil. TOPMODEL incorporates this vertical change in K_{sat} movement to simulate soil-water movement through the hillslope.

The scaling parameter (***m***) incorporates the *conmult* and is used by TOPMODEL to estimate spatial variability in saturation deficit across the landscape by linking the mean saturation deficit, or unfilled pore space in the soil, with the local difference in the topography (after Beven, 1984):

$$S_x = \overline{S} + (SpCf \times m)(\overline{TWI} - TWI_x), \quad (2)$$

where

S_x is local saturation deficit in a grid cell (10-m cells);

$\overline{S}$ is mean saturation deficit in basin;

m is scaling parameter;

SpCf is HRU-specific spatial coefficient determined during model optimization;

$\overline{TWI}$ is mean topographic wetness index in basin (discussed below); and

TWI_x is local topographic wetness index in grid cell;

with $$m \equiv \frac{porosity - field\ capacity}{f} \quad (3)$$

and $$f = \frac{\ln conmult}{soil\ thickness}. \quad (4)$$

Optimization for the individual HRUs, following the approach of Williamson and others (2009) and incorporating parameter exploration (Doherty, 2008), showed that streamflow simulation improved when the ***m*** directly calculated from the SSURGO database was multiplied by the HRU-specific spatial coefficient (*SpCf*; table 2) to empirically fit the relation between soil-water deficit and topography, given the resolution of those spatial data and the three different land-cover types. The scaling parameter (***m***) acts directly on the deficit calculation (equation 2). The magnitude of this parameter is critical to how much water is retained in the soil pores during dry periods and to the resultant hydrograph response in terms of flood peaks. A larger ***m*** results in an exaggeration of the topography (quantified by the TWI), resulting in more downslope movement of soil water and smaller peak flows in the stream. To optimize discharge estimates, some TOPMODEL-based research has estimated the *conmult* and ***m*** parameters without always maintaining the numerical link indicated by the equations (for example Band and others, 1993; Pellenq and others, 2003); this type of parameterization is not feasible without site-specific optimization, so it is not done for the regional approach used by WATER. Brasington and Richards (1998) showed that the magnitude of ***m*** is related to the spatial resolution of the input data and that, when DEM rasters on the order of 20 m are used, a laboratory-determined K_{sat} and correspondingly small ***m*** value produced the most accurate results. Use of this HRU-specific spatial coefficient (*SpCf*) allows the regional modeling approach to proceed by informing the model with spatially detailed soils data. At the same time, this spatial coefficient makes use of an optimization that has shown that the relation between the soil and topography differs for the different HRUs.

TOPMODEL uses a numerical characterization of landscape position called the topographic wetness index (*TWI*) to simulate streamflow and hillslope hydrology:

$$TWI = \ln\left(\frac{A}{\tan\beta}\right), \quad (5)$$

where

A is upslope contributing area per unit contour width (meters) and

β is local slope (degrees) of individual cells (that is, in the 10-m DEM resolution).

In general, lower TWI values indicate drier positions on the landscape (such as drainage divides and steep slopes); higher TWI values indicate wetter landscape positions (such as riparian areas). However, because the *TWI* incorporates both local slope and upslope area, it is possible for the TWI value to either decrease or increase from one cell to another in a downslope direction. Therefore, instead of basing computations on the TWI value of individual cells in a basin, TOPMODEL classifies the cells into a histogram (WATER uses a 30-bin histogram), and each bin of cells from the histogram, a quantitative representation of landscape position, is dealt with as a group on the basis of the mean TWI value of that bin; this mean TWI value is adjusted for developed areas by using the topographic adjustment parameter to decrease the topographic gradient and account for localized water retention (table 2). All of the cells from each bin are treated the same way for all future calculations; the TWI value for each bin for an individual basin is a constant and is used to calculate the changes in the local saturation deficit (equation 2 and fig. 2) on the principle that cells with a similar TWI value will have a similar hydrologic response (Beven and Kirkby, 1979). It is the integration of this approach to topography with a spatially detailed description of soil properties that enables the regional hydrologic modeling approach used in WATER without requiring site-specific optimization.

Data Used for Validating Simulations

Although a primary intention of WATER is to provide the ability to estimate streamflow at ungaged locations, the model development, optimization, and statistical evaluation documented in this report would be impossible without long-term streamflow monitoring sites. Statistical evaluation of model performance is an important part of developing WATER for a large region like the DRB—this involves comparison of WATER simulations to observations from long-term streamflow gages and other types of hydroclimatic monitoring. This statistical evaluation, in turn, allows the user to have confidence in WATER simulations and incorporate these results into the decision-making process.

Historical Streamflow and Optimization-Validation Basins

Observed mean daily streamflow (National Water Information System [NWIS] parameter code 00060; http://waterdata.usgs.gov/nwis) was first used to optimize hydrologic parameters (table 2) and then used to statistically evaluate mean daily streamflow simulated by WATER and to validate model output after development was completed. USGS streamgage sites were selected on the basis of the availability of streamflow data for 3 to 10 years during the 2001–10 time period. An additional selection criterion was that gaged streams be unaffected by reservoir releases or flow regulation. WATER parameters (table 2), most of which are HRU-specific, were optimized by using observations from 21 streamgage sites in the DRB (table 3 and fig. 4), each of which consisted primarily of a single HRU (either forested [>75 percent], agricultural [>60 percent], or developed [>70 percent] land cover); one of these sites, USGS site 01466500,

was only used for estimating a monthly water budget for ET optimization because it is a swamp, so it does not meet the underlying requirements for using TOPMODEL. An additional 28 streamgage sites with a mix of land cover were then used for validation of optimized model parameters and refinement of how water-use data were incorporated (discussed in "Water-Use Data Provided in WATER Application Utilities"). Finally, nine streamgage sites were tested after all model development had been completed. This brings the total to 57 sites that were used to statistically evaluate hydrologic simulations. In the remainder of the report, the terms "site" and "basin" are used interchangeably because WATER samples basin properties and simulates streamflow generated within a basin that delineates the total area upstream of a site along a stream.

Table 3. Fifty-eight USGS streamgage sites in the Delaware River Basin used for model optimization and statistical evaluation of simulations of the Water Availability Tool for Environmental Resources (WATER). Those 21 basins with relatively homogeneous land cover, consisting primarily of a single hydrologic response unit (HRU), were used for optimization of select WATER parameters (table 2); mixed land-cover basins were used to statistically evaluate select WATER parameters and to optimize incorporation of water-use data; nine basins were set aside for final testing of model performance. Basins were only included if the streamgage period of record overlapped with the climatic and land-cover datasets used by WATER. Only complete water years (October through September of the following year) were included. Locations are shown in figure 4.

[Optimization and statistical evaluation use numbers, with percentages based on NLCD 2006: a, greater than (>) 60 percent agricultural; d, >70 percent developed; f, >75 percent forested; m, mixed land cover; t, test basin. USGS, U.S. Geological Survey; ID, identification number; mi^2, square miles; km^2, square kilometers; %, percent; NJ, New Jersey; NY, New York; PA, Pennsylvania; U.S. United States; DE, Delaware; PET, potential evapotranspiration; AET, actual evapotranspiration]

USGS site ID and name		Drainage area		Hydrologic response unit (%)			Optimization and validation use	Period of record (water years)		Complete years
		(mi^2)	(km^2)	Forested	Agricultural	Developed		Begin	End	
01411500	Maurice River at Norma NJ	111.3	288.3	48.5	23.6	27.9	m	1933	2010	9
01413500	East Branch Delaware River at Margaretville NY	163.2	422.9	87.6	8.2	4.2	f	1937	2010	9
01414500	Mill Brook near Dunraven NY	25.1	65.1	93.8	3.9	2.3	f	1937	2010	9
01415000	Tremper Kill near Andes NY	33.1	85.7	79.0	17.3	3.7	f	1937	2010	9
01420500	Beaver Kill at Cooks Falls NY	242.4	628.0	93.2	2.4	4.4	f	1914	2010	9
01421618	Town Brook southeast of Hobart NY	14.3	37.0	64.9	32.4	2.7	t	1999	2010	9
01421900	West Branch Delaware River upstream from Delhi NY	134.4	348.2	64.0	31.0	5	t	1937	2010	9
01422389	Coulter Brook near Bovina Center NY	0.8	2.0	99.5	0.0	0.5	f	1999	2010	7
01422500	Little Delaware River near Delhi NY	49.8	129.1	75.4	19.5	5.1	f	1938	2010	9
01422738	Wolf Creek at Mundale NY	0.6	1.6	69.2	26.5	4.3	m	2000	2010	7

Table 3. Fifty-eight USGS streamgage sites in the Delaware River Basin used for model optimization and statistical evaluation of simulations of the Water Availability Tool for Environmental Resources (WATER). Those 21 basins with relatively homogeneous land cover, consisting primarily of a single hydrologic response unit (HRU), were used for optimization of select WATER parameters (table 2); mixed land-cover basins were used to statistically evaluate select WATER parameters and to optimize incorporation of water-use data; nine basins were set aside for final testing of model performance. Basins were only included if the streamgage period of record overlapped with the climatic and land-cover datasets used by WATER. Only complete water years (October through September of the following year) were included. Locations are shown in figure 4.—Continued

[Optimization and statistical evaluation use numbers, with percentages based on NLCD 2006: a, greater than (>) 60 percent agricultural; d, >70 percent developed; f, >75 percent forested; m, mixed land cover; t, test basin. USGS, U.S. Geological Survey; ID, identification number; mi^2, square miles; km^2, square kilometers; %, percent; NJ, New Jersey; NY, New York; PA, Pennsylvania; U.S. United States; DE, Delaware; PET, potential evapotranspiration; AET, actual evapotranspiration]

USGS site ID and name		Drainage area		Hydrologic response unit (%)			Optimization and validation use	Period of record (water years)		Complete years
		(mi^2)	(km^2)	Forested	Agricultural	Developed		Begin	End	
01422747	East Brook east of Walton NY	24.7	63.9	63.9	31.3	4.8	m	2000	2010	9
01423000	West Branch Delaware River at Walton NY	331.9	859.9	67.2	27.1	5.7	m	1951	2010	9
01424108	Sherruck Brook Tributary near Trout Creek NY	1.3	3.3	97.7	0.0	2.3	m	1999	2007	6
01428750	West Branch Lackawaxen River near Aldenville PA	40.6	105.1	60.8	31.0	8.2	t	1987	2010	9
01435000	Neversink River near Claryville NY	66.7	172.7	98.9	0.2	0.9	f	1938	2010	9
01439500	Bush Kill at Shoemakers PA	117.2	303.7	89.7	0.0	10.3	f	1909	2010	9
01440000	Flat Brook near Flatbrookville NJ	65.1	168.5	89.3	6.2	4.5	f	1924	2011	9
01440400	Brodhead Creek near Analomink PA	67.5	174.8	90.2	1.0	8.8	f	1958	2010	9
01442500	Brodhead Creek at Minisink Hills PA	260.6	675.0	74.5	4.0	21.5	f	1951	2010	9
01443500	Paulins Kill at Blairstown NJ	126.1	326.7	59.4	23.9	16.7	m	1922	2011	9
01445000	Pequest River at Huntsville NJ	31.0	80.2	66.0	17.2	16.8	m	1940	2011	8
01445500	Pequest River at Pequest NJ	106.1	274.9	60.5	26.1	13.4	m	1922	2011	9
01446000	Beaver Brook near Belvidere NJ	36.6	94.9	52.8	37.0	10.2	m	1923	2011	7
01447500	Lehigh River at Stoddartsville PA	91.8	237.7	88.2	0.3	11.5	t	1944	2010	9

Table 3. Fifty-eight USGS streamgage sites in the Delaware River Basin used for model optimization and statistical evaluation of simulations of the Water Availability Tool for Environmental Resources (WATER). Those 21 basins with relatively homogeneous land cover, consisting primarily of a single hydrologic response unit (HRU), were used for optimization of select WATER parameters (table 2); mixed land-cover basins were used to statistically evaluate select WATER parameters and to optimize incorporation of water-use data; nine basins were set aside for final testing of model performance. Basins were only included if the streamgage period of record overlapped with the climatic and land-cover datasets used by WATER. Only complete water years (October through September of the following year) were included. Locations are shown in figure 4.—Continued

[Optimization and statistical evaluation use numbers, with percentages based on NLCD 2006: a, greater than (>) 60 percent agricultural; d, >70 percent developed; f, >75 percent forested; m, mixed land cover; t, test basin. USGS, U.S. Geological Survey; ID, identification number; mi^2, square miles; km^2, square kilometers; %, percent; NJ, New Jersey; NY, New York; PA, Pennsylvania; U.S. United States; DE, Delaware; PET, potential evapotranspiration; AET, actual evapotranspiration]

USGS site ID and name		Drainage area		Hydrologic response unit (%)			Optimization and validation use	Period of record (water years)		Complete years
		(mi^2)	(km^2)	Forested	Agricultural	Developed		Begin	End	
01449360	Pohopoco Creek at Kresgeville PA	49.8	129.0	56.4	19.9	23.7	t	1967	2010	9
01450500	Aquashicola Creek at Palmerton PA	76.6	198.4	69.6	19.8	10.6	m	1940	2010	9
01451500	Little Lehigh Creek near Allentown PA	81.9	212.2	24.9	38.7	36.4	m	1946	2010	9
01451800	Jordan Creek near Schnecksville PA	53.0	137.3	29.7	59.4	10.9	m	1967	2010	9
01452000	Jordan Creek at Allentown PA	76.2	197.5	29.7	53.1	17.2	m	1945	2010	9
01452500	Monocacy Creek at Bethlehem PA	43.3	112.1	9.0	54.9	36.1	m	1949	2010	9
01464500	Crosswicks Creek at Extonville NJ	80.7	209.2	48.8	26.2	25	t	1938	2010	9
01464907	Little Neshaminy Creek at Valley Road near Neshaminy PA	27.0	70.1	21.3	12.0	66.7	t	2000	2010	9
01465798	Poquessing Creek at Grant Avenue at Philadelphia PA	21.4	55.4	13.4	4.9	81.7	d	1966	2010	9
01466500[1]	McDonalds Branch in Byrne State Forest NJ	2.3	6.1	92.6	0.0	7.4	f	1954	2010	9
01467048	Pennypack Creek at Lower Rhawn Street Bridge, Philadelphia PA	49.8	129.1	20.1	1.9	78	d	1966	2010	9

Table 3. Fifty-eight USGS streamgage sites in the Delaware River Basin used for model optimization and statistical evaluation of simulations of the Water Availability Tool for Environmental Resources (WATER). Those 21 basins with relatively homogeneous land cover, consisting primarily of a single hydrologic response unit (HRU), were used for optimization of select WATER parameters (table 2); mixed land-cover basins were used to statistically evaluate select WATER parameters and to optimize incorporation of water-use data; nine basins were set aside for final testing of model performance. Basins were only included if the streamgage period of record overlapped with the climatic and land-cover datasets used by WATER. Only complete water years (October through September of the following year) were included. Locations are shown in figure 4.—Continued

[Optimization and statistical evaluation use numbers, with percentages based on NLCD 2006: a, greater than (>) 60 percent agricultural; d, >70 percent developed; f, >75 percent forested; m, mixed land cover; t, test basin. USGS, U.S. Geological Survey; ID, identification number; mi^2, square miles; km^2, square kilometers; %, percent; NJ, New Jersey; NY, New York; PA, Pennsylvania; U.S. United States; DE, Delaware; PET, potential evapotranspiration; AET, actual evapotranspiration]

USGS site ID and name		Drainage area		Hydrologic response unit (%)			Optimization and validation use	Period of record (water years)		Complete years
		(mi^2)	(km^2)	Forested	Agricultural	Developed		Begin	End	
01467086	Tacony Creek at County Line, Philadelphia PA	16.2	42.0	13.2	0.3	86.5	d	1966	2010	5
01467150	Cooper River at Haddonfield NJ	17.1	44.3	25.9	0.8	73.3	d	1964	2010	9
01468500	Schuylkill River at Landingville PA	137.1	355.3	74.8	4.0	21.2	m	1948	2010	9
01470500	Schuylkill River at Berne PA	358.3	928.2	71.1	12.5	16.4	m	1948	2008	9
01470779	Tulpehocken Creek near Bernville PA	70.4	182.5	11.0	71.9	17.1	a	1976	2008	9
01471980	Manatawny Creek near Pottstown PA	85.5	221.5	43.6	36.5	19.9	m	1975	2004	3
01472157	French Creek near Phoenixville PA	59.0	153.0	51.3	29.7	19	m	1969	2008	9
01472198	Perkiomen Creek at East Greenville PA	37.7	97.5	42.6	31.3	26.1	m	1982	2008	9
01472199	West Branch Perkiomen Creek at Hillegass PA	23.1	59.8	44.9	32.8	22.3	m	1982	2008	9
01475530	Cobbs Creek at U.S. Highway 1 at Philadelphia PA	4.8	12.4	11.9	0.1	88	d	1965	2008	6
01475850	Crum Creek near Newtown Square PA	15.8	41.0	39.3	24.3	36.4	m	1982	2008	9
01477120	Raccoon Creek near Swedesboro NJ	26.0	67.3	29.6	49.0	21.4	m	1967	2010	9
01477800	Shellpot Creek at Wilmington DE	7.3	19.0	18.9	0.1	81	d	1945	2010	9

Table 3. Fifty-eight USGS streamgage sites in the Delaware River Basin used for model optimization and statistical evaluation of simulations of the Water Availability Tool for Environmental Resources (WATER). Those 21 basins with relatively homogeneous land cover, consisting primarily of a single hydrologic response unit (HRU), were used for optimization of select WATER parameters (table 2); mixed land-cover basins were used to statistically evaluate select WATER parameters and to optimize incorporation of water-use data; nine basins were set aside for final testing of model performance. Basins were only included if the streamgage period of record overlapped with the climatic and land-cover datasets used by WATER. Only complete water years (October through September of the following year) were included. Locations are shown in figure 4.—Continued

[Optimization and statistical evaluation use numbers, with percentages based on NLCD 2006: a, greater than (>) 60 percent agricultural; d, >70 percent developed; f, >75 percent forested; m, mixed land cover; t, test basin. USGS, U.S. Geological Survey; ID, identification number; mi^2, square miles; km^2, square kilometers; %, percent; NJ, New Jersey; NY, New York; PA, Pennsylvania; U.S. United States; DE, Delaware; PET, potential evapotranspiration; AET, actual evapotranspiration]

USGS site ID and name		Drainage area		Hydrologic response unit (%)			Optimization and validation use	Period of record (water years)		Complete years
		(mi^2)	(km^2)	Forested	Agricultural	Developed		Begin	End	
01478000	Christina River at Coochs Bridge DE	20.9	54.0	27.3	25.0	47.7	t	1943	2010	9
01479000	White Clay Creek near Newark DE	89.1	230.8	29.4	32.7	37.9	m	1932	2010	9
01480000	Red Clay Creek at Wooddale DE	47.3	122.6	33.6	33.3	33.1	m	1943	2010	9
01480300	West Branch Brandywine Creek near Honey Brook PA	18.5	47.8	23.9	59.9	16.2	m	1961	2008	9
01480675	Marsh Creek near Glenmoore PA	8.5	22.1	44.9	37.3	17.8	m	1967	2008	9
01482500	Salem River at Woodstown NJ	14.6	37.8	18.2	70.1	11.7	a	1940	2010	8
01484000	Murderkill River near Felton DE	12.5	32.5	34.7	57.5	7.8	m	1932	2009	1
01484050	Pratt Branch near Felton DE	3.1	8.1	12.6	64.4	23	a	1905	2009	1
01484100	Beaverdam Branch at Houston DE	3.5	9.1	37.4	58.3	4.3	t	1958	2010	9
01484270	Beaverdam Creek near Milton DE	6.9	17.9	34.7	54.4	10.9	m	1966	2005	3

[1]This basin was used only for statistical evaluation of PET and AET because of its proximity to three Ameriflux sites (Clark and others, 2012).

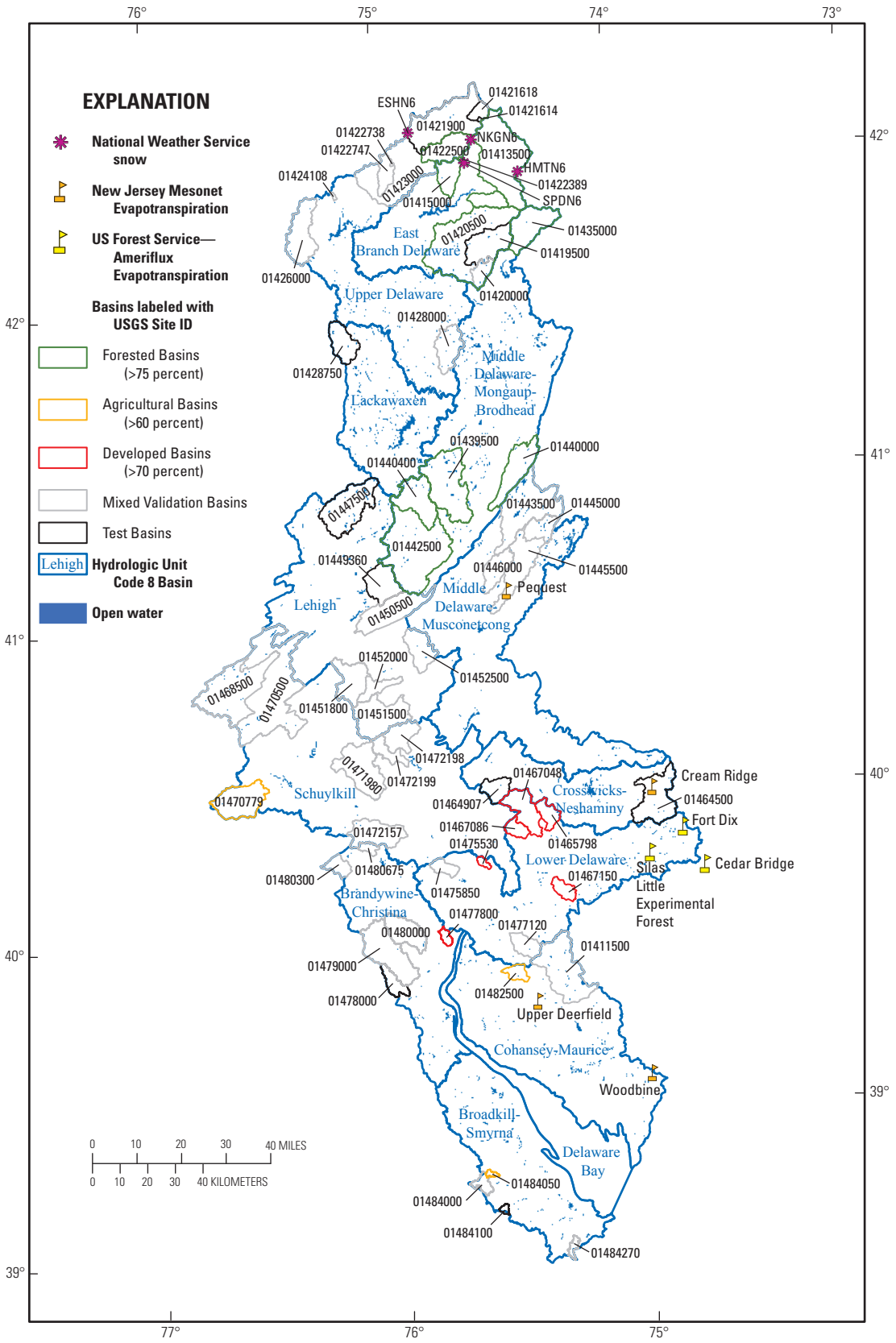

Figure 4. U.S. Geological Survey (USGS) streamgages and other monitoring sites used for model optimization and statistical evaluation of the Water Availability Tool for Environmental Resources (WATER) streamflow simulation and hydroclimatic variables for the Delaware River Basin. Details for each site are in tables 3 and 4. Basin color coincides with the optimization and statistical-evaluation use indicted in table 3. ID, identification number; %, percent.

Hydroclimatic Variables

To optimize the simulation of snow accumulation and snowmelt as well as both potential evapotranspiration (PET) and actual evapotranspiration (AET), simulated values were compared to observed values for basins with relatively homogeneous forest cover. For each of these hydroclimatic components of the water budget, the observed values were mostly point data, most of which were near (less than [<] 10 kilometers [km] away), but not within, the basins that had coincident streamflow observations (table 4 and fig. 4). Additionally, observations of snowpack thickness were available for only four sites in the DRB and were recorded monthly and (or) weekly during winter. In contrast, the daily WATER-simulations of snow accumulation and melting and PET are based on a maximum daily temperature that is an areal average for the entire basin. Consequently, no statistical analysis of these data is presented, and validation of these data is limited to a visual analysis.

Data That Enable Scenario Testing

Those process-based hydrologic models (TOPMODEL and TR–55) incorporated within WATER simulate how precipitation is transferred to streamflow. However, in much of the basin, water-resource management alters this relation. Incorporation of water-use data improves the ability of WATER to simulate streamflow in areas where streamflow withdrawals and returns significantly affect mean daily streamflow. The regional, process-based approach encapsulated by WATER also provides a DSS that can simulate streamflow under a range of forecasted climatic and land-use scenarios; it is estimated that maximum daily temperature will increase approximately 5.5 degrees Celsius (°C) and that precipitation will increase by 10 percent by 2100 (Frumhoff and others, 2007).

Water-Use Data Provided in WATER Application Utilities

Water-use data were acquired from the USGS National Water Census effort in the DRB (Hutson and others, in press). Data included in the model are seasonal totals for surface-water and groundwater use. Data are from 2010 except for New Jersey and Pennsylvania, for which multiyear data were available and the median values were used. Seasons are defined as January–March, April–June, July–September, and October–December; these breakdowns enable comparison to both calendar and water years (October to September). Water-use data are provided as million gallons per day for 12 categories (table 5) that can be differentiated as

- 12 groundwater and 12 surface water sources, or
- 17 withdrawal, 5 return, and 2 transfer types, or
- 19 point-specific and 5 areally-averaged classes.

Surface-water-use and groundwater-use data are in separate datasets for each category; withdrawals and return flows are also provided separately. However, the DSS applies a single, daily water-use total. Point data are included for over 6,000 sites (fig. 5) but do not include water use from Maryland (21 km^2 of the 35,075 km^2 DRB total). Areally averaged categories include irrigation, livestock, and domestic self-supply; for these categories, county-wide estimates were integrated with land-use and population data to provide a better spatial understanding of where this water use interacts with the hydrologic system. The reader is referred to Hutson and others (in press) for a detailed explanation of these water-use categories and their distribution in the basin.

Table 4. Sources of point observations used to optimize hydroclimatic components of water budget in the Delaware River Basin. Locations are shown in figure 4.

Hydroclimatic variable	Source	Site	Period of record
Evapotranspiration	Ameriflux (Clark and others, 2012)	Cedar Bridge, Fort Dix, and Silas Little, New Jersey	2006–8
Evapotranspiration	Office of the New Jersey State Climatologist at Rutgers University (Mathieu Gerbush, written commun., April 25, 2013)	Cream Ridge, Pequest, Upper Deerfield, and Woodbine, N.J.	2009–11
Snow accumulation and snowmelt	National Weather Service (2012)	ESHN6, HMTN6, NKGN6, SPDN6	2003–11

To protect the privileged information associated with these water-use data, point data were originally aggregated to 12-digit hydrologic unit code (HUC–12) basins for use in WATER. However, during optimization of WATER using the 28 mixed land-cover basins, it became apparent that data were distributed too generally for accurate streamflow simulation, so data were reaggregated to the 3,736 DEM-derived polygons; this is the spatial unit with which these water-use data are provided in the WATER database.

Water-use data are applied with the WATER Application Utilities that are provided with WATER. These utilities allow the user to increase, decrease, or remove individual water-use categories by using a factor approach. The water-use factor ranges from zero (no water use) and, for example, if the factor is set to 1, the data provided by the USGS National Water Census (Hutson and others, in press) are used without adjustment. A sum of seasonal water use is applied on a daily time step after the natural streamflow has been simulated for the entire period so that the user can compare the natural and water-use-affected records (two separate variables in WATER.txt output); no distinction is made between groundwater and surface-water sources. However, when considering water-use effects, users should remember that a seasonal median of the daily volume of water use is being used and that no daily or annual variability of water use is available.

Land-Cover Projection and Urbanization Forecasts Used to Replace the National Land Cover Database 2011 for Future Time Periods

To provide a land-cover snapshot that is contemporaneous with the 25-year climate records provided with WATER (centered on 2030 and 2060), two forecasted land-cover datasets are provided with WATER in addition to the 2011 NLCD (fig. 6). These forecasts were developed by using a stochastic (a random probability distribution) simulation model to forecast urbanization in large watersheds. The model was originally developed by the USGS for the Chesapeake Bay watershed and hence is called the Chesapeake Bay Land Change Model (CBLCM; table 6; Claggett and others [2014]). The CBLCM was parameterized and applied to the DRB to forecast urbanization from 2010 to 2060 in decadal increments. The CBLCM stochastically simulates the spatial location and extent of residential and commercial development; for the DRB, this simulation was run over 101 iterations for each time interval. The model is driven by exogenous projections of population produced by using the U.S. Environmental Protection Agency's Integrated Climate and Land Use Scenarios (ICLUS) model (ICLUS; U.S. Environmental Protection Agency, 2009). Historical population and employment data were analyzed for the period 1990–2010 to develop county-level trends in the ratio of population to employment. These trends were extrapolated to 2060 and multiplied by the population projections to estimate future employment.

Table 5. Water-use categories.

Water-use category	Type of water use		
	Surface water or groundwater	Withdrawal or return	Point data or areal average
Aquaculture	Both	Withdrawal	Point
Commercial	Both	Withdrawal	Point
Domestic self-supply	Groundwater	Withdrawal	Areally averaged
Industrial	Both	Both	Point
Irrigation	Both	Both	Both
Livestock	Groundwater	Withdrawal	Both
Mining	Both	Withdrawal	Point
Remediation	Groundwater	Withdrawal	Point
Thermoelectric	Both	Withdrawal	Point
Public water supply	Both	Both	Point
Sewage treatment	Surface water	Return	Point
Interbasin transfer	Surface water	Both	Point

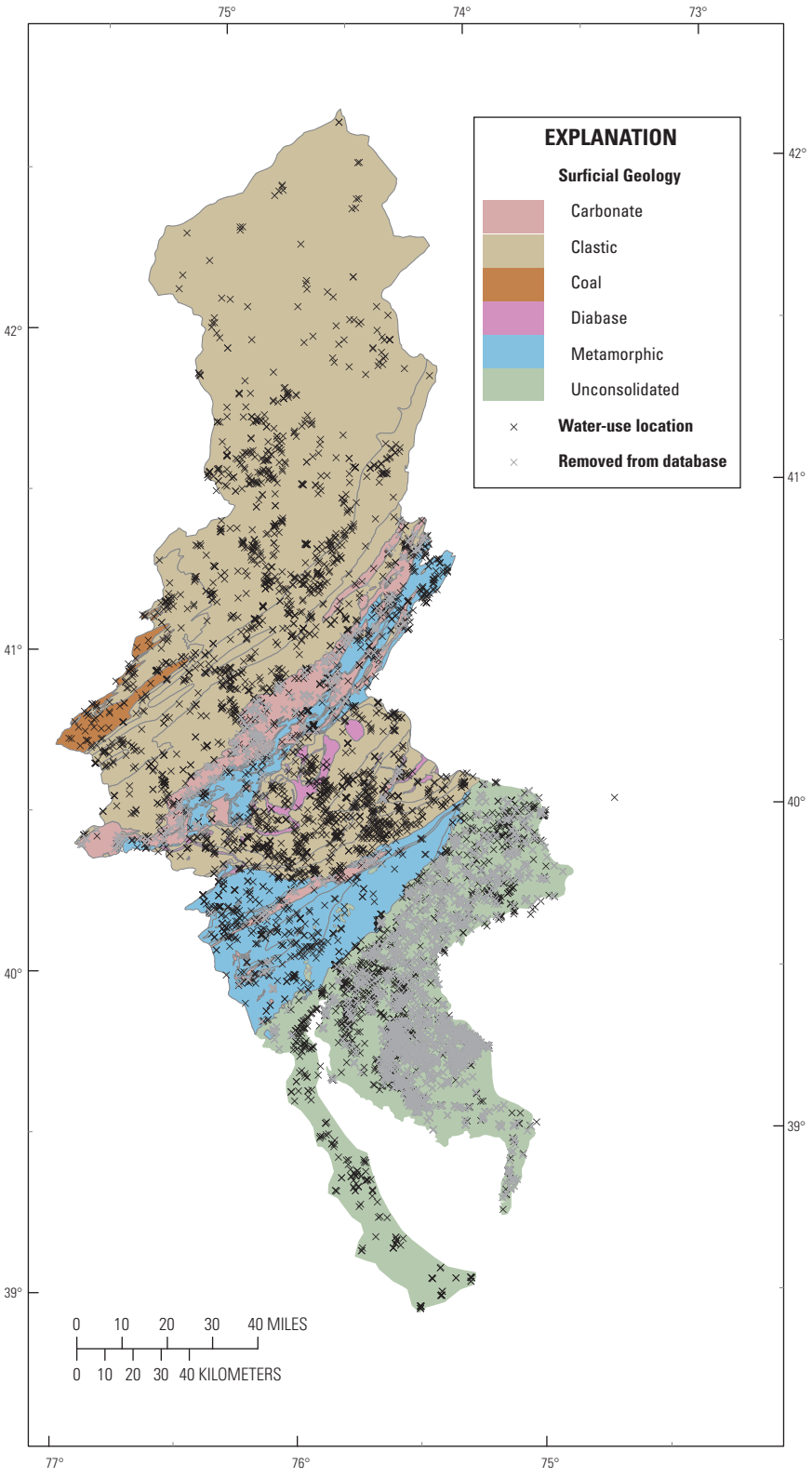

Figure 5. Water-use locations in the Delaware River Basin (DRB). Median, seasonal values of water use were provided as part of the DRB water-use effort (Hutson and others, in press) and are incorporated in the WATER Application Utilities. Surficial geology was used to isolate regions where streamflow simulation was less accurate after water use was incorporated. Consequently, groundwater withdrawals and returns were removed from the unconsolidated Coastal Plain as well as the carbonate region in the central part of the basin.

To spatially simulate development, a probability surface raster was created by relating observed changes in developed land cover (as captured by NLCD 2001 and 2011) with proximity to urban areas, proximity to recent growth in housing, and topographic slope (using NED; Gesch and others, 2002). The probability surface informed the likelihood of future growth at a given location. The sizes of simulated patches of residential and commercial development were informed by the cumulative frequency distribution of historical patches of developed land cover. The shapes of simulated patches were based on proximity to roads. In the model, growth occurs preferentially near roads, resulting in elongated patch shapes along roads and circular shapes far from roads. For each future decade, from 2020–60, the CBLCM was applied in a Monte Carlo simulation routine to produce 101 iterations of residential and commercial development mosaicked with the 2011 NLCD.

For each iteration, attribute data associated with individual patches of development were summarized over all iterations and all decades by HUC–12 (USGS and others, 2009). Data reported by HUC–12 included statistics on the mean, median, maximum, and minimum acres of commercial and residential development, forest and farmland acres converted to development, total employment, total population, total households, and median residential lot size. For all HUC–12s, the raster iterations representing the median amount of total development (commercial plus residential) were extracted and mosaicked together to spatially represent the median amount of future development in 2030 and 2060 throughout the DRB (fig. 6). The forecasted areas of commercial and residential growth in all 505 iteration rasters (five decadal snapshots for each of 101 iterations), in addition to the composite 2030 and 2060 median-condition rasters, were then translated into development intensities and impervious-surface values consistent with the 2011 NLCD and informed by the underlying housing densities.

Table 6. Data Sources for the Chesapeake Bay Land Change Model.

[The Chesapeake Bay Land Change Model (CBLCM) (Claggett and others, 2014). EPA, U.S. Environmental Protection Agency; USGS, U.S. Geological Survey; USDA, U.S. Department of Agriculture; NRCS, Natural Resources Conservation Service; GAP, Gap Analysis Program; NJDEP, New Jersey Department of Environmental Protection; Delaware OMB, Delaware Office of Management and Budget]

Data source	Contribution to CBLCM
2000 and 2010 U.S. Decennial Census of Population and Housing (U.S. Census Bureau, 2012)	Decadal housing and population values
2010 NAVTEQ Streets (Homeland Security Infrastructure Program, 2012), supplied through license agreement with the U.S. Environmental Protection Agency.	Production of asymmetric housing maps and refinement of urban land cover
Longitudinal Employer-Household Dynamics database (U.S. Census Bureau, 2013)	Estimates of total employment by census block
Integrated Climate and Land Use Scenarios v1.3.2 Population Forecasts (2005–2100) (US EPA, 2009)	Population projections
2010 Census TIGER/Line files (U.S. Census Bureau, 2011)	Census county and block boundaries,
National Watershed Boundary Database (USGS and others, 2009)	Summary units for reporting data; Delaware River Basin boundary
2001 and 2011 National Land Cover Database (Jin and others, 2013)	Patterns of growth and urban patch size distributions
National Elevation Dataset (Gesch and others, 2002)	Derive slope (percent) as a constraint on areas suitable for development
Protected Areas Database, v1.3 (USGS GAP, 2012)	Constrains areas suitable for development
2007 New Jersey land-use dataset (NJDEP, 2007)	Refines areas suitable for growth; refines estimates of housing and employment densities
2007 Delaware land-use dataset (Delaware OMB, 2007)	Refines areas suitable for growth; refines estimates of housing and employment densities

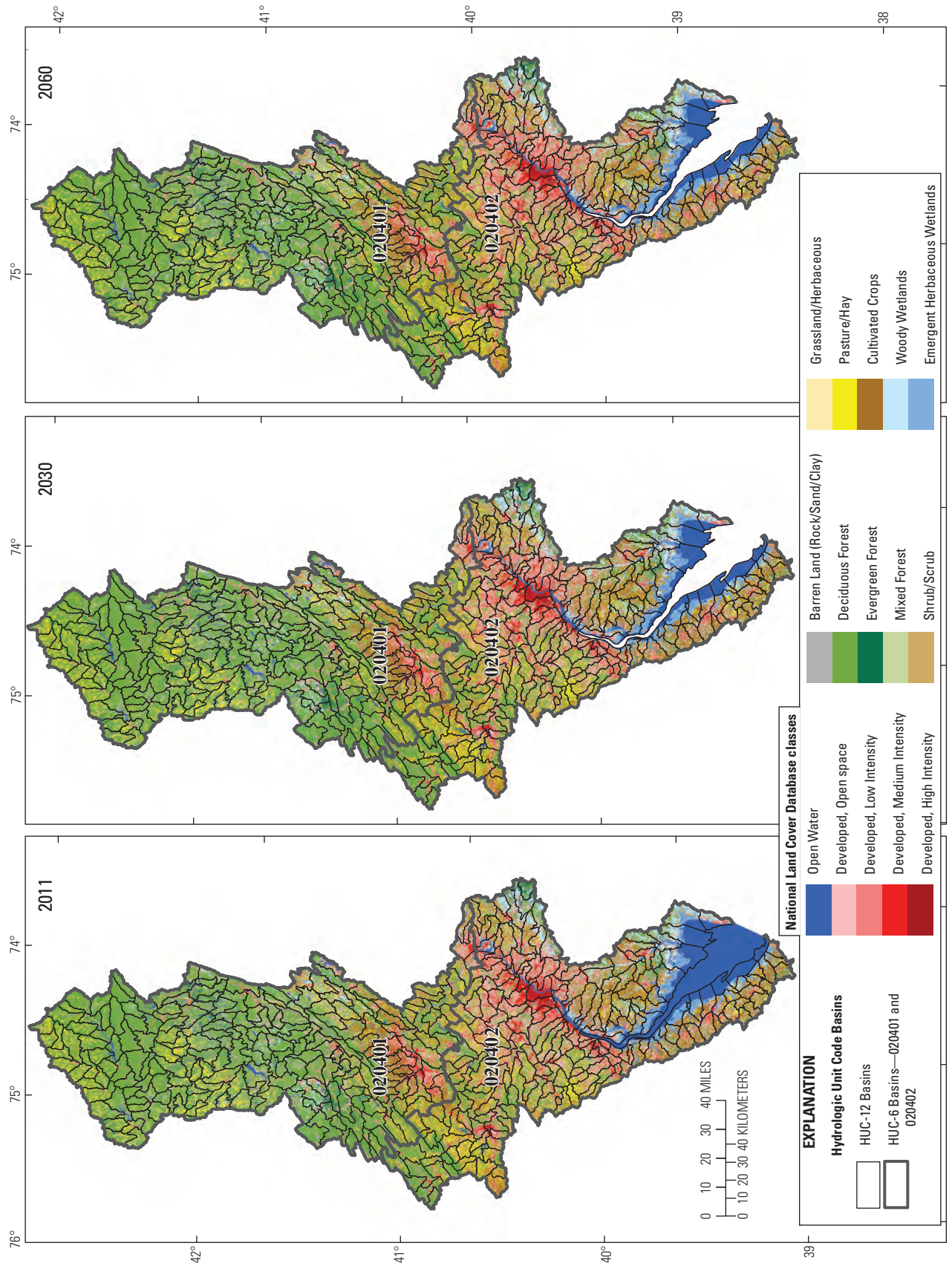

Figure 6. Land-cover data for the Delaware River Basin provided with the Water Availability Tool for Environmental Resources. *A*, Land-cover rasters for 2011 (National Land Cover Database; Fry and others, 2011), 2030, and 2060. The latter two are aggregations of Hydrologic Unit Code 12 (HUC–12) basins from the median of 101 Chesapeake Bay Land Change Model iterations. *B*, Forecasted development in each of 426 HUC–12 basins according to the median iterations of 101 simulations for 2030 and 2060.

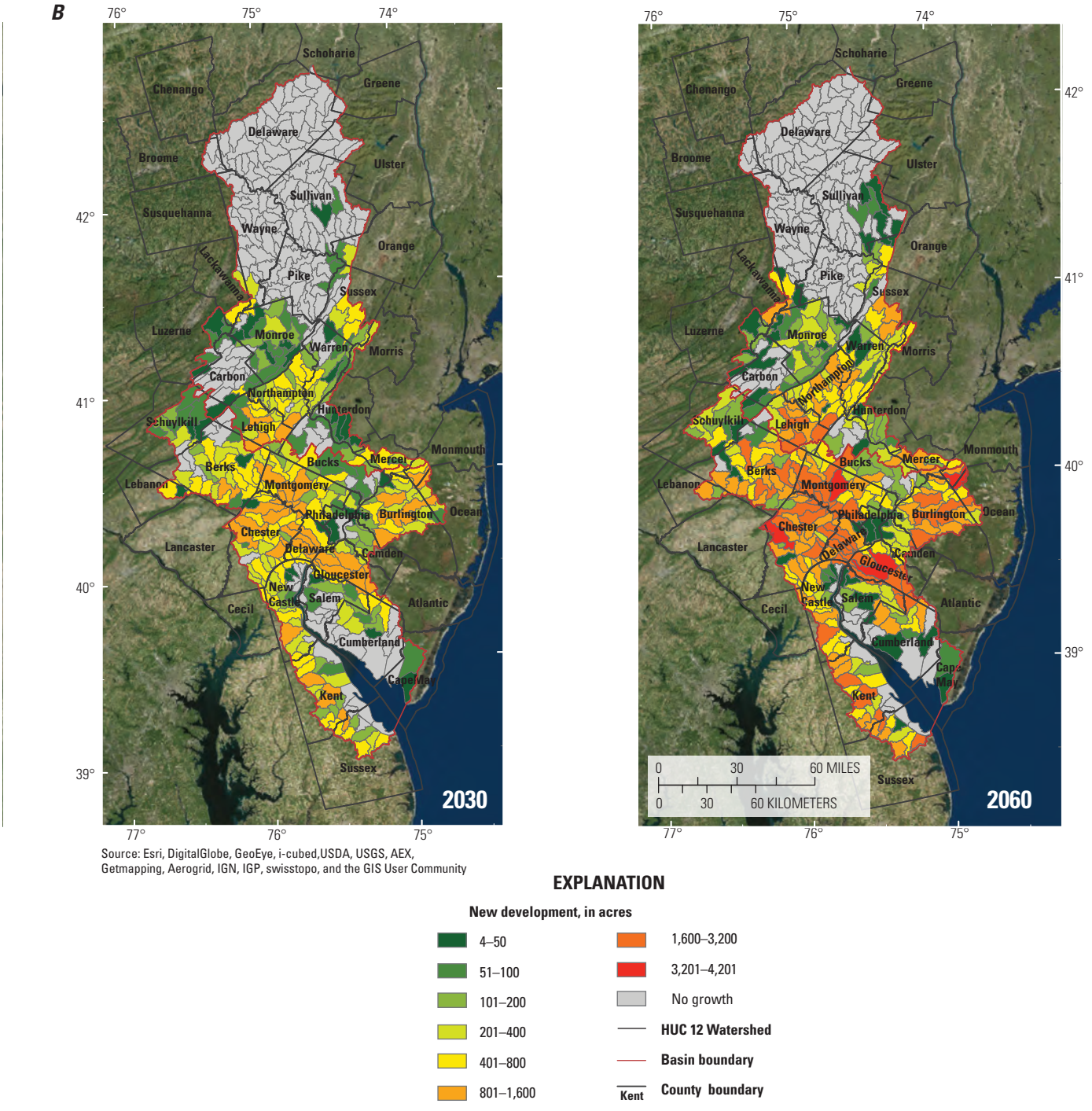

Figure 6. Land-cover data for the Delaware River Basin provided with the Water Availability Tool for Environmental Resources. *A*, Land-cover rasters for 2011 (National Land Cover Database; Fry and others, 2011), 2030, and 2060. The latter two are aggregations of Hydrologic Unit Code 12 (HUC–12) basins from the median of 101 Chesapeake Bay Land Change Model iterations. *B*, Forecasted development in each of 426 HUC–12 basins according to the median iterations of 101 simulations for 2030 and 2060.—Continued

General Circulation Models and Projections of Future Climate

A selection of general circulation models (GCMs) is provided with the WATER Application Utilities that characterize a range of how forecasted changes in precipitation, temperature, and available energy (surface net radiation minus ground heat flux) may alter streamflow and water availability in the DRB. These changes can be assessed in terms of the following:

- snow accumulation and timing of snowmelt;
- evapotranspiration (both potential and actual), frost-free days, and growing-season days in the year; and
- aggregated effects on seasonal streamflow variability.

GCM data are provided for two target time periods; these data forecast 25-year monthly normals (means) centered on 2030 and 2060. Change factors were derived for each of four Coupled Model Intercomparison Project Phase 5 (CMIP5; Taylor and others, 2011) GCM datasets (fig. 7 and table 7; Taylor and others, 2011) and two representative concentration pathways (RCPs) that forecast different amounts of change in the chemical composition of the atmosphere (representative concentration pathways 4.5 and 8.5; table 8). Change factors for the four GCMs and two RCP scenarios provide for consideration of how differences among individual climate models affect forecasts of streamflow; some researchers have found that these differences create an uncertainty that is larger than that associated with hydrologic modeling (for example Teng and others, 2011); consequently, this suite of GCMs provides a means of incorporating this range of forecasted conditions. All of these GCMs should be included in scenario testing and the overall trend among all models considered when results are interpreted.

These CMIP5 data are at a spatial resolution ranging from approximately 105-km to 310-km tile spacings; Daymet data were geospatially sampled by using the 3,736 DEM-derived polygons, which averaged 9.4 km^2 in size. To keep the spatial resolution provided by the initial Daymet historical climate record, monthly change factors, or deltas (δ), between the current and target time period were calculated for precipitation and temperature and are applied to the original climate record by the WATER Application Utilities (figs. 7*B* and 8).

A 25-year period was selected for the historical dataset provided with each CMIP5 model (1981–2005) and for the 2030 (2018–42), and the 2060 (2048–72) targets. Monthly-normal δ were calculated for precipitation (a multiplicative factor) and daily maximum temperature (an additive factor) by using the 25-year periods to estimate a monthly-normal δ between the historical and target time periods provided with each model and scenario combination; WATER then simulates snowpack on a daily time step by using the adjusted Daymet daily values of precipitation and temperature (fig. 8).

Previous researchers (for example Milly and Dunne, 2010) have noted a likely overestimation of PET when calculated by using a temperature-indexed approach and daily temperatures indicated by future climate projections. This concern is relevant to a Hamon (1963)-derived estimation of PET, such as that incorporated in WATER, because the equation used to estimate PET is based on a historical, empirical relation between temperature and energy availability that cannot be assumed to hold under anthropogenic climate change. For this reason, the forecasted PET in WATER can be calculated from a multiplicative δ factor based on a radiation-based PET (in energy units; Priestley and Taylor, 1972):

$$PET = \propto \frac{\Delta}{\Delta + \gamma}\left(R_n - G\right), \quad (6)$$

where

- α is 1.26 and is calibration constant (Priestley and Taylor, 1972);
- Δ is slope of the saturation vapor pressure temperature curve—a function of temperature;
- γ is psychrometric constant and is related to air pressure;
- R_n is net radiation; and
- G is heat flux density to the ground.

To implement this approach, a monthly-normalized δ was calculated for the available energy term (Rn–G) by using the ratio of the historical sum to the forecasted sum of the sensible heat flux and latent heat flux. This ratio was used as the change factor and was applied to the PET values calculated from the Daymet temperature record by using Hamon (1963):

$$PET_{FC} = PET_{Hh} * \partial_{PETptFC}, \quad (7)$$

where

- PET_{FC} is the daily PET value for forecasted conditions;
- PET_{Hh} is daily PET calculated using the Hamon (1963) method and the Daymet maximum daily temperature for the 1985–2005 time period; and
- $\delta_{PETpfFC}$ is the monthly, 25-year normalized δ for Priestley-Taylor-derived PET for the forecasted condition relative to the historical condition for that GCM.

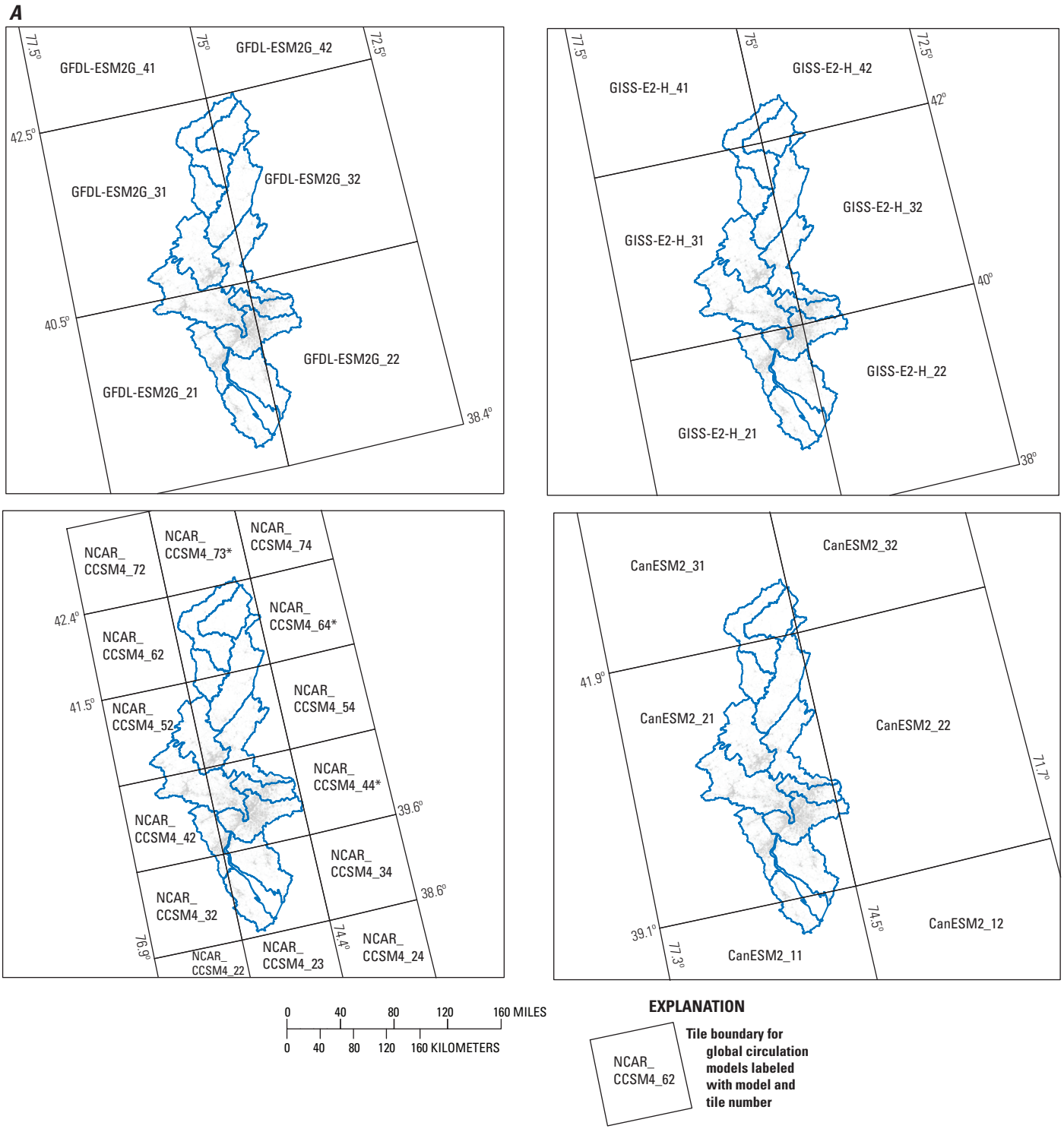

Figure 7. Summary of general circulation models (GCMs). *A*, Four GCM tile extents provided with the Water Availability Tool for Environmental Resources (WATER). All were accessed through the Coupled Model Intercomparison Project Phase 5 data portal (http://cmip-pcmdi.llnl.gov/cmip5/data_portal.html). Tile size differs among these GCMs (table 7). Those tiles in the NCAR_CCSM4 model marked with asterisks have been replaced, because of the small areas they cover, with data from the adjacent tile (63 or 43). *B*, Forecasted change factors (δs) for two time periods (2030 and 2060) and two scenarios (representative concentration pathways [RCP] 4.5 and 8.5) for four GCMs. Note that precipitation and potential evapotranspiration (PET) δs are both multiplicative and are shown with the same scale; a value of one indicates no change. Precipitation and PET are shown as a function of the forecasted change in the maximum daily temperature; this δ is additive and a value of zero indicates no change.

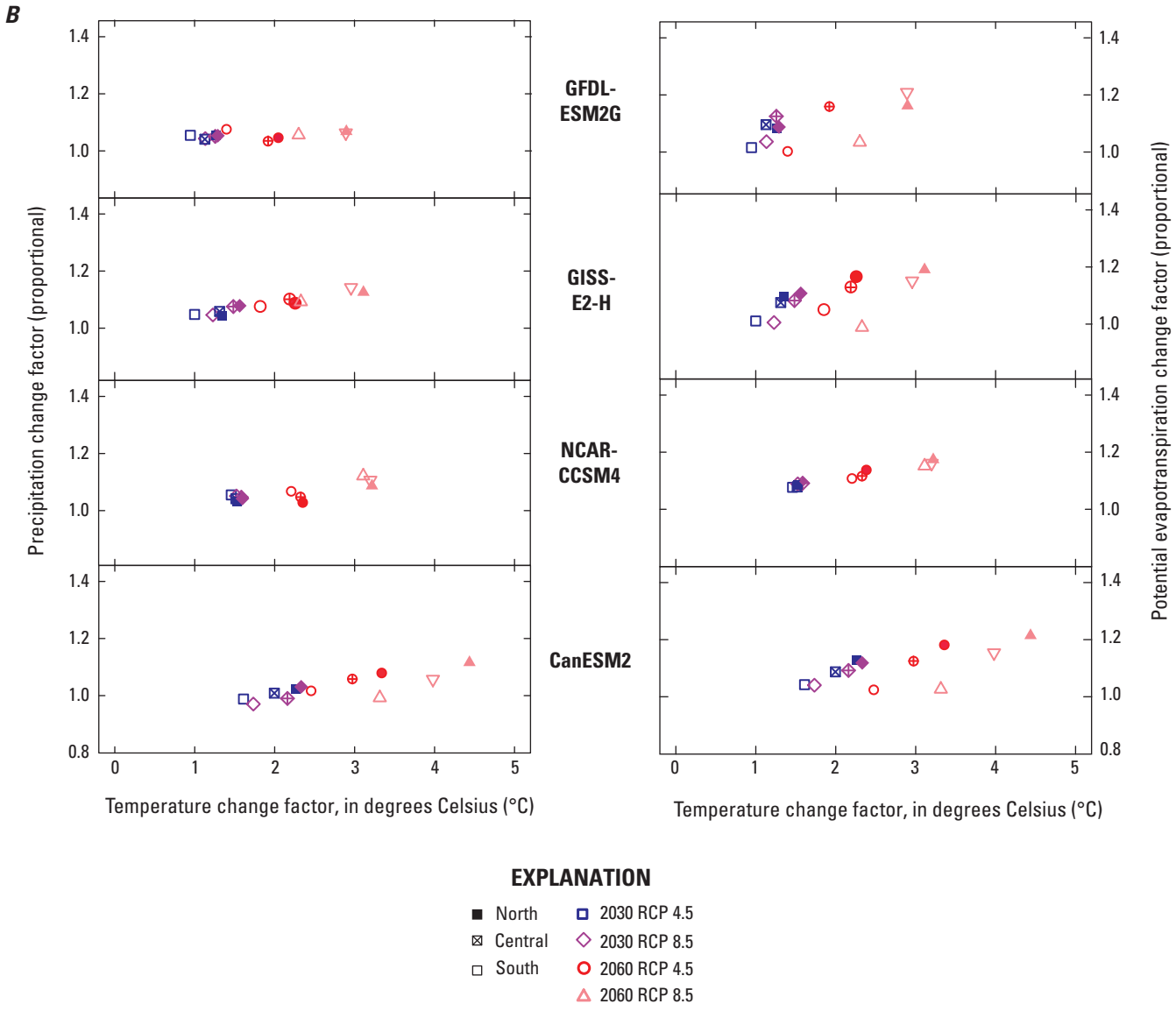

Figure 7. Summary of general circulation models (GCMs). *A*, Four GCM tile extents provided with the Water Availability Tool for Environmental Resources (WATER). All were accessed through the Coupled Model Intercomparison Project Phase 5 data portal (http://cmip-pcmdi.llnl.gov/cmip5/data_portal.html). Tile size differs among these GCMs (table 7). Those tiles in the NCAR_CCSM4 model marked with asterisks have been replaced, because of the small areas they cover, with data from the adjacent tile (63 or 43). *B*, Forecasted change factors (δs) for two time periods (2030 and 2060) and two scenarios (representative concentration pathways [RCP] 4.5 and 8.5) for four GCMs. Note that precipitation and potential evapotranspiration (PET) δs are both multiplicative and are shown with the same scale; a value of one indicates no change. Precipitation and PET are shown as a function of the forecasted change in the maximum daily temperature; this δ is additive and a value of zero indicates no change.—Continued

Table 7. General circulation models provided as part of the WATER database. The differences among models are detailed by Forster and others (2013).

Source	Abbreviation	General circulation model	Tile size (kilometers)	Documentation
National Oceanic and Atmospheric Administration—Geophysical Fluid Dynamics Laboratory	GFDL_NOAA	ESM2G	200	Dunne and others (2012)
National Aeronautics and Space Administration—Goddard Institute for Space Studies	GISS	E2-H	220	Nazarenko and others (2015)
National Center for Atmospheric Research—Community Climate System Model	NCAR_CCSM4	CCSM4	105	Gent and others (2011)
Canadian Centre for Climate Modelling and Analysis	CanESM2	CGCM4	310	von Salzen and others (2013)

Table 8. Representative concentration pathways (RCP; summarized from van Vuuren and others, 2011)—data are provided for RCPs 4.5 and 8.5 (bolded). For comparison, the January 2015 global mean CO_2 concentration was 400.14 parts per million (ppm), up from 397.42 ppm in January 2014 (Earth System Research Laboratory, 2015; verified March 25, 2015).

[RCP, representative concentration pathway; W/m^2, watts per square meter; ppm, parts per million]

Representative concentration pathway	Radiative forcing	Approximate carbon dioxide concentration
RCP 8.5	**Rising radiative forcing to 8.5 W/m^2 by 2100**	**1,370 ppm CO_2**
RCP 6	Stabilization at 6 W/m^2 after 2100	850 ppm CO_2
RCP 4.5	**Stabilization at 4.5 W/m^2 at 2100**	**650 ppm CO_2**
RCP 2.6	Peak at about 3 W/m^2 before 2100 and then decline to 2.6 W/m^2 by 2100	490 ppm CO_2

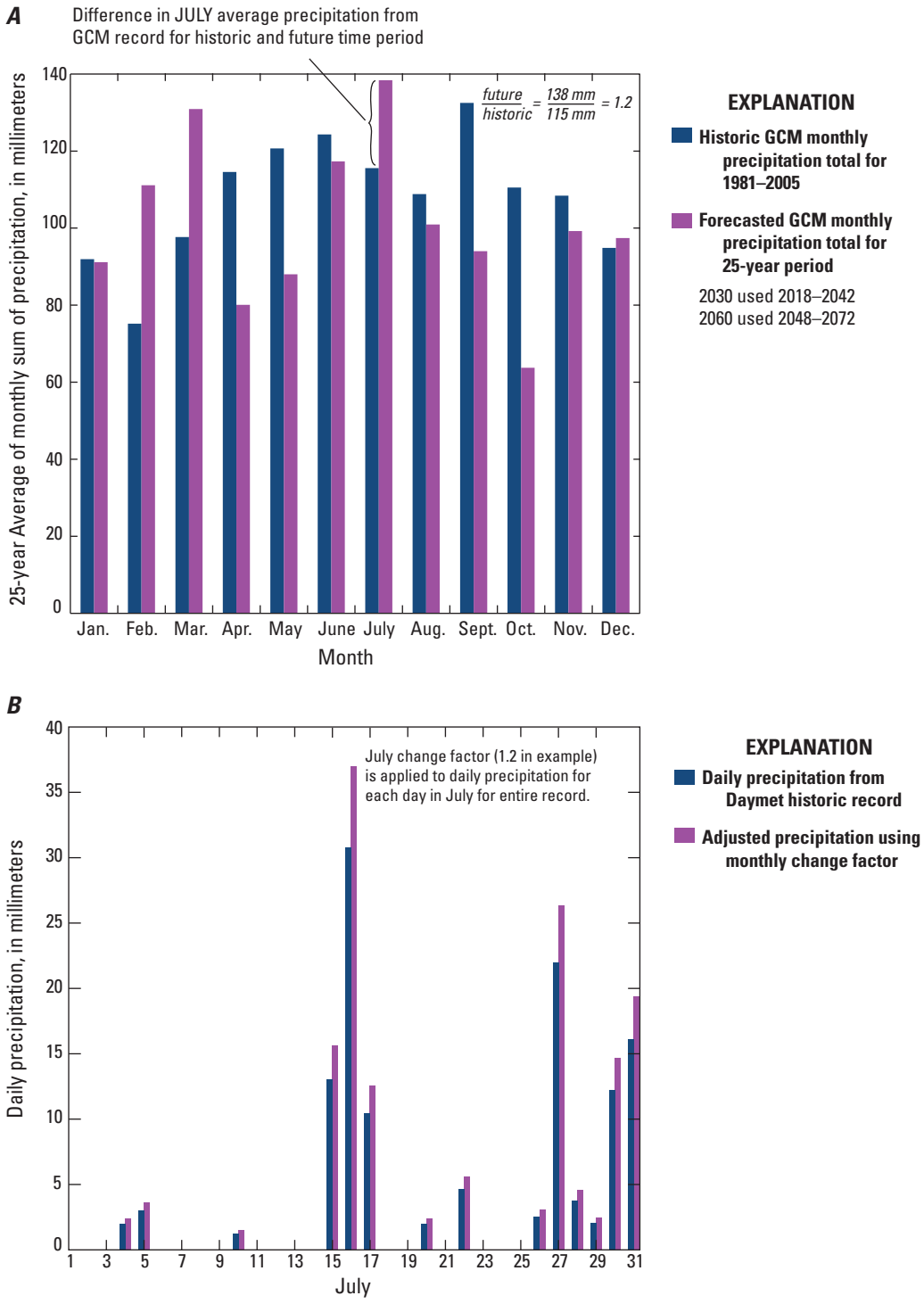

Figure 8. Example of how the monthly change factor (δ) is *A*, calculated and *B*, applied in order to incorporate general circulation model (GCM) data. The change factor is multiplicative for both precipitation and potential evapotranspiration. For temperature, the change factor is a difference instead of a ratio. mm, millimeter.

Evaluating Uncertainty for Scenario Testing

Statistical evaluation, validation, and uncertainty of WATER simulations are discussed in subsequent sections in terms of daily, mean monthly, and normalized mean monthly (that is, mean monthly averaged over the 25-year simulation period) streamflow simulations. These different time steps account for the difference in temporal resolution as one navigates from

- the historical record of daily precipitation to
- incorporation of seasonal median of water use to
- application of the monthly-normal δ used for forecasted climate to the historical climate record.

It is important to note, however, that only one land-cover dataset is provided for each target time period. These land-cover datasets are specific to 2011, 2030, and 2060. The simulations do not include the potential changes in land cover associated with the climate record. Instead, the 25-year climate record centered on each target year is used to understand the potential range of streamflow associated with this time period. It also follows that streamflow for the historical record will not incorporate land-cover and water-use changes between 1980 and 2010. Also, because the temperature-, precipitation-, and PET-δ factors are each based on a 25-year monthly normal, a similar time step should be used to identify significant changes in streamflow associated with these forecasted changes in climate. For example, mean monthly streamflow rather than daily streamflow should be assessed, and significant differences in mean mean-monthly streamflow for the period of record (that is, 25-year normals of mean monthly streamflow) are the best indicator of potential changes in streamflow and water availability due to forecasted climate change.

Model Development, Statistical Evaluation, and Validation of Hydroclimatic Components of WATER

Optimization and validation of different components of WATER proceeded concurrently and as data became available. Development and optimization of WATER used streamflow observations that extended from 2001–11. This time period was selected because it is at the intersection of those data available from NLCD (2006 and 2011; Fry and others, 2011) and the Daymet historical record of precipitation and temperature (Thornton and others, 2012). Although daily streamflow values simulated for the period before 2001 are expected to have more error because of changes in land and water use, WATER does provide a streamflow record extending from 1981–2011 because this longer record is critical in the consideration of aggregated streamflow metrics (monthly streamflow normals and flow-duration curves [FDCs]) that are of interest when incorporating land-cover and climate change forecasts. Streamflow was optimized and validated using the period 2001–10, including nine complete water years.

Hydroclimatic Water-Budget Components

The hillslope-hydrology model underlying WATER, TOPMODEL, is based on a water-budget approach. Independent aspects of the water budget, including PET and snow accumulation and snowmelt, are temperature indexed according to the daily precipitation and temperature provided by Daymet (Thornton and others, 2012). Daily precipitation amounts are randomly distributed within WATER as hourly precipitation amounts, with the model shifting to an hourly time step on days with precipitation. In its current configuration as a desktop DSS, WATER uses the same temperature time series for simulating both PET and snow to minimize processing time. As the following section explains, WATER uses the maximum daily temperature for both.

Accumulation and Melting of Snow

The maximum daily temperature (T_{max}; Thornton and others, 2012) is used by the model to simulate when precipitation occurs as rainfall as opposed to snowfall. Any simulated snowfall accumulates to create a snowpack that is melted using the temperature-indexed method of the USACE (1998); total snowmelt can not exceed standing snowpack. Each HRU uses a separate combination of snowmelt and rain-on-snowmelt coefficients (table 2) that apply the potential melt (M_s) to the standing snowpack:

$$M_s = C_m \left(T_{\max} - 0°C \right). \quad (8)$$

Simulation of snow accumulation and melt was evaluated with data from four National Weather Service (NWS) National Operational Hydrologic Remote Sensing Center stations (table 4; NWS, 2012). Daymet was also considered for evaluation of snowpack simulation; however, the transition between individual calendar years creates a bias after January 1 (Thornton and others, 2012). Consequently, only point data that are reported weekly or monthly were available for this comparison (figs. 4 and 9), and a direct, statistical comparison between observed and simulated values cannot be made. WATER converts precipitation from rain to snow (1 mm precipitation = 10 mm snow) when the temperature (averaged for the entire basin) is <0 °C; these basin-average values are reported in the WATER.txt file as snowpack (millimeters of snow) but are handled by the water budget as snow-water equivalent (millimeters of water). On the basis of comparison to the available observations, it was determined that the maximum daily temperature (T_{max}) was necessary in order to accurately model the accumulation and melt of snow. When the mean daily temperature was used, too much snow accumulated and the snowpack

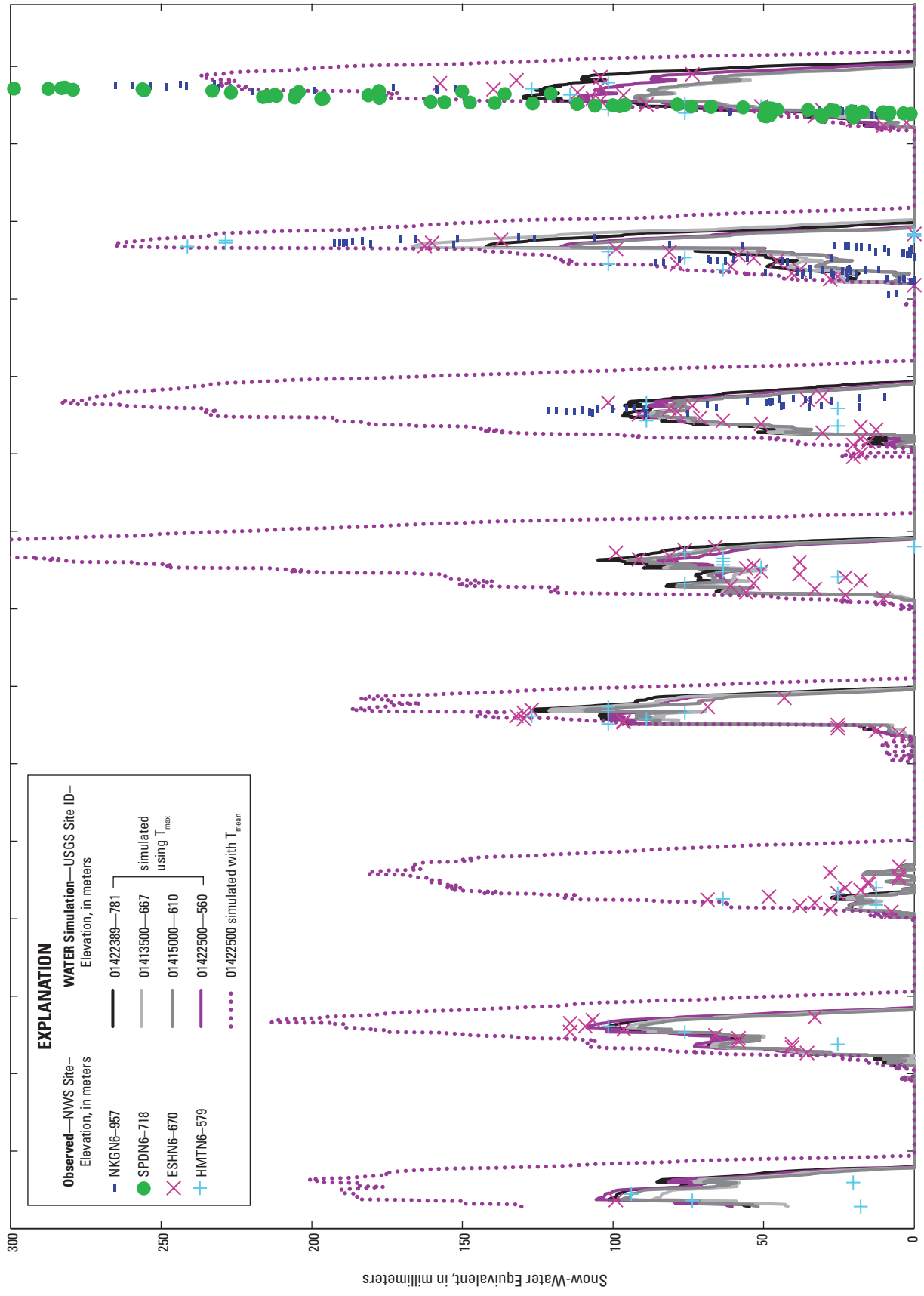

Figure 9. Comparison of Water Availability Tool for Environmental Resources (WATER)-derived daily basin averages of snow water equivalent for four northern validation basins to point observations from National Weather Service (NWS) observations in the Delaware River Basin. Locations are shown in figure 4; NWS sites are located along basin boundaries (topographic divides). Elevations for NWS sites and mean basin elevation are shown for comparison. Additional details about U.S. Geological Survey (USGS) and NWS sites are shown in tables 3 and 4, respectively. WATER simulations use maximum daily temperature to simulate the accumulation and melt of snow. Elevations are in meters (m) above the North American Vertical Datum of 1988.

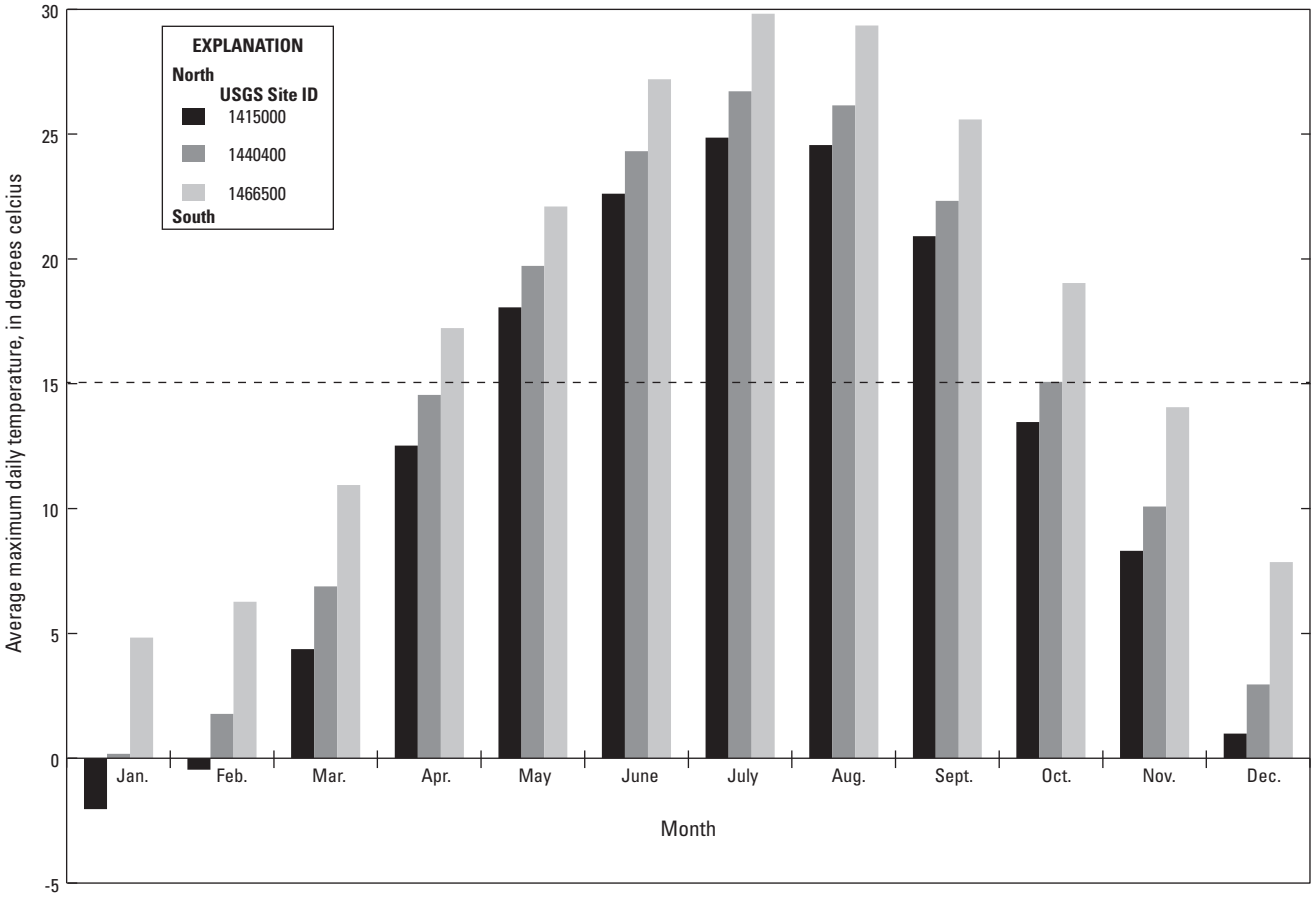

Figure 10. A north-south transect of maximum daily temperature for three basins with U.S. Geological Survey (USGS) gages. Basins are representative of the forested hydrologic response unit (more than 75 percent forested). A value of 15 degrees Celsius (°C) transitions the evapotranspiration protocol from dormancy to growing conditions. Sites are shown in figure 4.

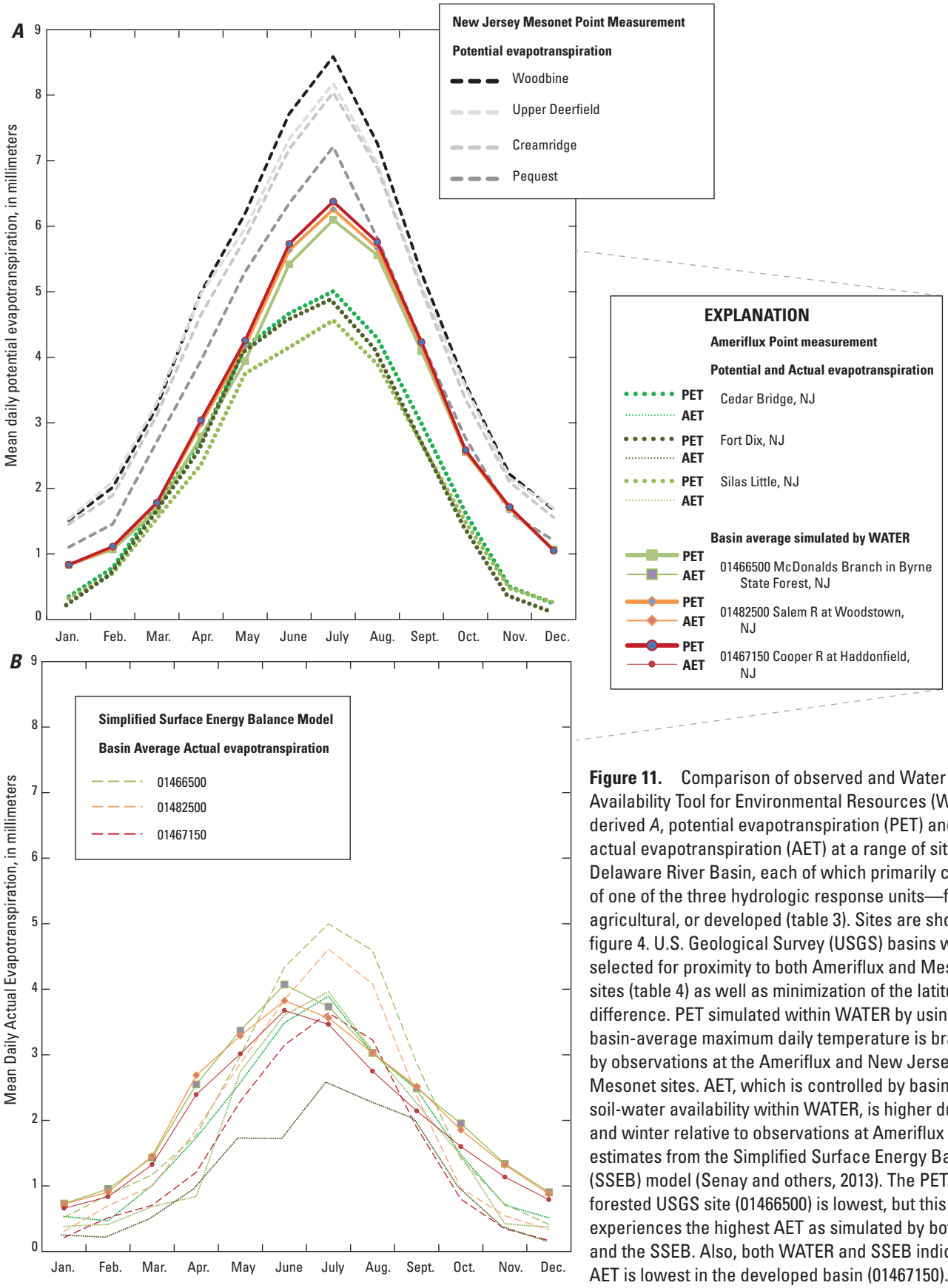

Figure 11. Comparison of observed and Water Availability Tool for Environmental Resources (WATER)-derived *A*, potential evapotranspiration (PET) and *B*, actual evapotranspiration (AET) at a range of sites in the Delaware River Basin, each of which primarily consists of one of the three hydrologic response units—forested, agricultural, or developed (table 3). Sites are shown in figure 4. U.S. Geological Survey (USGS) basins were selected for proximity to both Ameriflux and Mesonet sites (table 4) as well as minimization of the latitudinal difference. PET simulated within WATER by using the basin-average maximum daily temperature is bracketed by observations at the Ameriflux and New Jersey Mesonet sites. AET, which is controlled by basin-average soil-water availability within WATER, is higher during fall and winter relative to observations at Ameriflux sites and estimates from the Simplified Surface Energy Balance (SSEB) model (Senay and others, 2013). The PET at the forested USGS site (01466500) is lowest, but this site experiences the highest AET as simulated by both WATER and the SSEB. Also, both WATER and SSEB indicate that AET is lowest in the developed basin (01467150).

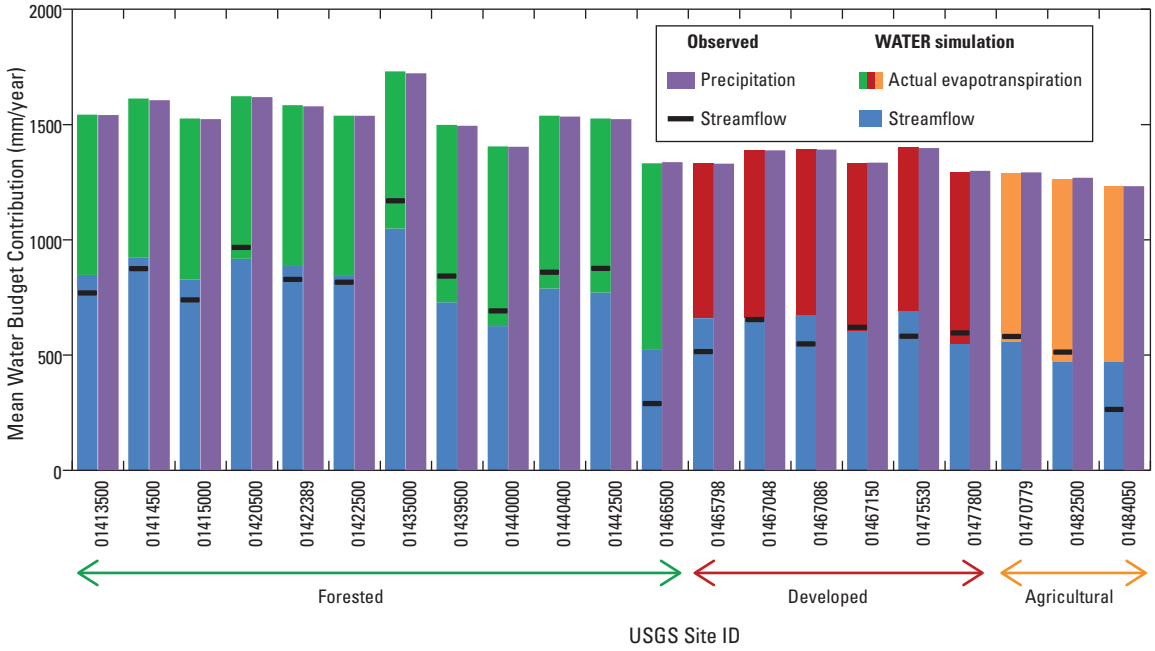

Figure 12. Water-budget components from Water Availability Tool for Environmental Resources simulations for homogeneous basins in the Delaware River Basin. Each is an annual sum normalized for the 9-year period of record from October 2001 through September 2010. The actual evapotranspiration portion of the water budget was used to help optimize the simulation of observed streamflow. Streamflow was normalized for basin area; both the observed and simulated values are shown. All water-budget components are in millimeters.

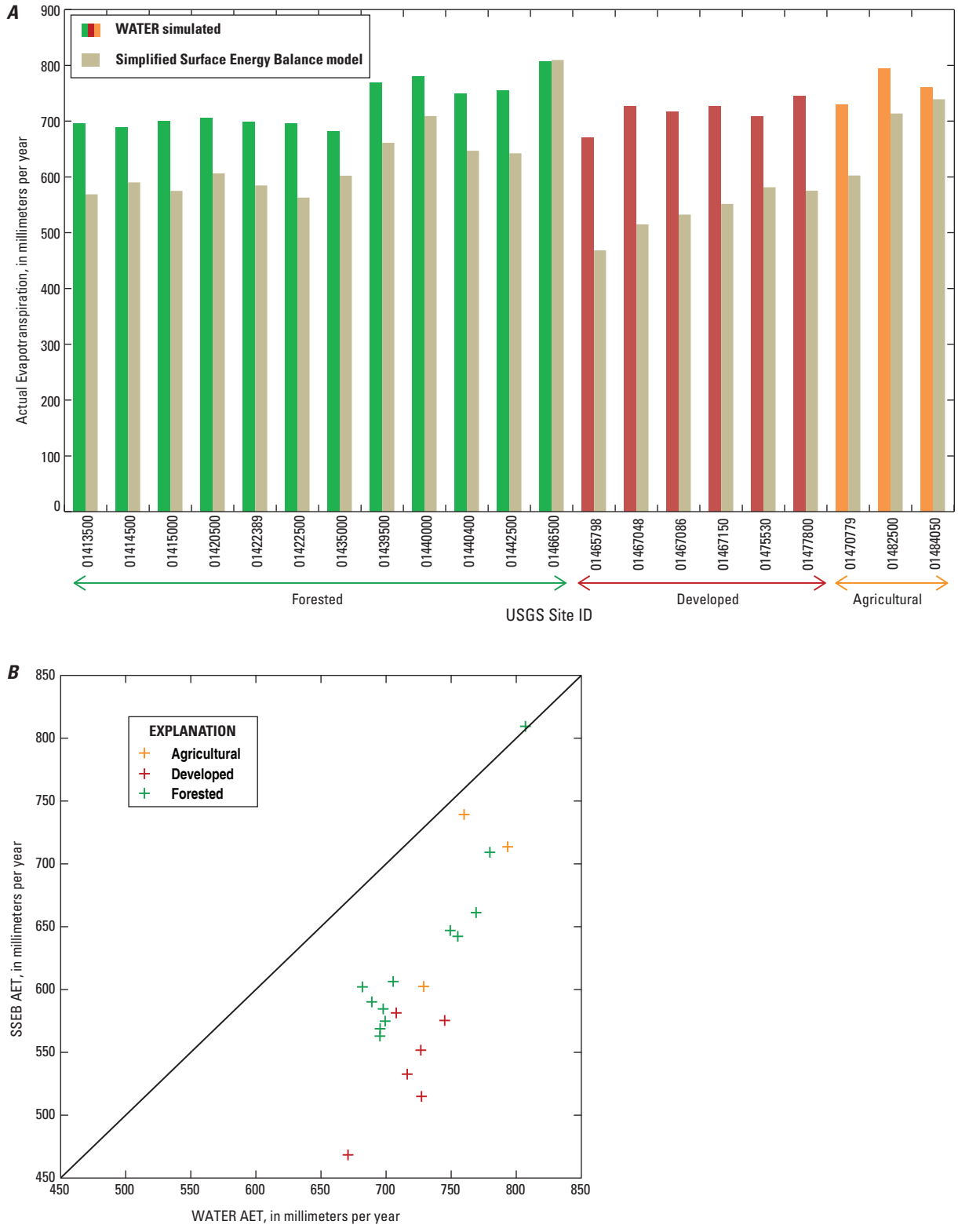

Figure 13. Statistical evaluation of actual evapotranspiration from the Water Availability Tool for Environmental Resources (WATER). *A*, Comparison of WATER-derived actual evapotranspiration (AET) at 21 sites in the Delaware River Basin to areal estimates from the Simplified Surface Energy Balance (SSEB) model (Senay and others, 2013). Sites are shown in figure 4. *B,* Scatterplot of observed versus simulated AET basin averages. WATER consistently estimates higher AET than SSEB does. However, a Spearman rank correlation test shows these two different estimates are significantly correlated (p-value = 0.0007), indicating that the relative AET is similar among the sites.

did not melt until late spring (fig. 9); this is in contrast to the normal melt period historically occurring by April. The melt coefficients (table 2) create an environment in which snowmelt is slowest in forested areas and most rapid in developed areas. This is logical given the protection provided by the forest canopy as well as the acceleration and management of melt that would be expected on the pavement and exposed land of urban areas (through salt application and snow removal).

Evapotranspiration

Potential evapotranspiration (PET) was simulated in WATER by using a temperature-indexed approach (Hamon, 1963), which combines daily temperature with estimates of day length and solar radiation that are based on latitude. The T_{max} was used as the daily temperature, and the evapotranspiration (ET) exponents (table 2) were used to control the relation between the daily PET and the soil-water storage calculated on the basis of the daily mean saturation deficit (S in equation 2). Because the model was designed to examine the potential effects of forecasted changes in climate, including increases in winter temperatures by as much as 6.5 °C (12 °Fahrenheit [F]; Frumhoff and others, 2007), instead of triggering the growing season by a calendar date, a temperature of 15 °C (60 °F) was selected to trigger the transition from dormancy to growing conditions and back. During the early season, before plant ET accelerates, only direct evaporation from the soil is expected to be underway. This growth-temperature threshold is applied on a daily time step—the beginning and end of the growing season may be punctuated by periods of decreased ET. For the historical time period (2001–11), this generally resulted in growing conditions and aggressive ET from approximately May through October and as early as April in the southern part of the basin (figs. 10 and 11). Comparison to observations at a combination of forested Ameriflux sites and mixed land-use Mesonet sites (table 4) shows that PET simulated in WATER is bounded by these observations.

WATER calculates actual evapotranspiration (AET) on a daily time step; the calculation is based on soil-water availability in the soil thickness that is accessible to roots, and it uses parameters that were optimized to differentiate dormancy from growing conditions (table 2). For each group of homogeneous land-cover basins, AET was used as a means of empirically optimizing streamflow as part of the overall water budget for each basin (fig. 12). As a consequence of these ET and soil parameters, more water is accessed for AET in the forested areas (table 2 and figs. 11–13), relative to agricultural and developed areas, because of a combination of the following:

- the smaller percentage of water that bypasses the root-zone as a function of macroporosity,
- the larger proportion of the soil that is accessible to roots, and
- the effect of the larger ***m***, which slows movement of soil-water downslope towards the stream.

AET estimates from WATER are consistently higher than point observations from the Ameriflux sites (fig. 11*B*), each of which is from the top of the forest canopy. AET was also compared to estimates from the Simplified Surface Energy Balance (SSEB) model (Senay and others, 2013), which was geospatially sampled for each of the 21 homogeneous land-cover basins in the DRB by using the USGS Geo Data Portal. WATER consistently estimates a significantly higher AET than that from the SSEB (paired Wilcoxon signed-rank test, p-value <0.0001; figs. 11 and 13*A*); however a Spearman rank correlation test shows these estimates are significantly correlated (rho=0.6974; p-value = 0.0006), indicating that the relative AET is similar among the sites regardless of which model is used (fig. 13*B*). Most of this excess AET is in the fall and winter months; the spring AET estimates from WATER are bounded by observations from the Ameriflux sites and SSEB simulations. The range of AET estimates in the WATER simulations differs from the range of estimates in the SSEB simulations, with more similarity among land-cover types in the WATER estimates than the SSEB estimates. This may be related to the difference in spatial resolution. WATER simulations use 10-m resolution topography combined with temperature averaged for 3,736 DEM-derived basins that average 9.4 km^2. In contrast, SSEB uses topographic and satellite data at a resolution of 1 km^2 (Senay and others, 2013).

Optimization of Remaining Hydrologic Parameters and Differentiation of Hydrologic Response Units

After optimization of individual hydroclimatic variables, including PET and snow accumulation and snowmelt, the remaining parameters that link topography, soils, and land cover were evaluated (first eight parameters in table 2). Each of these was optimized by using 21 relatively homogeneous basins (table 3), and the resultant combination was validated by using those 28 basins with mixed land cover—no additional changes were made on the basis of statistical evaluation of those mixed land-cover basins. Each of these parameters would be expected to vary among the HRUs because of a combination of differences in preservation of natural soil properties, natural and managed plant communities, anthropogenic infrastructure, and connectivity of impervious surface. For example, the importance of individual parameters for hydrologic simulation of forested areas follows:

- The relatively large spatial coefficient (*SpCf*; 0.4) preserves the topographic gradient characterized by the TWI and enables storage of soil water in the landscape that provides base flow.
- The topographic adjustment (1) focuses on the natural topography instead of the anthropogenic infrastructure.

- The proportion of the soil available to plant roots (0.75) reflects the perennial vegetation and permanent, deep roots that characterize the forest environment.
- The percentage of precipitation (15 percent) that is routed through macropores by the model is similar to natural estimates and does not assume tile- or storm-drains that might cause water to bypass the root zone and AET.
- The long water-body delay (15 days) reflects the size of the water-bodies and resultant storage.
- The effective-impervious multiplier (0.7) decreases the percentage of impervious area estimated from NLCD for forested areas, where impervious areas are likely discontinuous, in order to simulate how much of the water falling on impervious areas can run onto pervious areas and infiltrate the soil instead of being routed by the model directly to the stream.
- The impervious runoff delay (0.1) is relatively low, causing the majority of the precipitation that falls on impervious areas to be delivered to the stream that day instead of delaying the runoff in retention basins that might be present in more developed areas.
- The impervious curve number (90) is lower than that used in developed areas and causes the TR–55 model (USDA, 1986) to generate relatively less runoff for the same amount of impervious area in developed areas.

Incorporation of Water-Use Data

Water-use data were originally aggregated to a HUC–12 basin in order for this study to stay aligned with the rest of the water-use reporting for the USGS Water Census Focus Area Studies. However, optimization of the incorporation of these water-use data, by using the 21 homogeneous basins that were used to optimize the rest of the modeling approach ("f," "a," and "d" in table 3) plus 28 additional basins of mixed land-cover ("m" in table 3), indicated that the aggregation of data to a HUC–12 basin caused excessive error in the streamflow simulations. Use of the original point locations improved model performance. However, there were still areas of poor performance, where summer and fall withdrawals were far in excess of streamflow, in the unconsolidated sediments of the Coastal Plain as well as the carbonate regions (fig. 5). Residents in these areas of the DRB are dependent on groundwater from deep aquifers (Hutson and others, in press). Surficial geology (fig. 5) was used to isolate these regions, and groundwater withdrawals and returns in the Coastal Plain and carbonate regions were removed from the point database because each of these areas includes groundwater withdrawals from deep aquifers that are a combination of confined and unconfined aquifers (in the Coastal Plain) or fracture systems (in the carbonate regions) that are not in equilibrium with the daily hydrology simulated by TOPMODEL. Point data were then reaggregated to those 3,736 DEM-derived polygons; this protects the individual locations by placing them in areas >0.1 km^2; these basins have a mean area of 9.4 km^2 and a maximum area of 132.4 km^2.

Statistical Evaluation, Validation, and Uncertainty of Streamflow Simulated by Using WATER

A total of 57 basins were used for statistical evaluation of hydrologic simulation by the WATER DSS (table 3). As discussed previously, 21 of these basins, used for optimization of model parameters (table 2), were relatively homogeneous in land cover that corresponded to the HRUs used by WATER; one basin was excluded from streamflow validation because it drains a hardwood swamp with a surface water-groundwater interaction that is not captured by this TOPMODEL approach (USGS site 01466500, McDonalds Branch in Lebanon State Forest, N.J.; Mast and Turk [1999]). The remaining 37 basins were mixed in land cover. Twenty-eight of these mixed basins were used to validate model parameters and to optimize the incorporation of water-use data. Nine mixed basins were set aside and used as test basins for final validation that WATER would perform similarly in areas not used to optimize the hydrologic models or datasets. The WATER output discussed in this section uses streamflow estimates that have been adjusted by seasonal water-use-median totals for specific point locations (discussed in "Incorporation of Water-Use Data"); these are streamflow estimates from WATER to which water-use data were applied with WATER Application Utilities.

Goodness-of-Fit Statistics

A series of goodness-of-fit statistics were run on observed versus simulated streamflow by using the USGS EflowStats R-statistics package (Thompson and Archfield, 2014) to evaluate overall model performance as well as the ability of the model to distinguish individual streamflow components associated with high-streamflow, midrange, and low-streamflow conditions. A combination of statistics for evaluating overall model performance is presented; each statistic evaluated a comparison of daily streamflow for the period of October 2001 through September 2010 (3,287 days; 12 sites had 366–2,922 days; table 3); these statistics were run with only complete water years. Groups were compared through paired, Wilcoxon signed-rank tests, and the comparisons are two sided unless otherwise noted. Statements of significance indicate a p-value <0.05. The goodness-of-fit statistics used included those described as follows:

- The Nash-Sutcliffe efficiency (E_f) statistic ranges from negative infinity to 1 (Nash and Sutcliffe, 1970):

$$E_f = 1 - \frac{\sum (y_i - x_i)^2}{\sum (x_i - \bar{x})^2}. \quad (9)$$

A value of 1 indicates that the simulation perfectly matches those observed data for each day of the comparison. A value of zero indicates that the simulation provides no more information than a mean annual streamflow value. Each of the E_f values reported was calculated by using the natural log (ln) of the daily streamflow (observed [x_i] and simulated [y_i]) to better represent all parts of the hydrograph and not concentrate on the largest streamflow events.

- The normalized root mean squared error (*RMSEn*) calculates the error as a multiple of the daily observed streamflow value:

$$RMSEn = \sqrt{\frac{\sum (y_i - x_i)/x_i)^2}{n}}. \quad (10)$$

The RMSEn provides an estimation of uncertainty for the simulations that can be transitioned to simulations at ungaged sites and those involving scenario testing; this statistic is essentially a proportional error relative to daily streamflow. This same statistic also is used to estimate uncertainty for aggregated streamflow.

- The ratio of the root mean squared error to the standard deviation of the observed streamflow (*RSR*) calculates the error as a proportion of variability in observed streamflow:

$$RSR = \frac{\sqrt{\frac{\left(\sum (y_1 - x_1)^2\right)}{n}}}{\sqrt{\frac{\left(\sum (\bar{x} - x_i)^2\right)}{n}}}. \quad (11)$$

The RSR helps to identify those sites and seasons during which observed streamflow variability caused by anthropogenic controls (such as water use) or weather patterns (such as snowmelt) may affect the ability to simulate streamflow because of water storage or redistribution that is not represented in those datasets used by WATER.

- The Spearman rank correlation coefficient (*rho*) incorporates ranks (R) of daily observed and simulated streamflow within the entire record:

$$rho = \frac{\sum (Rx_i Ry_i) - n\left(\frac{n+1}{2}\right)^2}{n\left(n^2 - 1\right)/12}. \quad (12)$$

This statistic quantifies the ability of the simulation to accurately separate individual streamflow components in terms of how individual days rank among the entire streamflow record.

- The bias (B) calculates error as a percentage of the daily streamflow value:

$$B = 100 * \frac{\sum (y_i - x_i)}{\sum x_i}. \quad (13)$$

The bias helps to identify whether the model consistently overestimates or underestimates streamflow for individual sites or time periods. A positive bias indicates that WATER overestimates streamflow.

Evaluation of Daily Streamflow

This group of goodness-of-fit statistics shows how WATER performs throughout the DRB (fig. 14). Fifty-three of 57 basins have an E_f between 0.39 and 0.83. Normalized root mean squared error ranges from 0.32 to 3.11, and RSR ranges from 0.45 to 1.64. Bias ranges from -26.7 to 27.4 percent, with 35 of 57 basins between ±10 percent. The Spearman rank correlation coefficient ranges from 0.69 to 0.92 (not shown in figure 14).

Three basins in particular have poor performance relative to the other validation basins. Two of these (01451500—Little Lehigh Creek at Allentown, Pa.; and 01452500—Monocacy Creek near Bethlehem, Pa.) are populated regions in the carbonate area of the DRB, where groundwater use makes it difficult to simulate streamflow (fig. 5). A third basin (01484270—Beaverdam Creek near Milton, Del.) is in the Coastal Plain region and may be influenced by high tides (fig. 3). The RMSEn of several basins in the midlatitudes of the DRB, including basins where the land cover is relatively equally split among the three HRUs, ranges from 0.76 to 0.90; daily water use may be more difficult to characterize from seasonal estimates for the mixed land-cover environment than for basins with primarily one HRU. The RMSEns of several basins in the northern part of the DRB shows relatively high values; however, comparison to the observed variability (RSR) suggests that there is a high variability in daily streamflow for these basins. For each basin, a 3-day moving average of streamflow significantly improved model performance (p<0.01); this 3-day average accounts for the random distribution of precipitation events, the potential for a precipitation event to span more than 1 day, and the variable snow-water equivalent among and within events. There is no apparent spatial pattern in the bias.

For an understanding of the accuracy of hydrologic simulations for different streamflow conditions, streamflows were divided into six percentiles (≤10 percent, >10–25 percent, >25–50 percent, >50–75 percent, >75–90 percent, and >90 percent) and compared to overall model performance (fig. 15). The RMSEn (fig. 15*A*) indicates no significant difference in model performance for streamflows larger than the 25th percentile, and the average value is less than 1 for these streamflows. The RMSEn is significantly larger for the

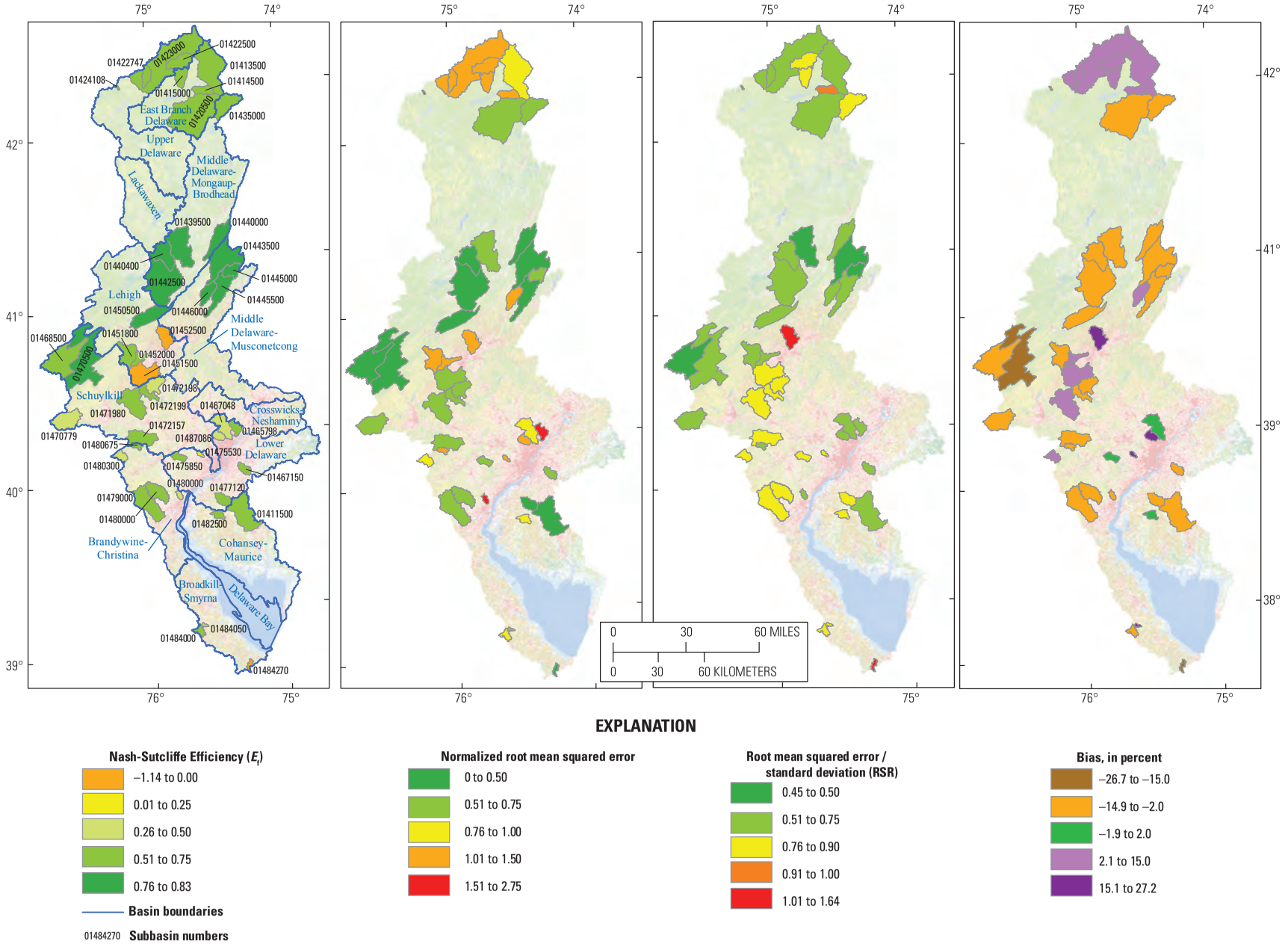

Figure 14. Statistical evaluation of hydrologic simulations for 48 basins in the Delaware River Basin. For each statistic, green indicates better performance. The first three of these statistics are unitless. The Nash-Sutcliffe efficiency (E_f) was evaluated by using the natural log of the daily streamflow value. The Nash-Sutcliffe efficiency has a range of negative infinity to 1; a value of 1 indicates that the simulation perfectly matches those observed data for each day of the comparison. The normalized root mean squared error (RMSEn) describes error as a proportion of observed daily streamflow. The ratio of the root mean squared error (RMSE) to the standard deviation of observed streamflow (RSR) describes error in terms of variability of observed streamflow. Bias is reported as a percent (%); a positive bias indicates an overestimation by the Water Availability Tool for Environmental Resources simulation.

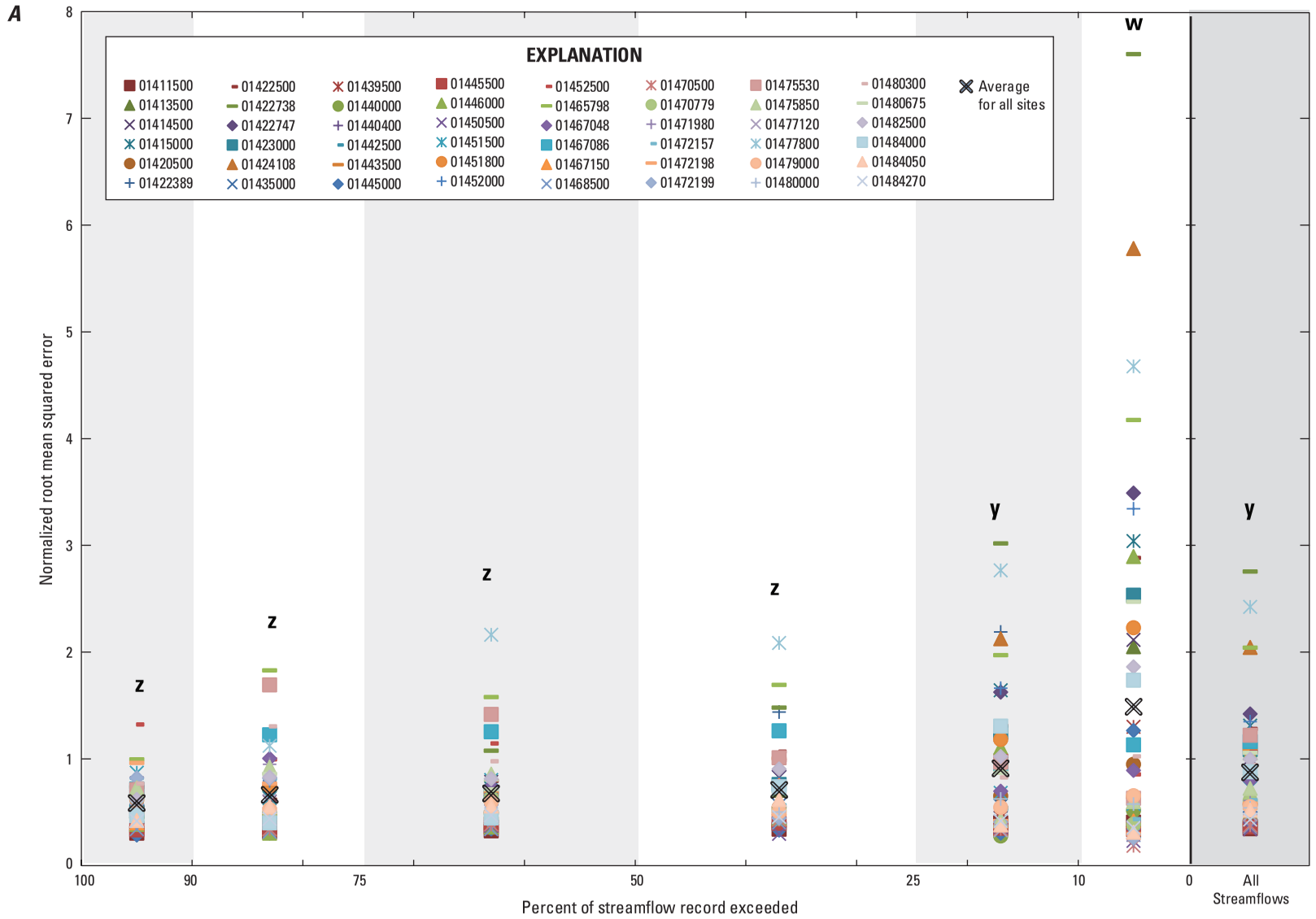

Figure 15. Goodness-of-fit statistics for 48 basins in the Delaware River Basin as a function of individual streamflow percentiles: *A*, normalized root mean squared error, *B*, root mean squared error / standard deviation (RSR), *C*, Spearman rank correlation coefficient, and *D*, Bias. The values for the entire streamflow record are shown all the way to the right. Those largest streamflows are shown to the left such that, for example, points between 90 and 100 include those that exceed 90 percent (%) of the observed streamflow record. Letters indicate statistically different groupings (p-value <0.05) among streamflow components according to two-sided, paired Wilcoxon signed-ranked tests. Streamflow percentiles labeled with different letters significantly differ from each other. Groups labeled with multiple letters are not different from other groups with the same letter. For example, those streamflow percentiles noted with a ***w*** are significantly different from those labeled with a ***y***, but neither group significantly differs from those labeled as ***yw***.

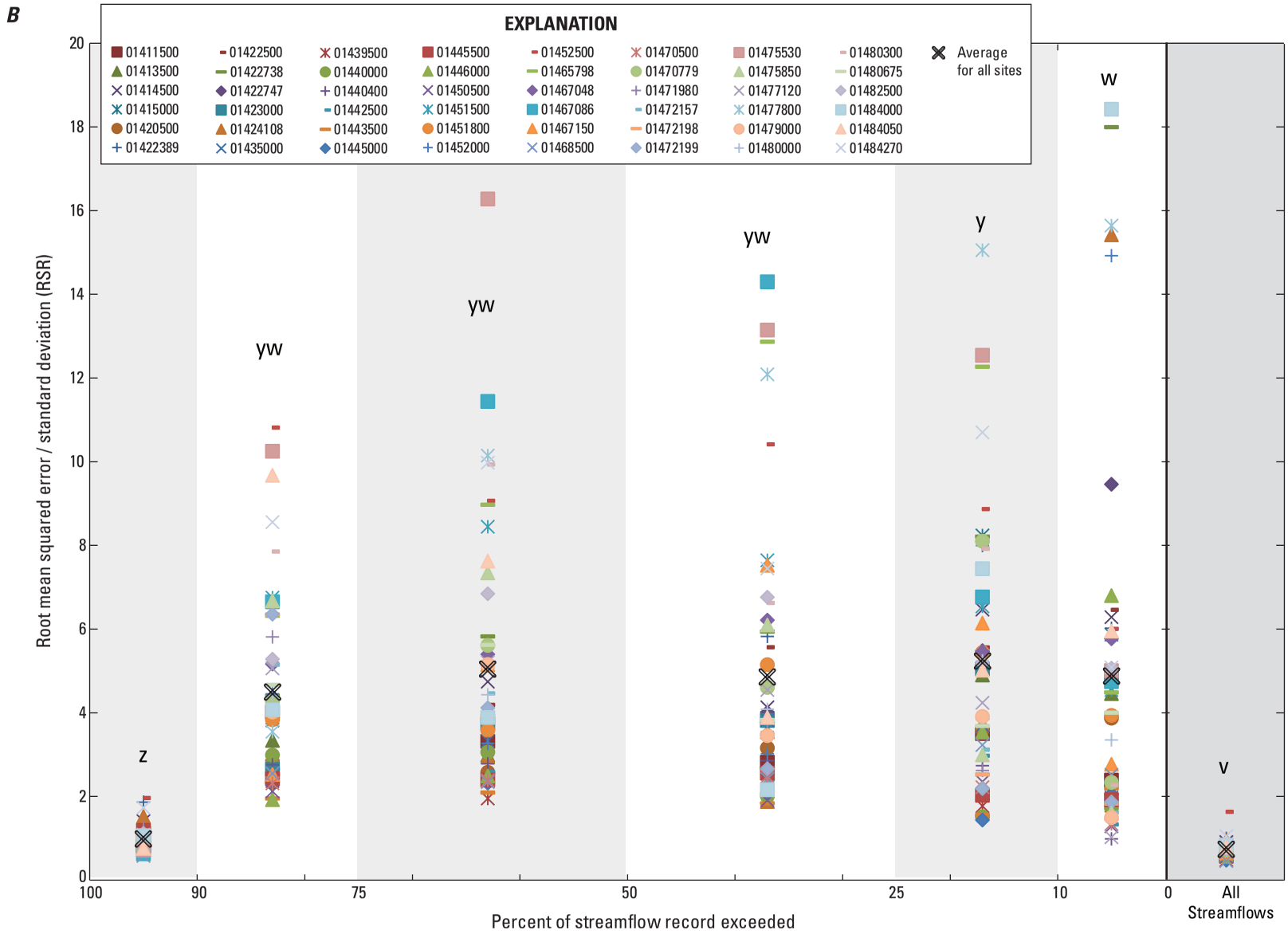

Figure 15. Goodness-of-fit statistics for 48 basins in the Delaware River Basin as a function of individual streamflow percentiles: *A*, normalized root mean squared error, *B*, root mean squared error / standard deviation (RSR), *C*, Spearman rank correlation coefficient, and *D*, Bias. The values for the entire streamflow record are shown all the way to the right. Those largest streamflows are shown to the left such that, for example, points between 90 and 100 include those that exceed 90 percent (%) of the observed streamflow record. Letters indicate statistically different groupings (p-value <0.05) among streamflow components according to two-sided, paired Wilcoxon signed-ranked tests. Streamflow percentiles labeled with different letters significantly differ from each other. Groups labeled with multiple letters are not different from other groups with the same letter. For example, those streamflow percentiles noted with a ***w*** are significantly different from those labeled with a ***y***, but neither group significantly differs from those labeled as ***yw***.—Continued

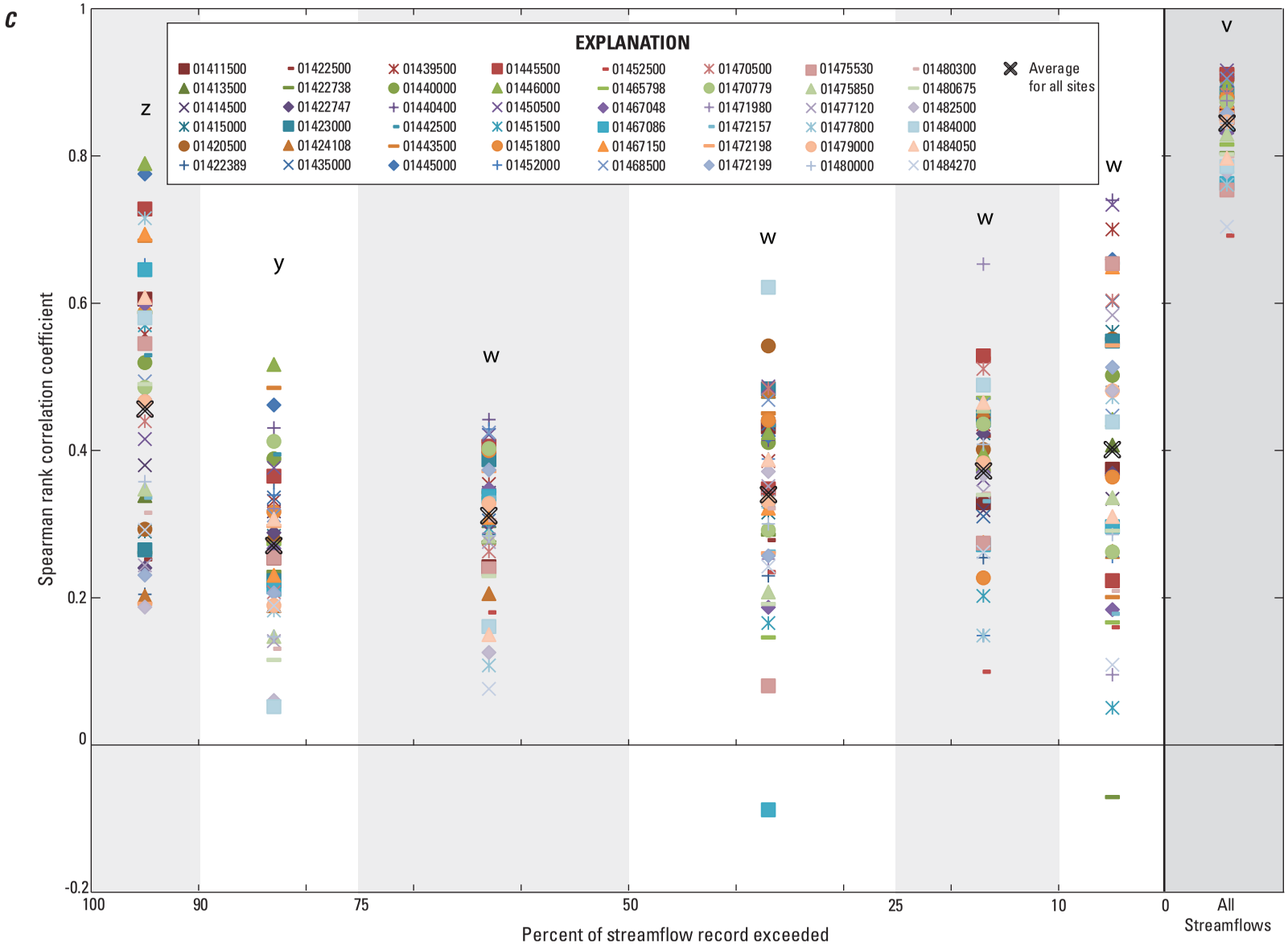

Figure 15. Goodness-of-fit statistics for 48 basins in the Delaware River Basin as a function of individual streamflow percentiles: *A*, normalized root mean squared error, *B*, root mean squared error / standard deviation (RSR), *C*, Spearman rank correlation coefficient, and *D*, Bias. The values for the entire streamflow record are shown all the way to the right. Those largest streamflows are shown to the left such that, for example, points between 90 and 100 include those that exceed 90 percent (%) of the observed streamflow record. Letters indicate statistically different groupings (*p*-value <0.05) among streamflow components according to two-sided, paired Wilcoxon signed-ranked tests. Streamflow percentiles labeled with different letters significantly differ from each other. Groups labeled with multiple letters are not different from other groups with the same letter. For example, those streamflow percentiles noted with a ***w*** are significantly different from those labeled with a ***y***, but neither group significantly differs from those labeled as ***yw***.—Continued

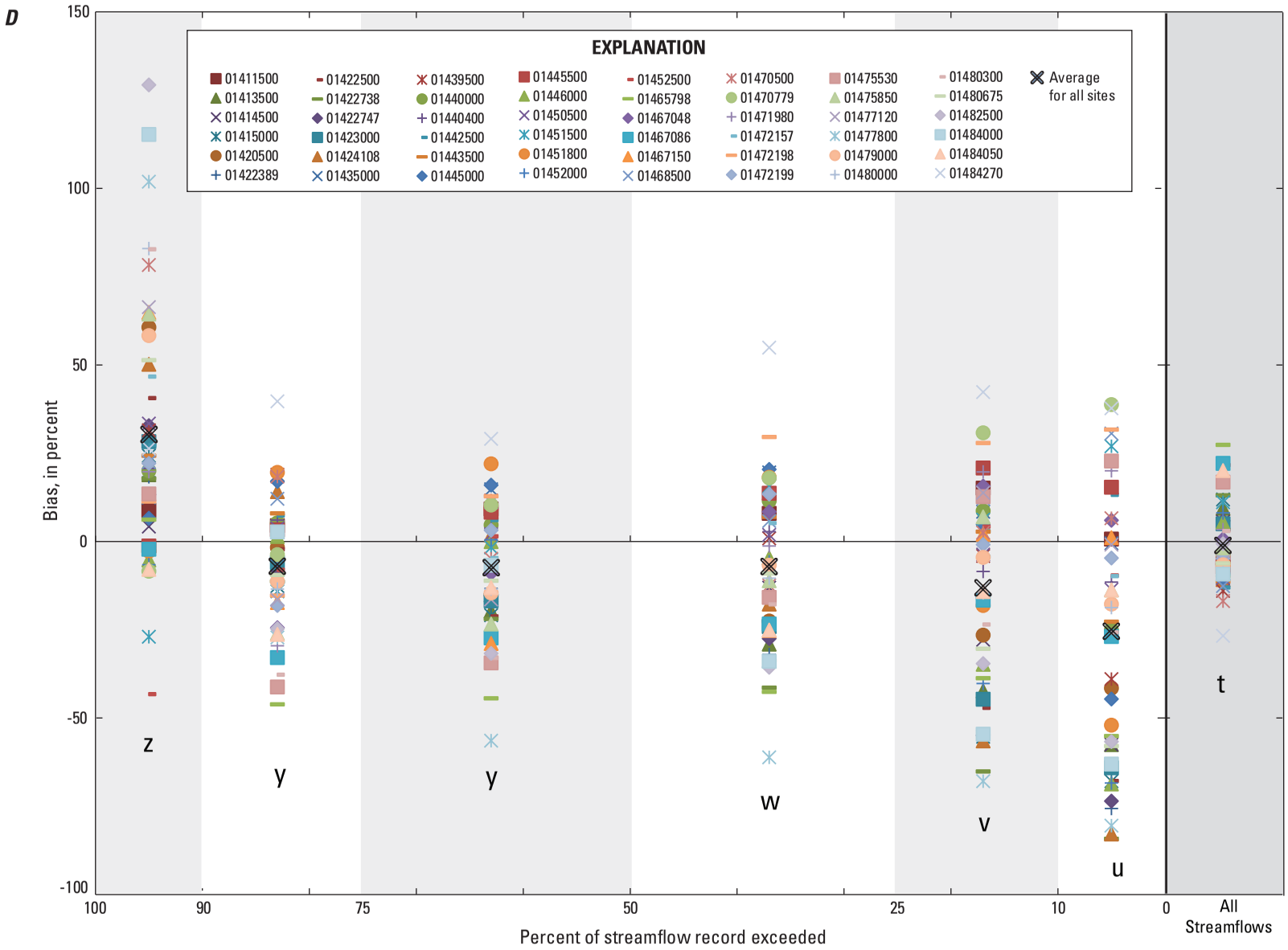

Figure 15. Goodness-of-fit statistics for 48 basins in the Delaware River Basin as a function of individual streamflow percentiles: *A*, normalized root mean squared error, *B*, root mean squared error / standard deviation (RSR), *C*, Spearman rank correlation coefficient, and *D*, Bias. The values for the entire streamflow record are shown all the way to the right. Those largest streamflows are shown to the left such that, for example, points between 90 and 100 include those that exceed 90 percent (%) of the observed streamflow record. Letters indicate statistically different groupings (p-value <0.05) among streamflow components according to two-sided, paired Wilcoxon signed-ranked tests. Streamflow percentiles labeled with different letters significantly differ from each other. Groups labeled with multiple letters are not different from other groups with the same letter. For example, those streamflow percentiles noted with a ***w*** are significantly different from those labeled with a ***y***, but neither group significantly differs from those labeled as ***yw***.—Continued

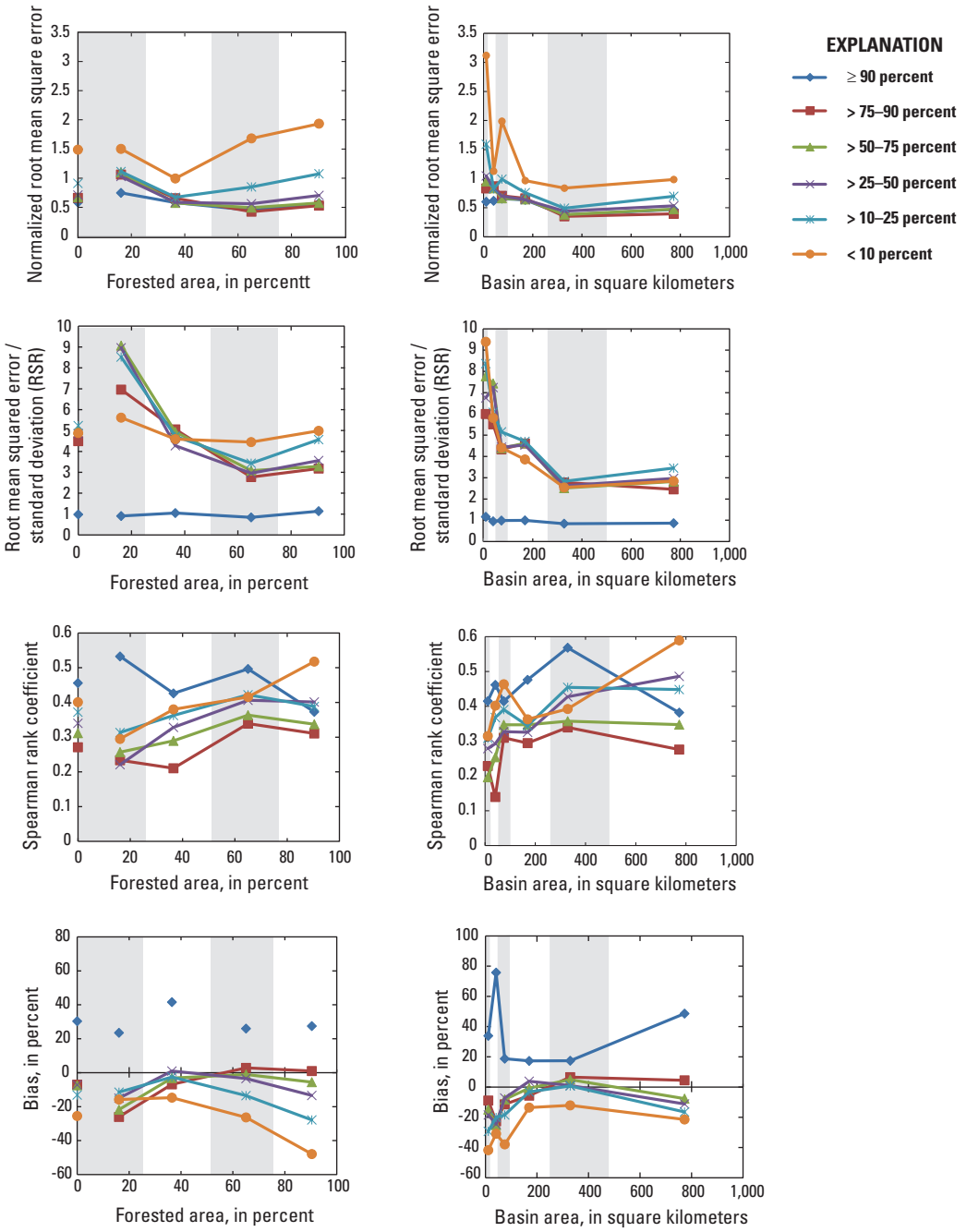

Figure 16. Goodness-of-fit streamflow-percentile statistics grouped as a function of basin area and percentage of forested area. Forested-area categories are 0–25 percent (%), >25–50 percent, >50–75 percent, and >75–100 percent. Basin-area categories are 0–25 square kilometers (km^2), >25–50 km^2, >50–100 km^2, >100–250 km^2, >250–500 km^2, and >500–928 km^2; points are shown at basin average for the range. For each statistic, the overall mean for all 48 sites is shown at 0 percent forested area on left. >, greater than; <, less than.

smallest streamflows (<25th percentile). However, when the root mean squared error is normalized by the natural variability for each basin (RSR; fig. 15*B*), there is no significant difference among those streamflows smaller than the 90th percentile. This suggests that the larger error in streamflow simulation, as indicated by the RMSEn, is a function of day-to-day variability in observed streamflow that might be caused, for example, by temporal distribution of precipitation events or actual water use during summer and fall. The RSR also shows that for the largest streamflows (90–100th percentiles), on average the root mean squared error is equal to the standard deviation of observed streamflow for this streamflow percentile (RSR=0.98) and is similar to that for all streamflows (RSR=0.73).

The Spearman rank correlation coefficient (fig. 15*C*) shows that within individual streamflow percentiles, the simulations are less accurate when the entire flow record is considered; there is no significant difference in performance for streamflows <75th percentile. However, the notably higher value for all streamflows (rho=0.84) indicates that the model successfully differentiates individual daily streamflow in terms of where these rank in the entire streamflow record. The evaluation of bias (fig. 15*D*) shows the most difference among the streamflow percentiles. Overall, the largest streamflows show a positive bias (30 percent), indicating that these largest streamflows are overestimated; this is likely a function of how precipitation is randomly distributed within WATER, making it difficult to accurately simulate the timing of peak streamflow. The average bias for the entire streamflow record in all basins is -1.14 percent, and streamflows from the 90th–25th percentile have a bias of approximately -7 percent and a similar distribution of positive and negative bias among individual basins. The two smallest streamflow percentiles (>25-10th and <10th) also show a similar spread of positive and negative bias, but with a more negative average bias (-13 and -25 percent, respectively). In both cases, the absolute percent

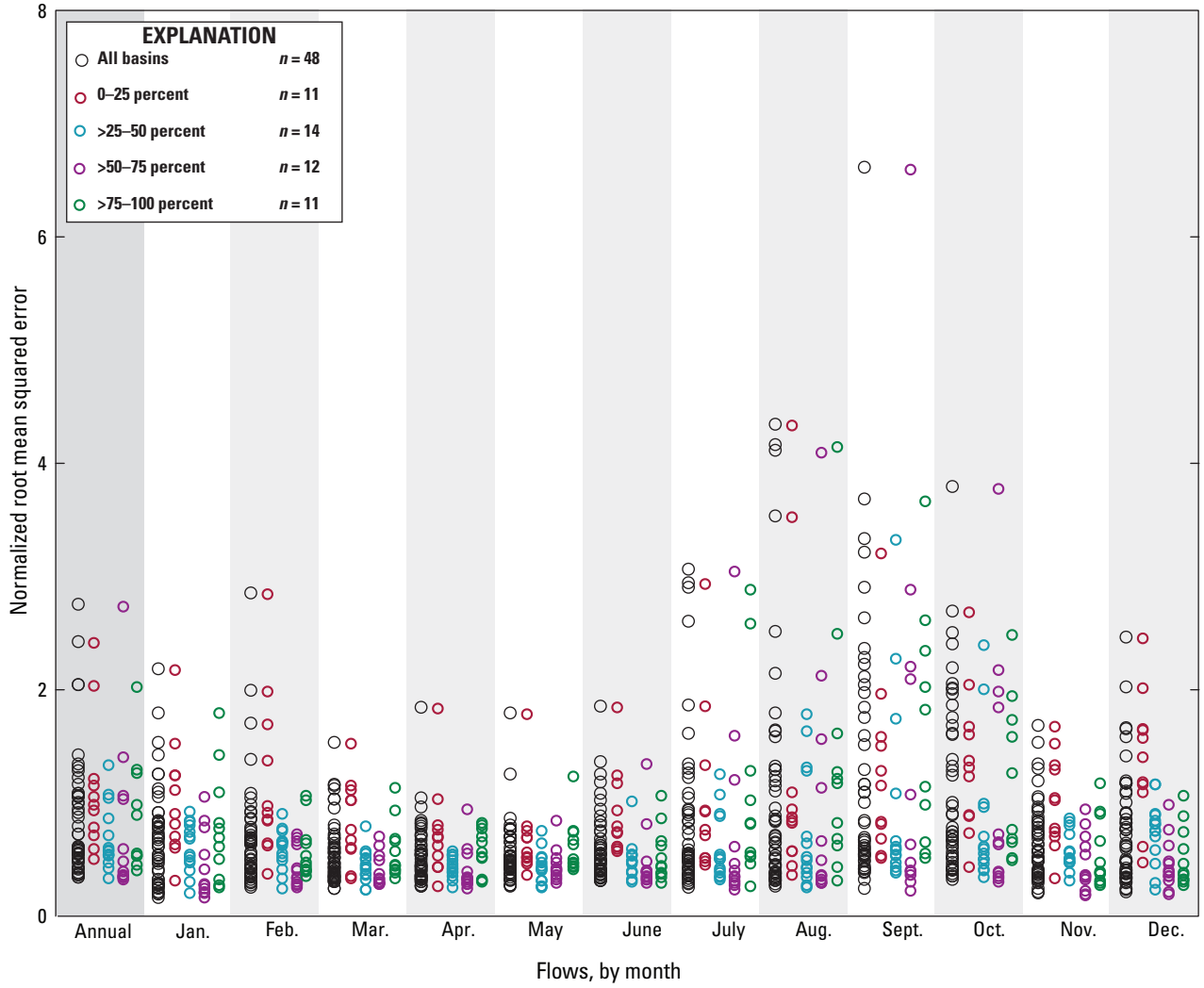

Figure 17. Normalized root mean squared error (RMSEn) as a function of percentage of forested area. Forested-area categories are 0–25 percent, >25–50 percent, >50–75 percent, and >75–100 percent. Note that U.S. Geological Survey site 01422389 has zero-streamflow days in September and October, so no RMSEn is reported for those months or as annual value and only five forested sites are shown for these time periods.

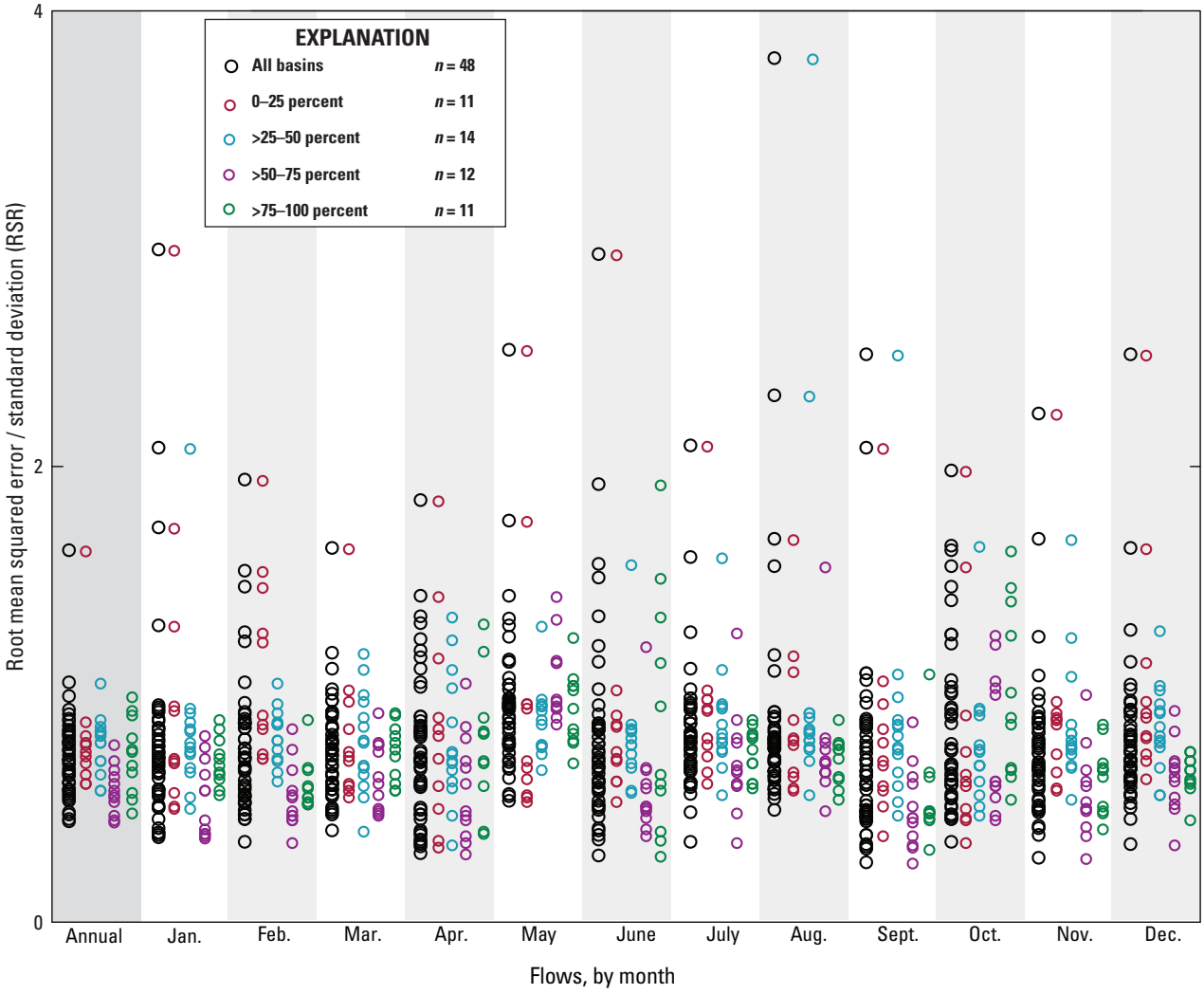

Figure 18. Root mean squared error/standard deviation (RSR) as a function of percentage of forested area. Forested-area categories are 0–25 percent, >25–50 percent, >50–75 percent, and >75–100 percent.

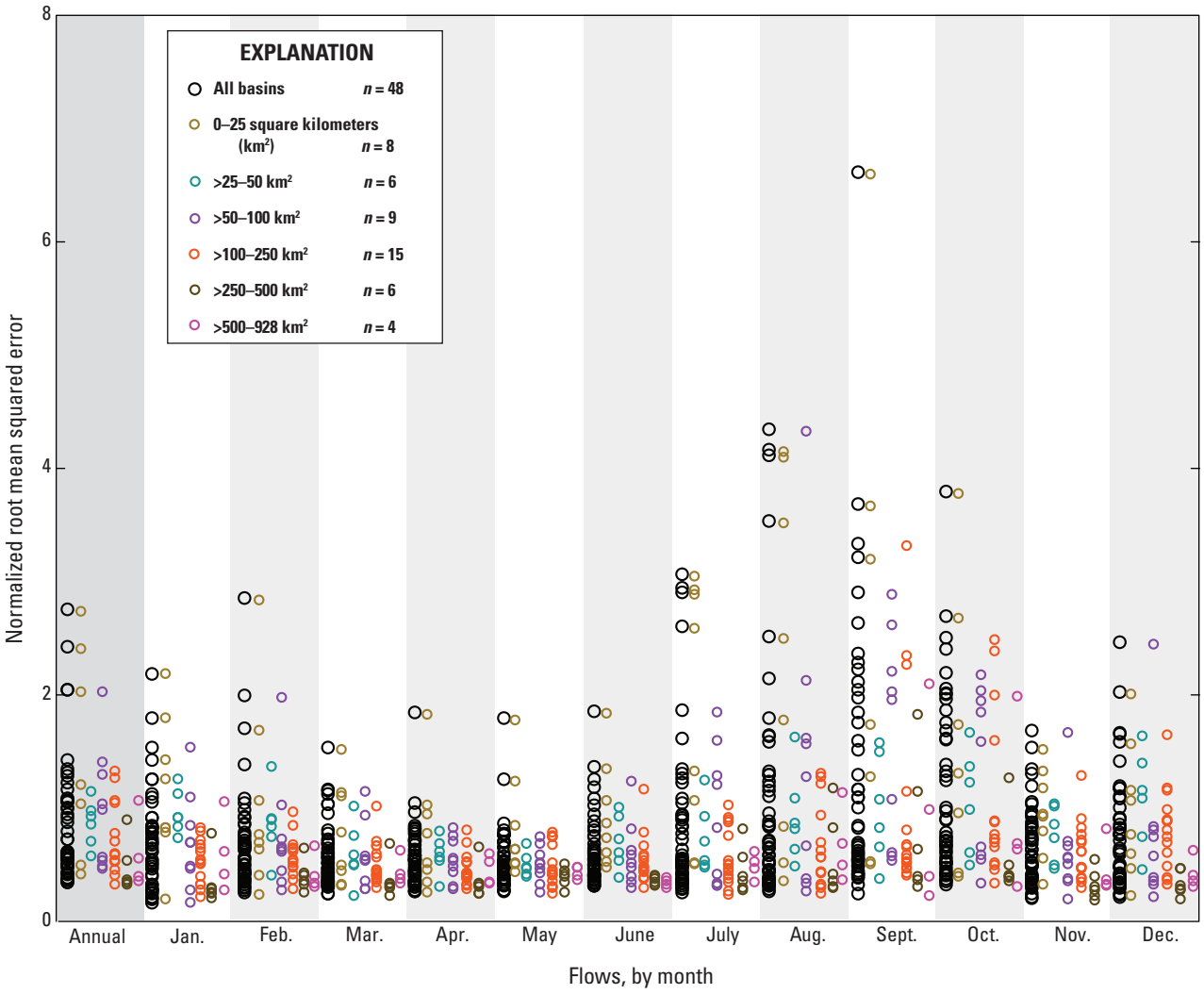

Figure 19. Normalized root mean squared error (RMSEn) as a function of basin area. Area categories are 0–25 square kilometers (km²), >25–50 km², >50–100 km², >100–250 km², >250–500 km², and >500–928 km². Note that U.S. Geological Survey site 01422389 has zero-streamflow days in September and October, so no RMSEn is reported for those months or as an annual value and only five forested sites are shown for these time periods.

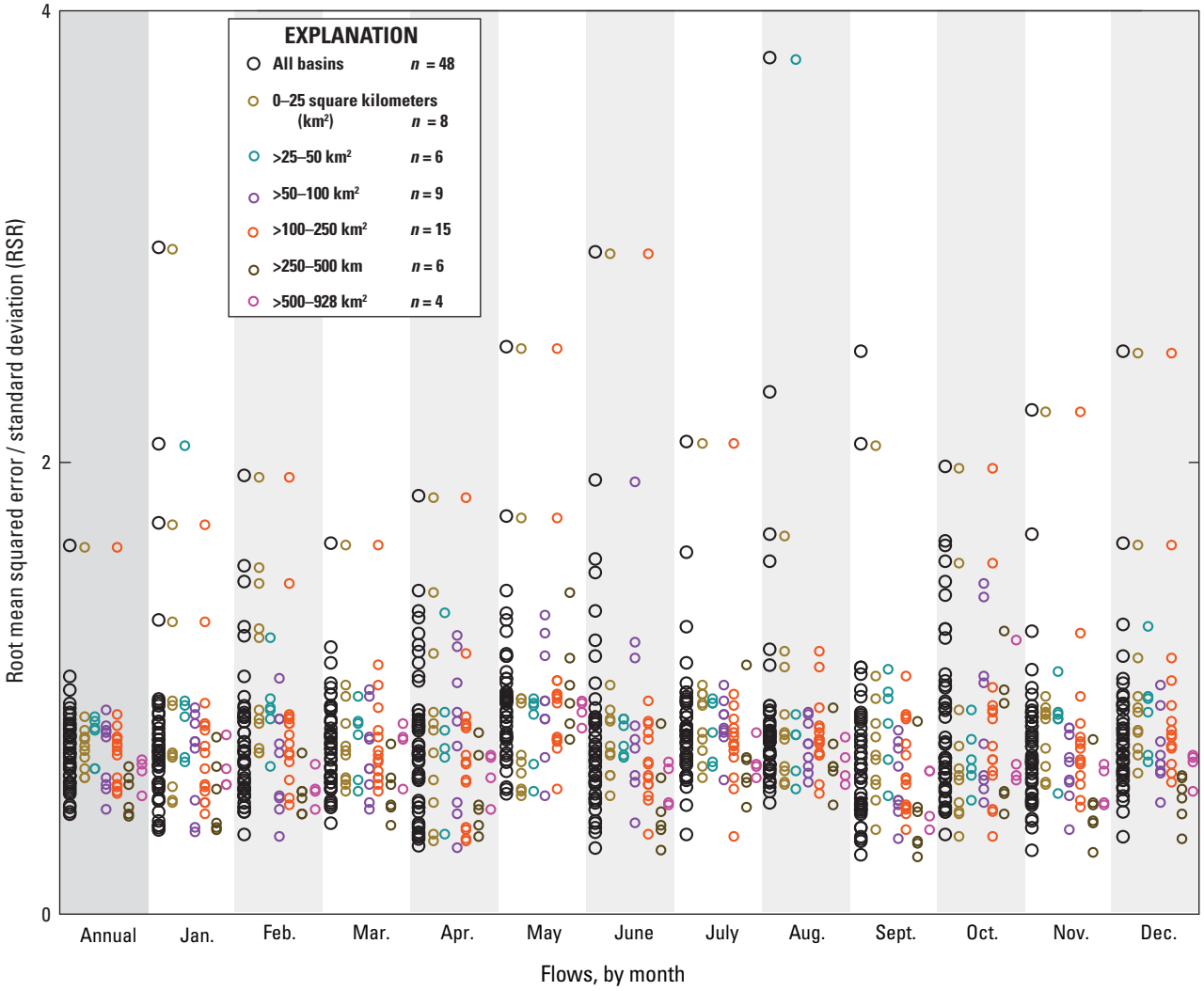

Figure 20. Root mean squared error/standard deviation (RSR) as a function of basin area. Area categories are 0–25 square kilometers (km²), >25–50 km², >50–100 km², >100–250 km², >250–500 km², and >500–928 km².

bias is significantly larger for the smallest streamflows than for the 25–50th streamflow component (p-value = 0.018 and p-value <0.001, respectively); the difficulty in simulating these small streamflows is compounded by the day-to-day deviation of the seasonal water-use estimate from the actual daily value.

Individual streamflow percentiles were also assessed in order to understand if there was a relation of streamflow to land-cover distribution (0–25 percent, >25–50 percent, >50–75 percent, >75–100 percent) or basin size (0–25 km^2, >25–50 km^2, >50–100 km^2, >100–250 km^2, >250–500 km^2, and >500 km^2) (fig. 16); each of the four goodness-of-fit statistics was averaged for sequential ranges of basin area and percentage of forested area. The RMSEn, RSR, and Spearman rho all show similar trends for each of the streamflow percentiles when evaluated as a function of basin area and percentage of forested area. The largest streamflows (≥90th percentile) are the general exception to this and exhibit different bias and RSR relative to the other streamflow percentiles. For example, the RSR for the largest streamflows is lower than that for the other streamflow percentiles; this is true in terms of both forested area and basin size. This is further evidence that bias in the largest streamflows is a function of how precipitation is distributed in the model as opposed to other aspects of the model, because this error is consistent regardless of location within the DRB, basin size, or land-cover distribution. Similarly, those basins smaller than 25 km^2 have the largest RSR and lowest Spearman rho for streamflows <90th percentile; an accurate and precise precipitation distribution, beyond what is available in WATER, is critical in these small basins, where

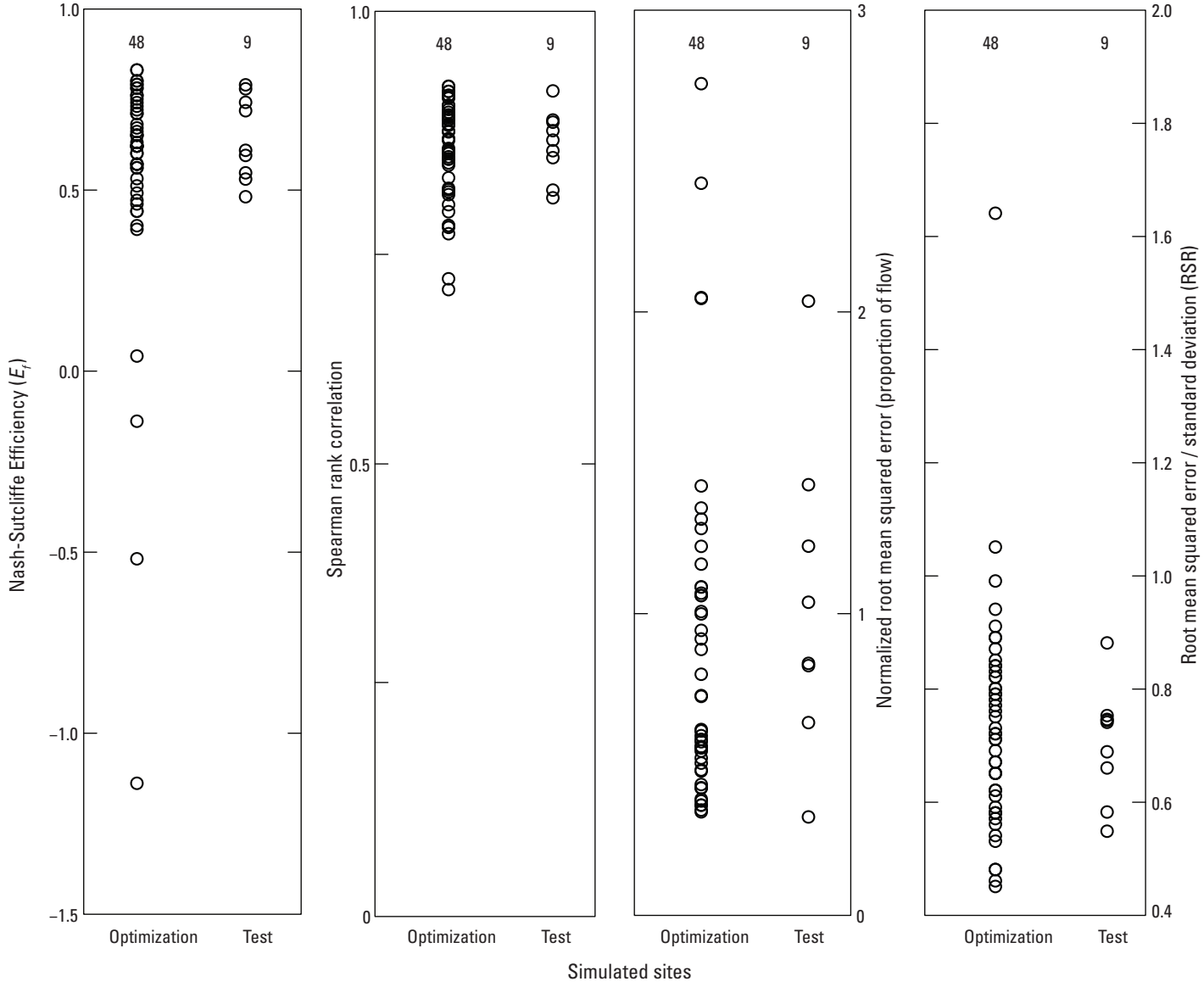

Figure 21. Comparison of four goodness-of-fit statistics for 48 optimization basins and 9 test basins. Note that for each statistic, the nine test basins perform comparably to those basins use for optimization.

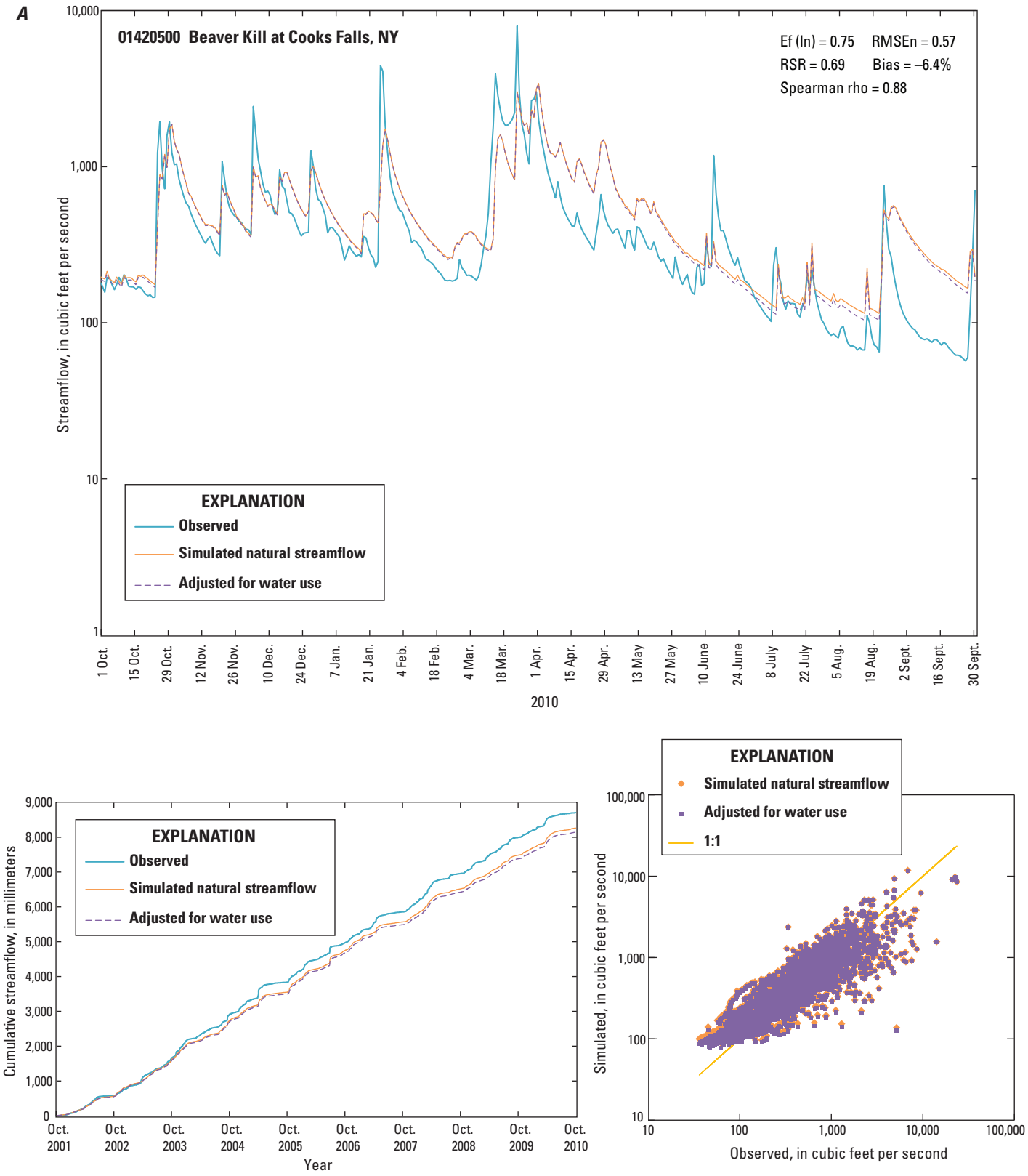

Figure 22. Observed and simulated streamflow for October 1, 2009, through September 30, 2010, with and without water use, together with cumulative streamflow for the 2001–10 period in *A*, a forested basin (01420500 Beaver Kill at Cooks Falls, NY) and *B*, an agricultural basin (01470779 Tulpehocken Creek near Bernville, PA). Note that for the forested basin, there is little change when water use is applied. All plots are at the same scale. Site-specific statistics have also been included. E_f(ln), Nash-Sutcliffe efficiency of the natural log of streamflow; RMSEn, normalized root mean squared error; RSR, ratio of the root mean squared error to the standard deviation of observed streamflow.

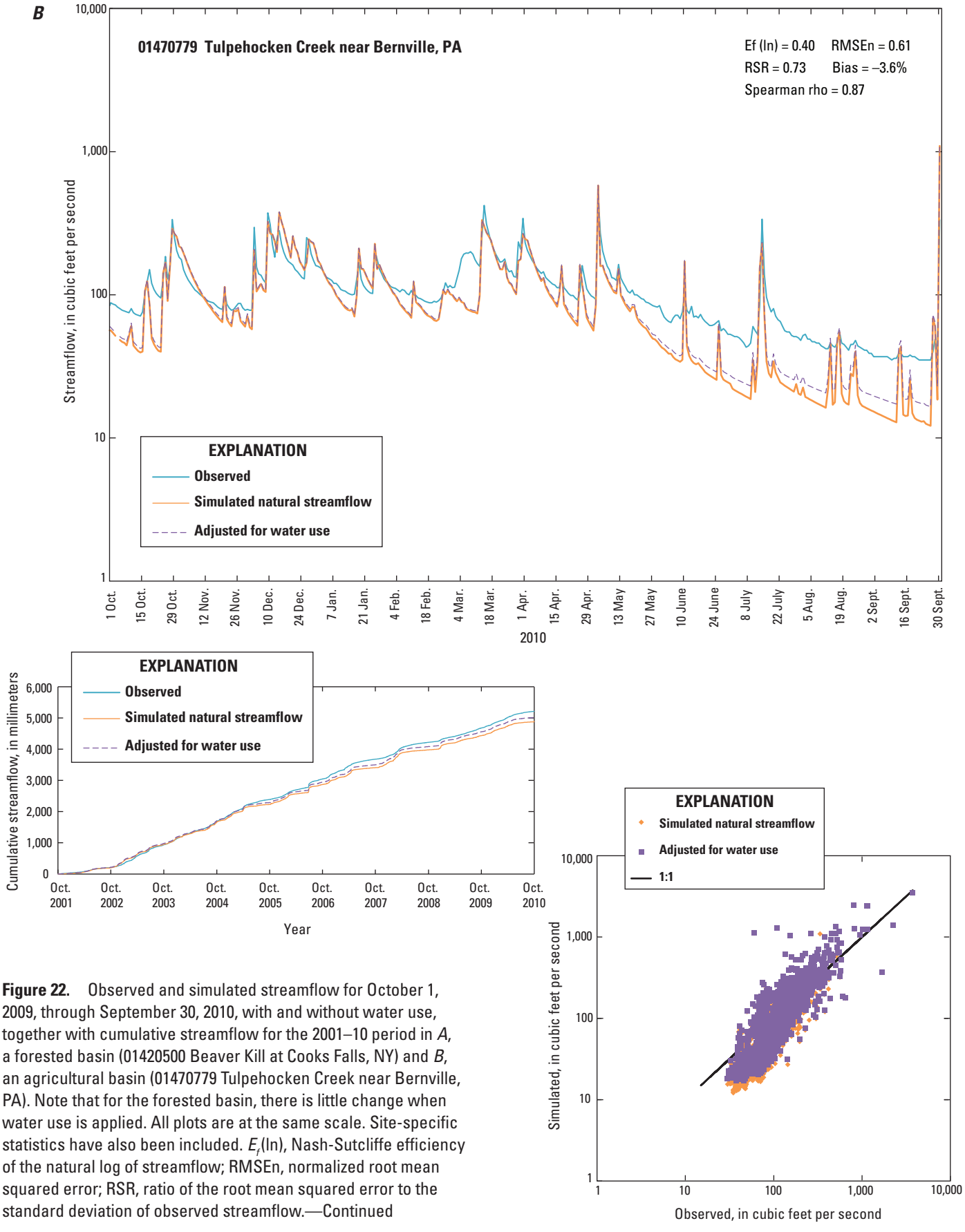

Figure 22. Observed and simulated streamflow for October 1, 2009, through September 30, 2010, with and without water use, together with cumulative streamflow for the 2001–10 period in *A*, a forested basin (01420500 Beaver Kill at Cooks Falls, NY) and *B*, an agricultural basin (01470779 Tulpehocken Creek near Bernville, PA). Note that for the forested basin, there is little change when water use is applied. All plots are at the same scale. Site-specific statistics have also been included. E_f(ln), Nash-Sutcliffe efficiency of the natural log of streamflow; RMSEn, normalized root mean squared error; RSR, ratio of the root mean squared error to the standard deviation of observed streamflow.—Continued

response to individual events can be rapid and directly reflects the magnitude and duration of precipitation as well as local soil-water storage capacity; in contrast, spatial and temporal differences in precipitation and soil-water storage are masked by channel storage and tributary integration that occurs in larger basins (Dingman, 2002). Finally, those basins with the smallest percentage of forested area, where the variability in daily water use combines with localized snowpack management, have a relatively large RSR for streamflows <90th percentile.

To further understand the variability in streamflow simulation, the RMSEn and RSR were examined as a function of both percentage of forested area and basin size by using monthly streamflow distributions (figs. 17–20). The highest monthly RMSEn (fig. 17) is in September for 01422738—Wolf Creek at Mundale, N.Y., the smallest basin evaluated (1.6 km^2); this is one of the two months for which a nearby basin (01422389–Coulter Brook near Bovina, N.Y. [2.0 km^2]) has zero-streamflow days. In general, RMSEn is higher in the warmer and drier months (July–October) when individual plant species, beyond the specification of the forested HRU, can increase their rooting depth in response to soil-water stress and access deeper soil layers not used during the rest of the growing season. Those basins with >75-percent-forested area also have higher RMSEn in January relative to the February–June period—most of these basins are in the northern part of the DRB, where simulation of daily snow accumulation and snowmelt processes are likely compounding model error. The RSR of these same basins is larger in October and June, a month later in the spring than for those basins with 25–50-percent-forested area (fig. 18). This may be related to the transition into and out of the aggressive ET period of the year, which starts later in the northern part of the DRB, where those basins with >75-percent-forested area are concentrated (fig. 4). The highest monthly RSR is in August for USGS site 01484000—Murderkill River near Felton, Del.; this site is at the fringe of the tidally influenced area, where the low streamflows may be impacted by high tides (fig. 3).

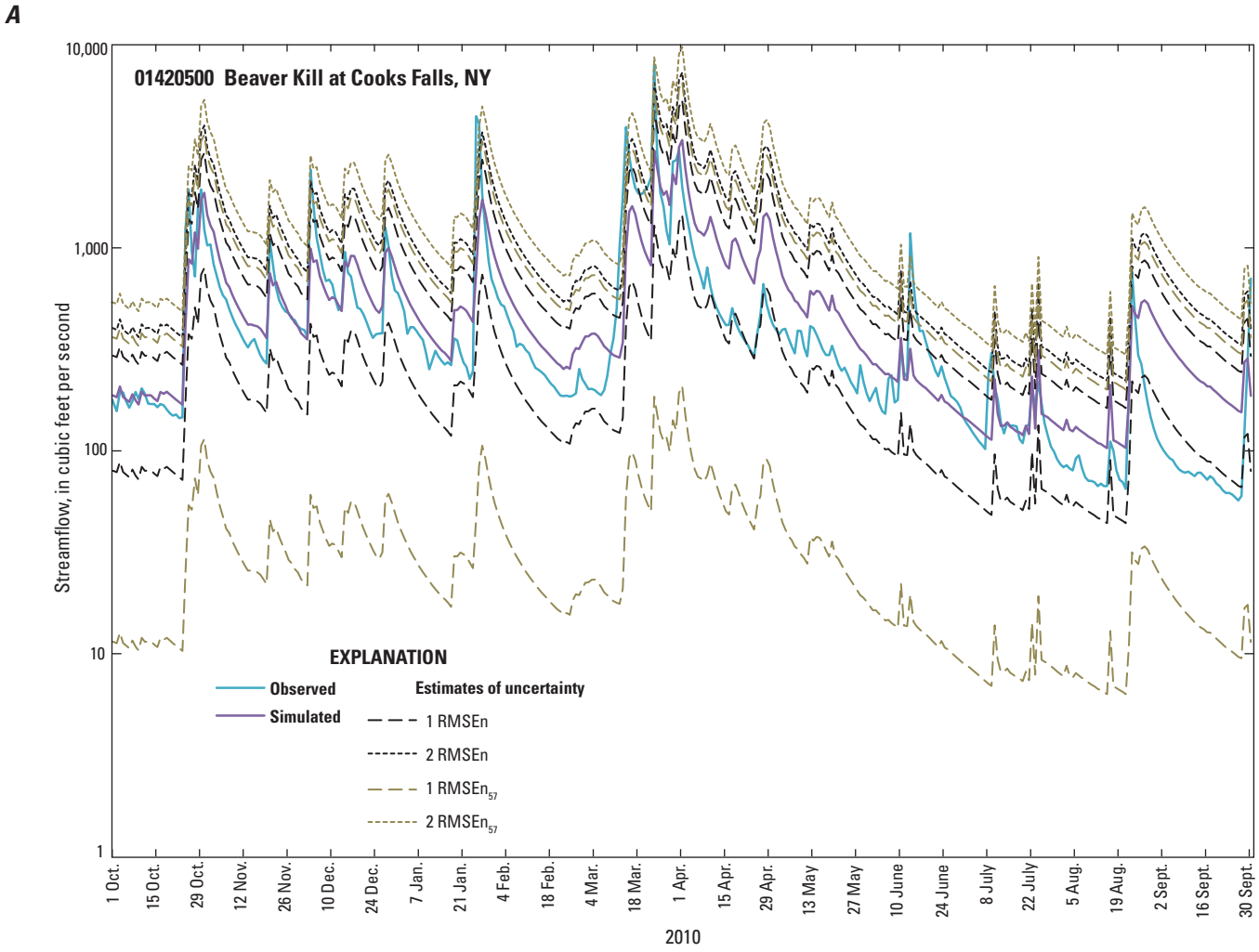

Figure 23. Examples of observed and simulated streamflow for *A*, a forested basin and *B*, an agricultural basin with four different uncertainty ranges: ±1 normalized root mean squared error from individual sites (RMSEn), ±2 RMSEn, ±1 normalized root mean squared error averaged from all sites ($RMSEn_{57}$), and ±2 $RMSEn_{57}$.

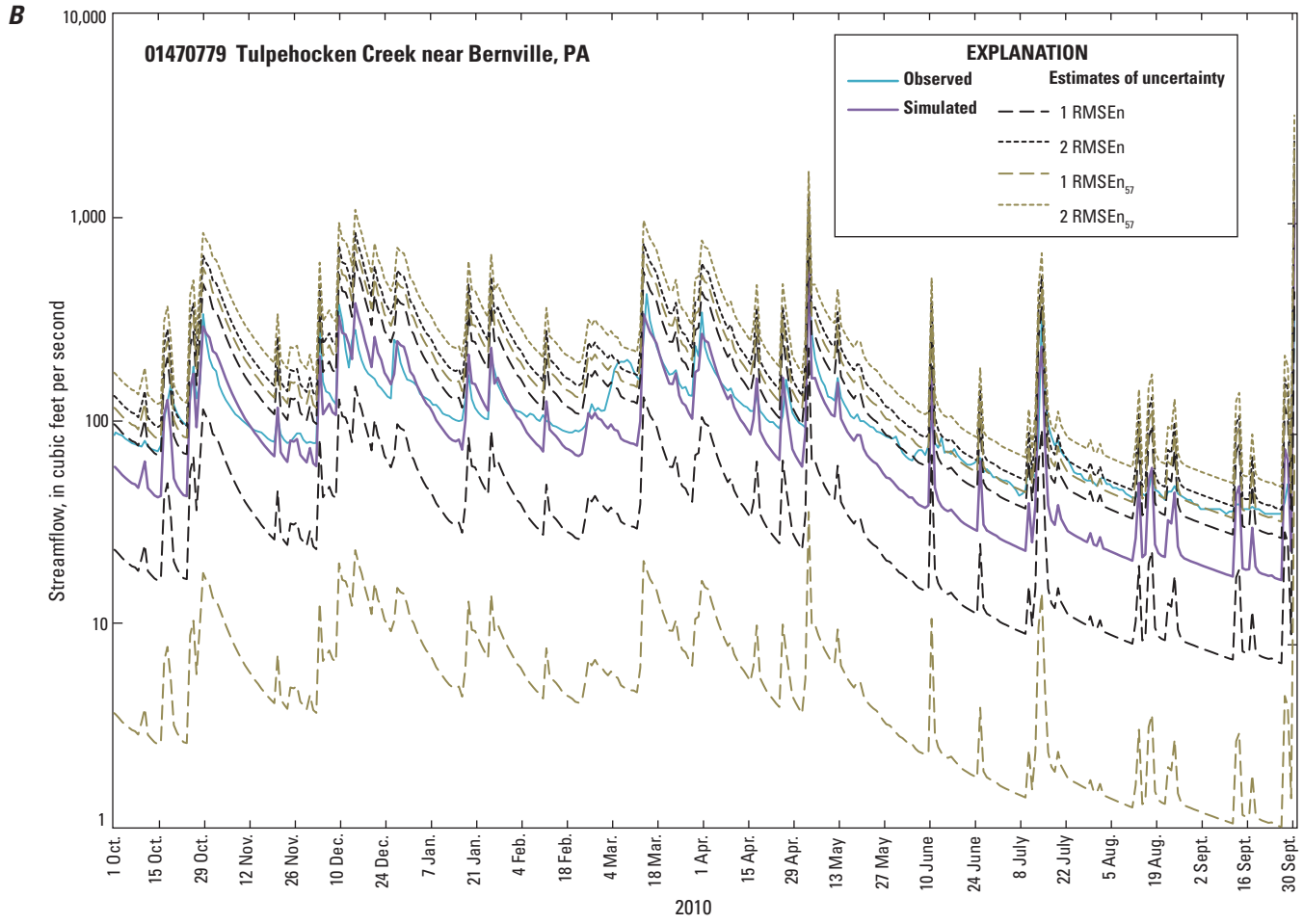

Figure 23. Examples of observed and simulated streamflow for *A*, a forested basin and *B*, an agricultural basin with four different uncertainty ranges: ±1 normalized root mean squared error from individual sites (RMSEn), ±2 RMSEn, ±1 normalized root mean squared error averaged from all sites ($RMSEn_{57}$), and ±2 $RMSEn_{57}$.—Continued

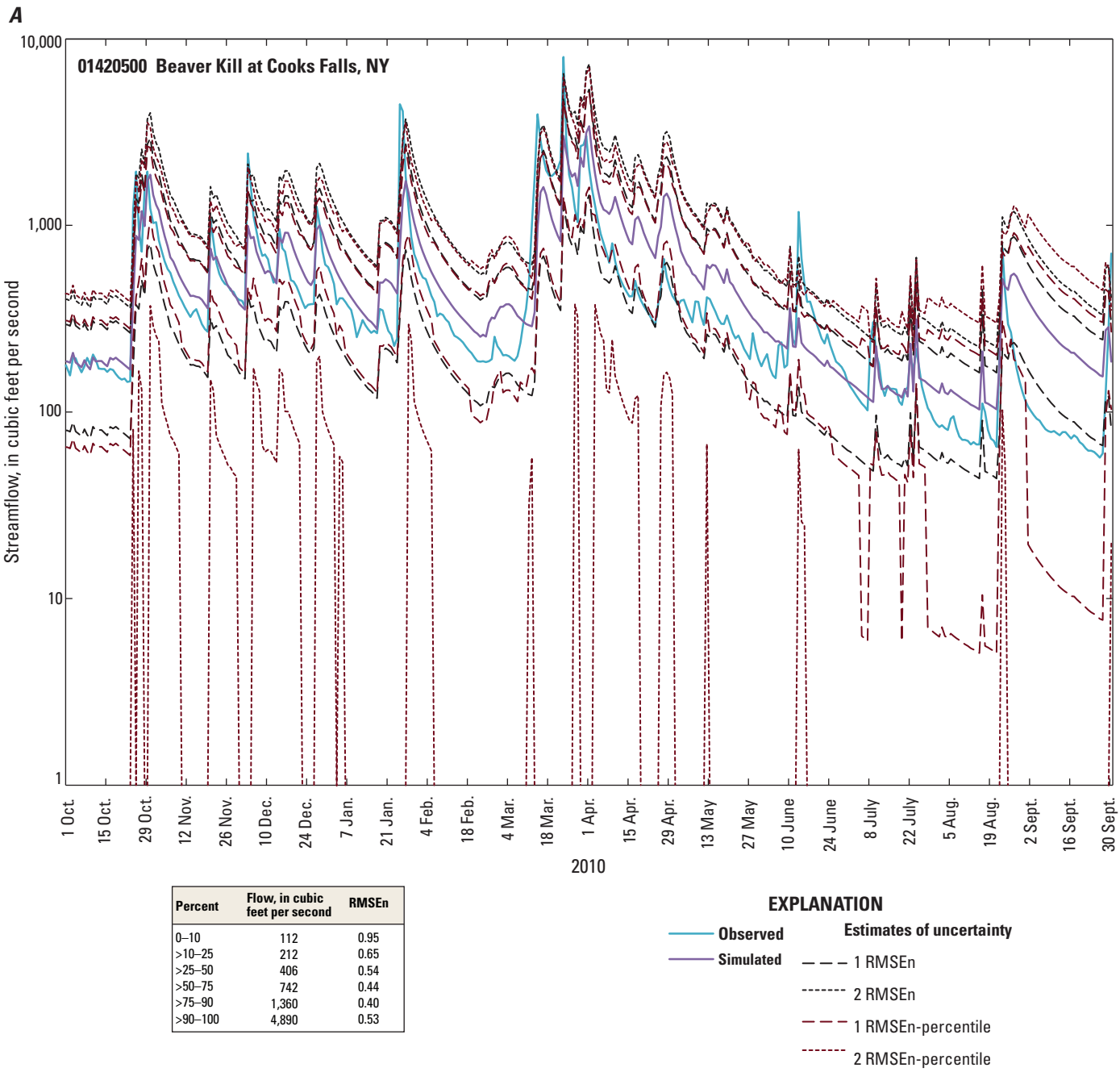

Figure 24. Examples from *A*, a forested basin (01420500 Beaver Kill at Cooks Falls, NY) and *B*, an agricultural basin (01470779 Tulpehocken Creek near Bernville, PA) of observed and simulated streamflow with site-specific uncertainty ranges from normalized root mean squared error (±1 RMSEn and ±2 RMSEn from figure 23) and for individual streamflow components (±1 RMSEn-percentile and ±2 RMSEn-percentile, values shown as inset). Note that axis has been shifted for agricultural basin B but that the range shown includes the same orders of magnitude.

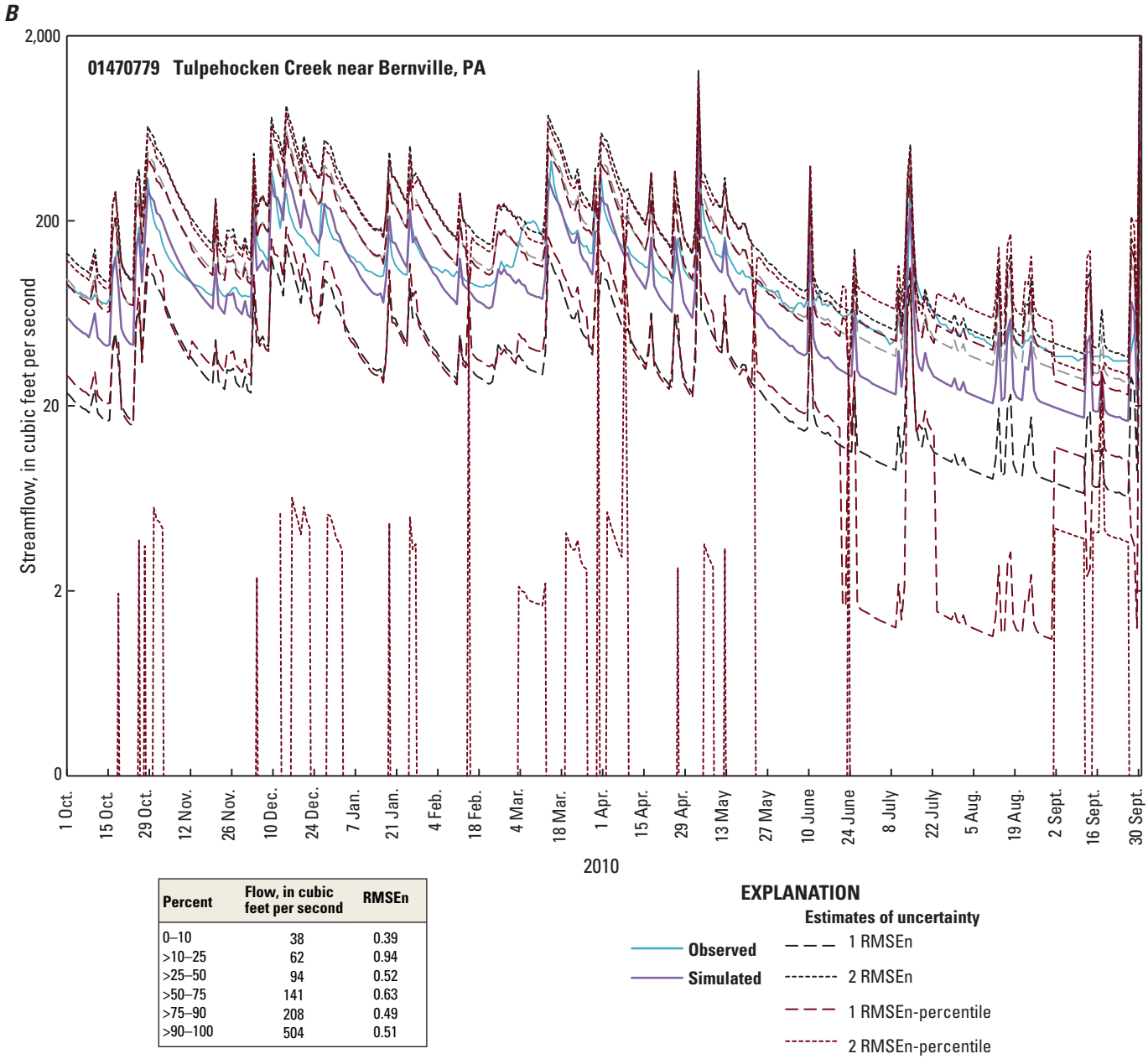

Percent	Flow, in cubic feet per second	RMSEn
0–10	38	0.39
>10–25	62	0.94
>25–50	94	0.52
>50–75	141	0.63
>75–90	208	0.49
>90–100	504	0.51

Figure 24. Examples from *A*, a forested basin (01420500 Beaver Kill at Cooks Falls, NY) and *B*, an agricultural basin (01470779 Tulpehocken Creek near Bernville, PA) of observed and simulated streamflow with site-specific uncertainty ranges from normalized root mean squared error (±1 RMSEn and ±2 RMSEn from figure 23) and for individual streamflow components (±1 RMSEn-percentile and ±2 RMSEn-percentile, values shown as inset). Note that axis has been shifted for agricultural basin B but that the range shown includes the same orders of magnitude.—Continued

Table 9. Number of days of observed streamflow not bounded by normalized root mean squared error (RMSEn)-based confidence intervals over the period of record at two sites in the Delaware River Basin, including the site-specific RMSEn, the average RMSEn from 57 sites, and the site-specific RMSEn for the observed streamflow percentile.

[*n*=3,287 days. USGS, U.S. Geological Survey; ID, identification number; RMSEn, normalized root mean squared error; %, percent]

USGS site ID	Observed streamflow not bounded by confidence interval, in days			
	+1 RMSEn	-1 RMSEn	+2 RMSEn	-2 RMSEn
	Site specific			
01420500	345 (10%)	108 (3.3%)	163 (5.0%)	0 (0%)
01470779	1165(35%)	39 (1.2%)	219 (6.7%)	0 (0%)
	Average for all sites (n=57)			
01420500	207 (6.3%)	0 (0%)	74 (2.3%)	0 (0%)
01470779	618 (19%)	1 (0.03%)	42 (1.3%)	0 (0%)
	By observed streamflow percentile			
01420500	414 (12.6%)	147 (4.5%)	208 (6.3%)	0 (0%)
01470779	1165 (35.4%)	39 (1.2%)	219 (6.7%)	0 (0%)

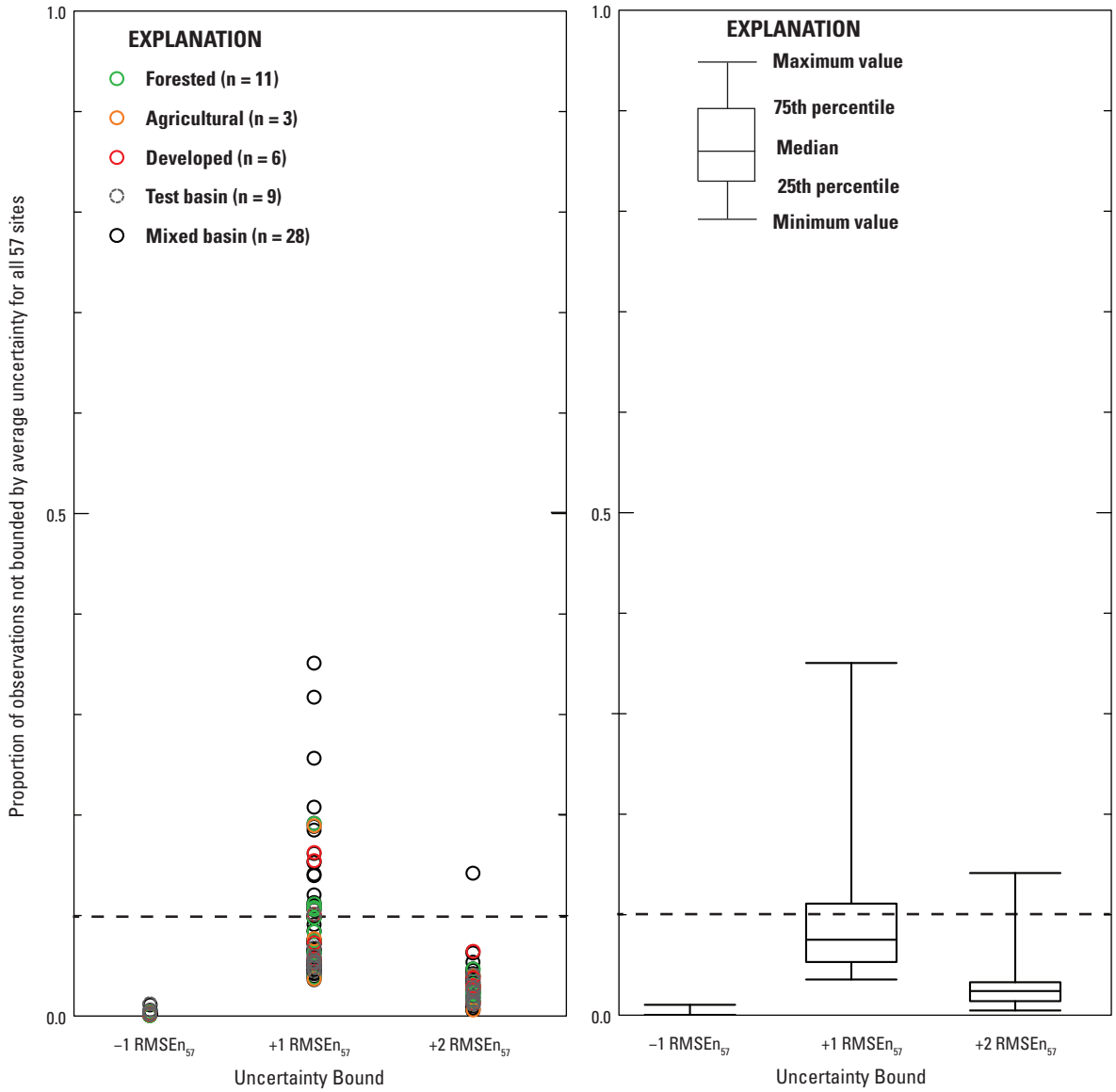

Figure 25. The proportion of days, over the period of record for all 57 statistical evaluation sites in the Delaware River Basin, on which observed streamflow is not bounded by the confidence interval based on the average normalized root mean squared error ($RMSEn_{57}$) for all sites. Only Monocacy Creek near Bethlehem, Pennsylvania, has less than 90 percent of the streamflows bounded by +2/-1 RMSEn. Data are shown both as individual points, with basin types differentiated, and as a boxplot for all 57 observations.

When these same statistics are considered as a function of basin area (figs. 19 and 20), the error in the smallest basins appears to follow a seasonal trend, with higher error optimization in winter and summer relative to spring and fall. These small basins include those with 11.9–99.5-percent-forested area, so this error is not interpreted to be a function of land use. Again, this higher error is likely a function of the random distribution of precipitation by the model, which is unlikely to perfectly mimic actual events; this precipitation distribution is especially important in smaller basins where response to individual events can be rapid (Dingman, 2002). The seasonal trend in error becomes less apparent as basin size increases.

Nine basins, ranging in size from 2 to 348 km^2, were used to test model performance for basins not included in any part of the optimization process (figs. 4 and 21). For each statistic, these test basins performed comparably to those 48 basins used for optimization of WATER parameters and incorporation of water-use data. When these nine sites are incorporated, the mean RMSEn for all sites increases from 0.875 to 0.939, and the median changes from 0.614 to 0.762; the mean RMSEn for the nine test basins is 1.27, and the median is 1.04.

Two basins will be used as examples to further illustrate model performance; one is predominantly forested (fig. 22*A*), and the other is predominantly agricultural (fig. 22*B*). Over the 9-year period evaluated, there was an average underestimation of cumulative streamflow of 62.3 millimeters per year (mm/yr; 49.1 mm/yr without water use) in the forested basin. The agricultural basin had an average underestimation of 20.8 mm/yr (36.0 mm/yr without water use).

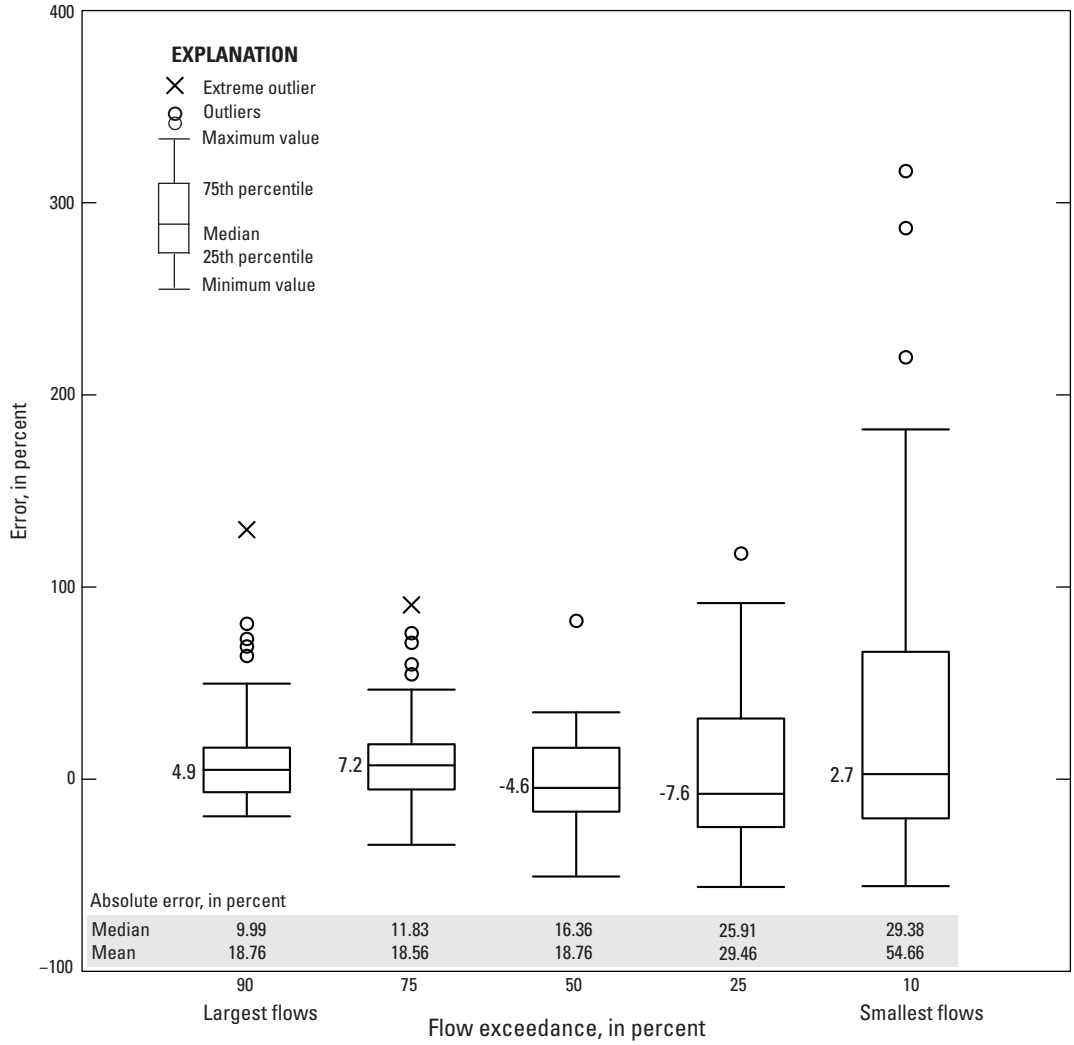

Figure 26. The percentage of error for each streamflow percentile (*n*=57 sites) in the flow-duration curve; median error is notated on the graph. Median and mean values of absolute error for each percentile are summarized at bottom. All data are shown.

Estimating Uncertainty for Daily Streamflow Simulations by Using the Normalized Root Mean Squared Error

The RMSEn provides an estimation of uncertainty for the simulations that can be transitioned to simulations at ungaged sites and those involving scenario testing; this statistic is essentially a proportional error of daily streamflow simulation. For each of the 57 sites, the site-specific RMSEn was applied to the simulated discharge and compared to uncertainty bounds by using the mean RMSEn (an average of the RMSEn for all 57 sites; $RMSEn_{57}$) as well as the site-specific RMSEn for each streamflow percentile as indicated by the observed streamflow. For the two basins shown (figs. 23 and 24), on the basis of the site-specific RMSEn, >90 percent of the streamflows are bounded by the addition of 2 RMSEn and subtraction of 1 RMSEn (+2/-1 RMSEn; fig. 23); this is also true for the mean $RMSEn_{57}$ (0.939; n=57) and for the RMSEn specific to the observed streamflow percentile for each site (fig. 24 and table 9). When all 57 sites are considered (fig. 25) by using the mean $RMSEn_{57}$, only Monocacy Creek near Bethlehem, Pa., has <90 percent of the streamflows bounded by +2/-1 $RMSEn_{57}$; the remaining 56 sites have >93 percent of the individual days bounded by +2/-1 $RMSEn_{57}$, and 53 of these have >95 percent of days bounded by +2/-1 $RMSEn_{57}$. Note that this error is not a function of land cover as is shown by the distribution of the different land-cover groupings (table 3) in the plot.

Evaluation of Daily Streamflow Distribution by Using the Flow-Duration Curve

As was discussed in a comparison of hydrologic flow models for the southeast U.S. (Farmer and others, 2015), the daily flow-duration curve (FDC) is a representation of the distribution of daily streamflow at a given site. The FDC is used to understand the average streamflows and extreme events in a basin for the period of record by quantifying, for example, the streamflow value that exceeds 90 percent of the streamflow record (percentile = 0.9). Five streamflow percentiles (0.1, 0.25, 0.5, 0.75, 0.9) were evaluated for each of the 57 evaluated sites by using the RMSEn and bias statistics used for daily streamflow. When this cumulative distribution function is compared for each site (n=5 streamflow percentiles), there is a median RMSEn of 0.44 for all sites. When the streamflow percentiles are evaluated independently (n=57 sites; fig. 26 and table 10), there are significant differences in percentage of error (100 × [sim–obs]/obs) among the streamflow percentiles, with absolute error decreasing as the magnitude of streamflow increases. This is consistent with the statistical evaluation of daily streamflow, which indicates that the smallest streamflows have the largest proportion of error; however these smallest streamflows also have the largest observed variability (fig. 15). Together, this statistical evaluation of daily streamflow and the aggregated streamflow percentiles indicates that although there is a difference in the ability to differentiate among the individual streamflow percentiles, the higher observed variability during low-streamflow conditions, relative to those that exceed the smallest 25 percent of streamflows, suggests that uncertainty is similar for the entire streamflow record.

Evaluation of Mean Monthly Streamflow Simulations by Using Normalized Root Mean Squared Error

The WATER DSS was developed to provide a modeling environment that could be used to evaluate land-cover, climate, and water-use-allocation scenarios. For scenario testing, each of these variables is altered on a monthly, seasonal, and (or) decadal time step. Consequently, it is recommended that the change associated with scenarios be evaluated at a monthly time step that is normalized for the 25-year climatic record.

Evaluation of mean monthly streamflow simulations focused on the RMSEn, a statistic that quantifies error as a percentage of the streamflow value so can be most easily transferred to streamflow simulation at ungaged sites; site period of record ranged from 12 to 108 months for 57 sites. Two sites, Beaver Kill at Cooks Falls, N.Y., and Tulpehocken Creek near Bernville, Pa., were used to illustrate the difference in observed and simulated mean monthly streamflows over the 2001–10 time period (fig. 27). The RMSEn for mean monthly streamflows ranged from 0.226–6.253 for all 57 sites, with a mean of 1.15 and a median of 0.526. However, when only those 45 sites with a full 108 months (9 years) were included (table 1), the maximum was 1.61, the mean was 0.527, and the median was 0.400. This mean RMSEn for (0.527, n=45)

Table 10. Results of Wilcoxon signed-rank test comparing the error for each streamflow percentile from the flow-duration curve for all 57 sites in the Delaware River Basin. Values shown are p-values from paired tests. Significant differences are indicated by asterisks (*). For example, there is no significant difference (p-value = 0.263) between error in simulation of the lowest 10 percent of streamflows and the error in simulation of the highest 10 percent of streamflows (90th percentile). Data are shown in figure 26.

[%, percent, <, less than; —, not applicable]

p-values		Streamflow percentile			
		25%	50%	75%	90%
Streamflow percentile	10%	<0.001*	0.001*	0.201	0.263
	25%	—	0.505	0.029*	0.066
	50%	—	—	<0.001*	0.008*
	75%	—	—	—	0.703

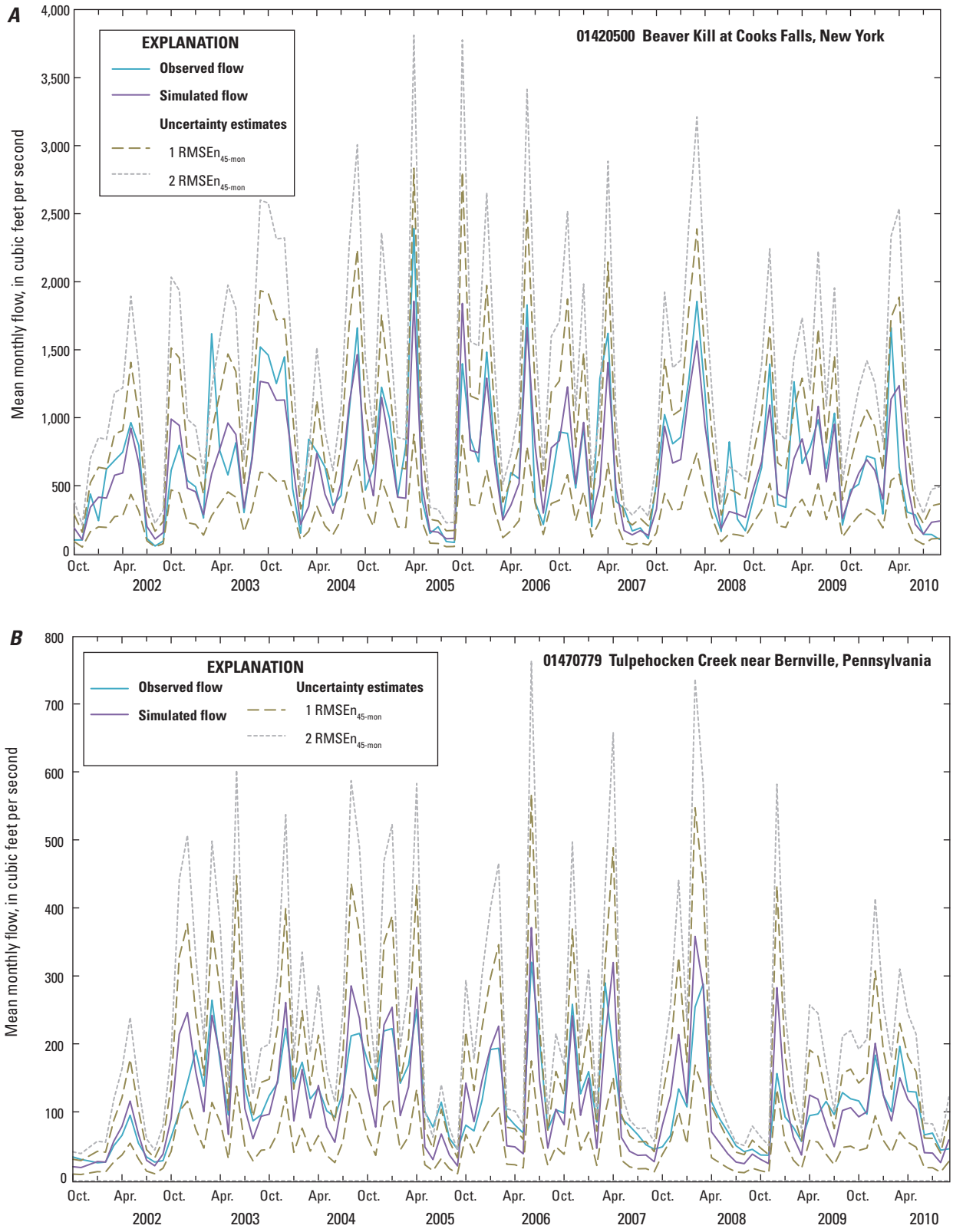

Figure 27. Examples from *A*, a forested basin (01420500 Beaver Kill at Cooks Falls, NY) and *B*, an agricultural basin (01470779 Tulpehocken Creek near Bernville, PA) of observed and simulated mean-monthly streamflow with uncertainty ranges from normalized root mean squared error (RMSEn) averaged from all sites in the Delaware River Basin with 108-month (9-year) records ($RMSEn_{45\text{-}mon}$ = 0.527).

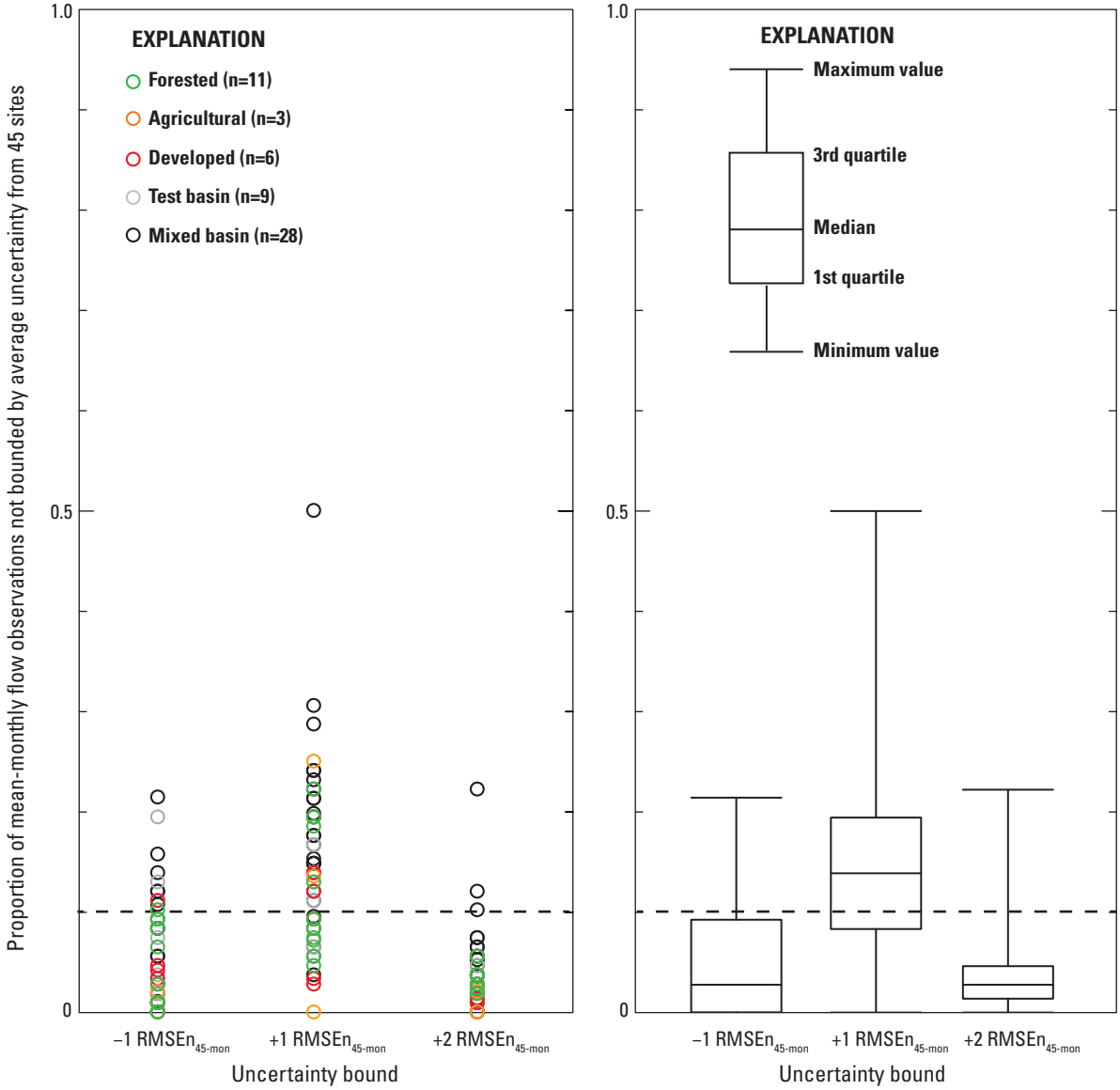

Figure 28. The proportion of period of record during which the mean monthly observed streamflow is not bounded by the confidence interval based on the normalized root mean squared error (RMSEn) over the period of record for all 45 validation sites in the Delaware River Basin with an observation period of 108 months ($RMSEn_{45\text{-}mon}$=0.527). Fourteen sites have less than 90 percent of the streamflows bounded by +2/-1 $RMSEn_{45\text{-}mon}$. Data are shown both as individual points, with basin types differentiated, and as a boxplot for all 57 observations.

Table 11. Number of months of observed mean monthly streamflow not bounded by the confidence interval based on the mean normalized root mean squared error (RMSEn) over the period of record for all 45 validation sites in the Delaware River Basin with an observation period of 108 months ($RMSEn_{45\text{-}mon}$=0.527), for Beaver Kill, New York, and Tulpehocken Creek, Pennsylvania, sites in the Delaware River Basin.

[USGS, U.S. Geological Survey; ID, identification number; RMSEn, normalized root mean squared error; %, percent]

USGS site ID	Months not bounded by confidence interval, as total (and percentage)			
	+1 RMSEn	-1 RMSEn	+2 RMSEn	-2 RMSEn
01420500	9 (8.3%)	1 (0.9%)	4 (3.70%)	0 (0%)
01470779	27 (25.0%)	1 (0.9%)	2 (1.85%)	0 (0%)

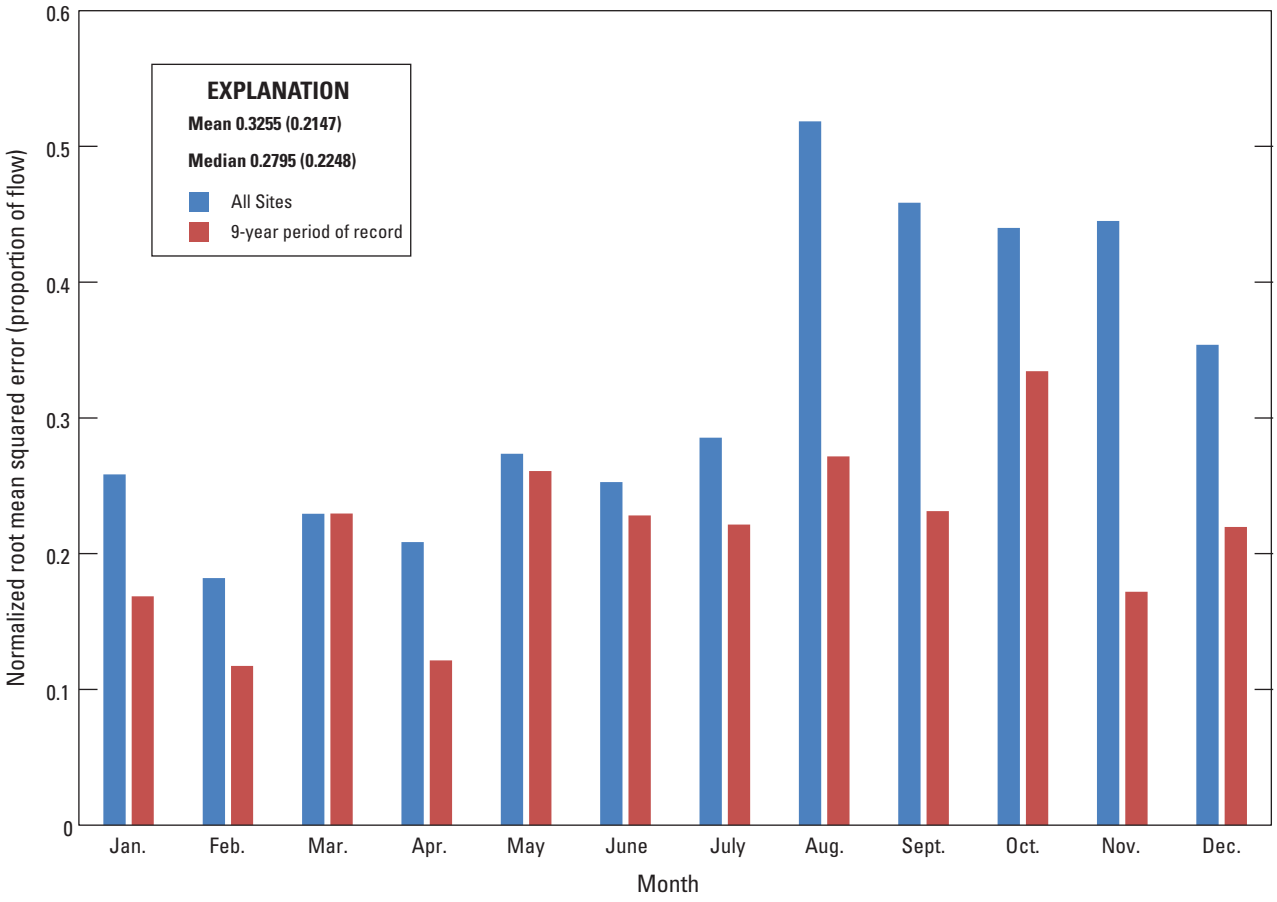

Figure 29. Root mean squared error (RMSEn) for mean monthly streamflow normalized for the period of record for all 57 sites in the Delaware River Basin and for the 45 sites with a 9-year period of record (in parentheses).

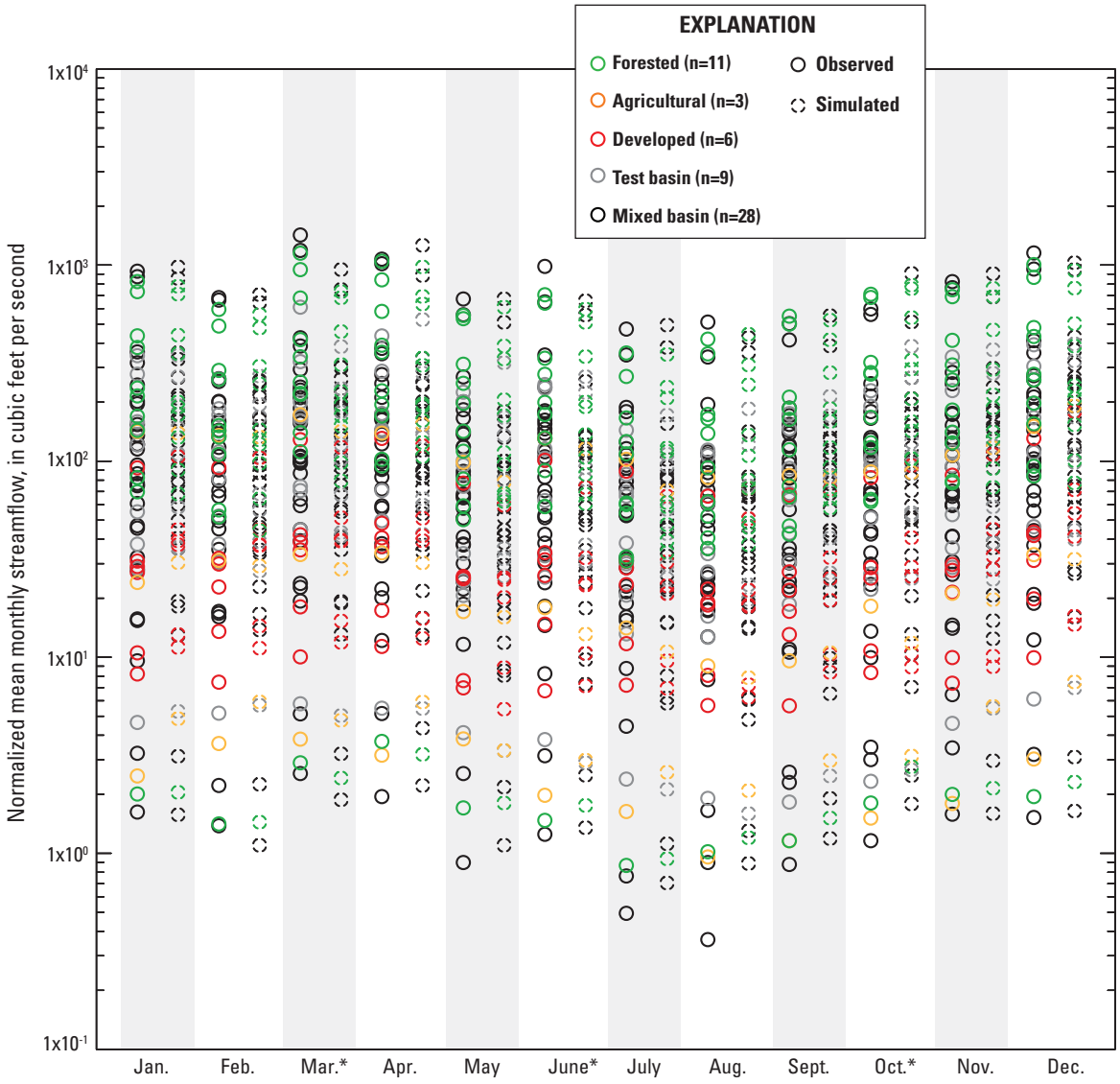

Figure 30. Observed and simulated mean-monthly streamflow normals for 2001–10 time period for 57 sites in the Delaware River Basin. Asterisk (*) indicates that observed and simulated monthly normals significantly differ for those 45 sites with a full 108-month period of record.

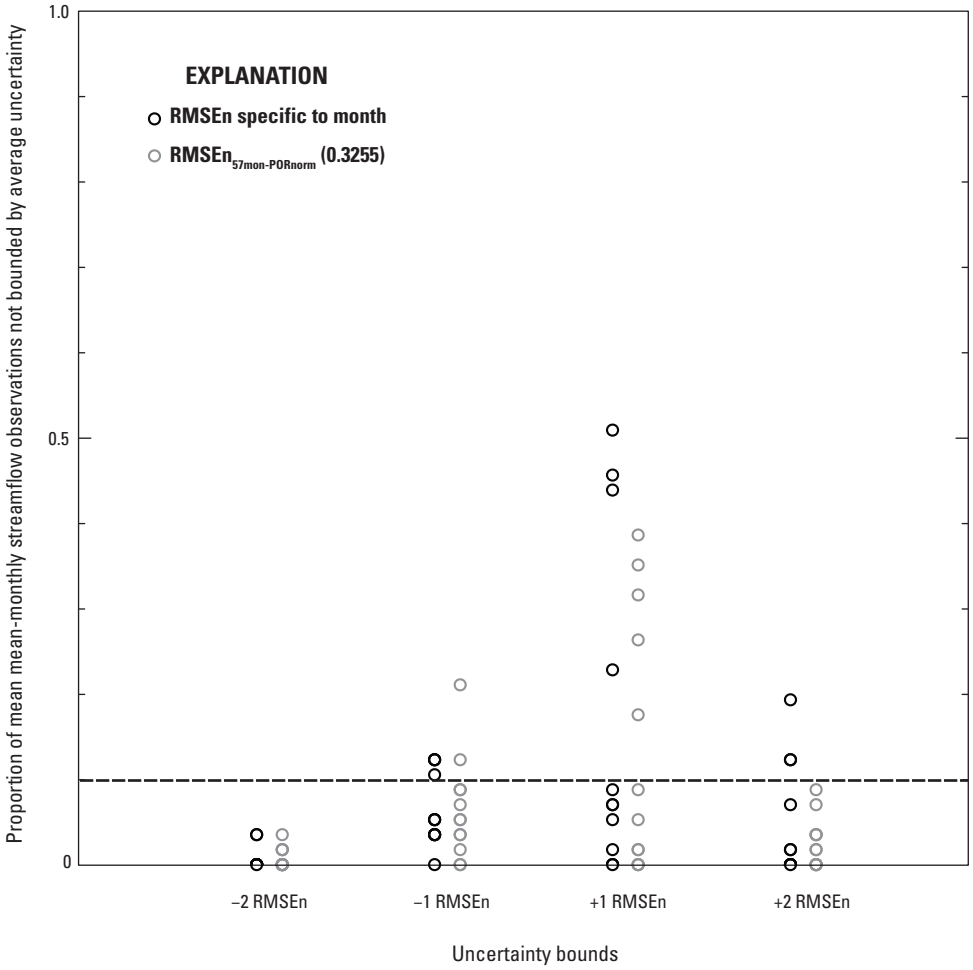

Figure 31. Proportion of mean monthly-streamflow normals (*n*=12 months) not bounded by simulated discharge if using either the month-specific (shown in figure 29) or averaged nomralized root mean squared error (RMSEn) of the normalized mean-monthly streamflow ($RMSEn_{57mon\text{-}PORnorm}$) for all 57 sites in the Delaware River Basin.

was used to estimate uncertainty for mean monthly streamflow simulations ($RMSEn_{45\text{-}mon}$). Similarly to the daily simulations, a confidence interval of +2/-1 $RMSEn_{45\text{-}mon}$ bounds >95 percent of the streamflows for the two example sites (fig. 28 and table 11). When these uncertainty bounds are applied to all 57 validation sites, two sites have >10 percent of mean monthly streamflows not bounded by +2 $RMSEn_{45\text{-}mon}$, and 12 sites have >10 percent of mean monthly streamflows that are not bounded by -1 $RMSEn_{45\text{-}mon}$. Monocacy Creek near Bethlehem, Pa., is the most poorly estimated, with 24 of 108 months not included in the +2 $RMSEn_{45\text{-}mon}$/-1 $RMSEn_{45\text{-}mon}$ uncertainty bounds. Again, it should be noted that this uncertainty is not a function of land-cover; this is critical if scenario testing will incorporate land-cover forecasts.

When the mean monthly streamflow is normalized for the period of record, with a single mean for each month for each site, error is generally highest during the late summer and fall (fig. 29), although this seasonal difference is smaller when only those sites with a full 9-year period of record are included. When the observed and simulated mean streamflow for each month are compared for all 57 sites, only March, June, and October significantly differ (fig. 30). When the mean monthly streamflow normalized for the period of record is bounded by using the mean RMSEn uncertainty ($RMSEn_{57mon\text{-}PORnorm=0}$.3255), a +2/-2 $RMSEn_{57mon\text{-}PORnorm}$ is needed to bound >90 percent of the monthly streamflow estimates (fig. 31). Depending on the question being asked, one could use the RMSEn normalized for each month (fig. 31); however, there is little difference between this and using the overall mean.

Evaluating the mean monthly streamflow over the period of record used for validation is analogous to evaluating mean monthly streamflows by using monthly normals when implementing scenario testing for land-cover, climate, or water-use changes. Consequently, applying an uncertainty of +2/-2 $RMSEn_{57mon\text{-}PORnorm}$ (0.3255 × mean monthly streamflow) is recommended for quantifying expected streamflow magnitudes.

Summary

The Water Availability Tool for Environmental Resources (WATER) decision support system (DSS) was developed to provide the Delaware River Basin community an ability to investigate the potential effects of different management decisions, forecasted changes in climate, and land-cover change. Although the WATER DSS can be used for the entire Delaware River Basin, there are some streams, including those downstream of regulated reservoirs and those within the tidal zone, where simulations should only be used for general information. WATER provides consistent simulation of hydrologic conditions, including high and low streamflows, for basins with ranges of size, land cover, and location within the Delaware River Basin. Individual hydroclimatic components of the water budget are also effectively simulated. Consequently, this process-based, regionally calibrated DSS can be used to investigate the sustainability and resiliency of water-resources as a result of forecasted environmental and management scenarios. Scenario testing can be accomplished because the WATER DSS provides for potential changes in both the natural and the anthropogenic environment by independently incorporating land-cover, climate, and landscape (topography and soils) characteristics.

Ultimately, it is the responsibility of the user to interpret results. However, some precautions and suggestions for use of the WATER DSS follow:

1. An uncertainty range of +2/-1 normalized root mean squared error averaged from all sites ($RMSEn_{57}$; 0.939) is recommended for daily streamflow simulations.

2. For those scenarios involving general circulation model (GCM) data and land-cover change, mean monthly streamflows, not mean daily streamflows, should be the finest unit considered because GCM data are applied by using a monthly normal and land-cover simulations were derived at a decadal time step. Normalized mean monthly streamflow (in other words, streamflow averaged for each month for the 25-year climate record) should be used with the normalized root mean squared error that has been normalized for the period of record for all 57 sites ($RMSEn_{57mon\text{-}PORnorm}$; 0.3255) to quantify the forecasted range of streamflow and water availability for a given scenario.

3. All scenarios should be compared to simulation of the same site by using the historical conditions (2011 National Land Cover Database and 2010 water use) provided with the DSS. This is similar to the approach illustrated with the determination of the GCM change factor calculations. Multiple GCMs and representative concentration pathways should be incorporated in scenario testing, and the overall trend in streamflow and other hydroclimatic variables among multiple GCM simulations should be used to plan for forecasted change.

References Cited

Band, L.E., Patterson, Pitman, Nemani, Ramakrishna, and Running, S.W., 1993, Forest ecosystem processes at the watershed scale—Incorporating hillslope hydrology: Agricultural and Forest Meteorology, v. 63, nos. 1–2, p. 93–126.

Band, L.E., Peterson, D.L., Running, S.W., Coughlan, Joseph, Lammers, Richard, Dungan, Jennifer, and Nemani, Ramakrishna, 1991, Forest ecosystem processes at the watershed scale—Basis for distributed simulation: Ecological Modelling, v. 56, p. 171–196.

Beven, K.J., 1984, Infiltration into a class of vertically non-uniform soils: Hydrological Sciences Journal, v. 29, no. 4, p. 425–434.

Beven, K.J., 1986a, Hillslope runoff processes and flood frequency characteristics, in Abrahams, A.D., ed., Hillslope processes: London, Allen and Unwin, p. 187–202.

Beven, K.J., 1986b, Runoff production and flood frequency in catchments of order n—An alternative approach, in Gupta, V.K., Rodríguez-Iturbe, Ignacio, and Wood, E.F., eds., Scale problems in hydrology—Runoff generation and basin response: Dordrecht, The Netherlands, D. Reidel Publishing Company, p. 107–131.

Beven, K.J., and Kirkby, M.J., 1979, A physically based, variable contributing area model of basin hydrology/Un modèle à base physique de zone d'appel variable de l'hydrologie du bassin versant: Hydrological Sciences Bulletin, v. 24, no. 1, p. 43–69.

Beven, K.J., Kirkby, M.J., Schofield, N., and Tagg, A.F., 1984, Testing a physically-based flood forecasting model (TOPMODEL) for three U.K. catchments: Journal of Hydrology, v. 69, nos. 1–4, p. 119–143.

Beven, K.J., and Wood, E.F., 1983, Catchment geomorphology and the dynamics of runoff contributing areas: Journal of Hydrology, v. 65, nos. 1–3, p. 139–158.

Beven, K.J., Wood, E.F., and Sivapalan, Murugesu, 1988, On hydrological heterogeneity—Catchment morphology and catchment response: Journal of Hydrology, v. 100, nos. 1–3, p. 353–375.

Brasington, James, and Richards, Keith, 1998, Interactions between model predictions, parameters and DTM scales for TOPMODEL: Computers and Geosciences, v. 24, no. 4, p. 299–314.

Claggett, P.R., Irani, F.M., Thompson, R.L., and Stubbs, Q., 2014, A new approach to regional urban change modeling: introducing the CBLCM v3a, in Chesapeake community modeling program's annual symposium, Annapolis, MD, accessed August 26, 2015 at http://www.chesapeakemeetings.com/CheMS2014/sessions.php.

Clark, K.L., Skowronski, Nicholas, Gallagher, Michael, Renninger, Heidi, and Schäfer, Karina, 2012, Effects of invasive insects and fire on forest energy exchange and evapotranspiration in the New Jersey pinelands: Agricultural and Forest Meteorology, v. 166–167, p. 50–61.

Delaware Office of Management and Budget [Delaware OMB], 2007, 2007 Delaware land use dataset: Delaware Office of Management and Budget dataset, accessed November 7, 2013, at http://opendata.firstmap.delaware.gov/.

Delaware River Basin Commission [DRBC], 2013, Delaware River Basin code (December 4, 2013 ed.): West Trenton, New Jersey, p. 175, accessed September 19, 2015, at http://www.nj.gov/drbc/library/documents/watercode.pdf.

Delaware River Basin Commission [DRBC], 2015, Modeling the Delaware River Basin with DRB-PST: Model documentation, available upon request from the Delaware River Basin Commission, Email contact@drbc.nj.gov).

Dingman, S.L., 2002, Physical hydrology (2d ed.): Upper Saddle River, N.J., Prentice Hall, 646 p.

Doherty, John, 2008, FORTRAN 90 modules for implementation of parallelised, model-independent, model-based processing: Watermark Numerical Computing, 236 p.

Dunne, J.P., John, J.G., Adcroft, A.J., Griffies, S.M., Hallberg, R.W., Shevliakova, Elena, Stouffer, R.J., Cooke, William, Dunne, K.A., Harrison, M.J., Krasting, J.P., Malyshev, S.L., Milly, P.C.D., Phillipps, P.J., Sentman, L.T., Samuels, B.L., Spelman, M.J., Winton, Michael, Wittenberg, A.T., and Zadeh, Niki, 2012, GFDL's ESM2 global coupled climate-carbon Earth System Models; Part I—Physical formulation and baseline simulation characteristics: Journal of Climate, v. 25, no. 19, p. 6646–6665.

Earth System Research Laboratory, 2015, Trends in atmospheric carbon dioxide: National Oceanic and Atmospheric Administration, Earth System Research Laboratory, Global Monitoring Division Web page, accessed March 25, 2015, at http://www.esrl.noaa.gov/gmd/ccgg/trends/global.html.

Famiglietti, J.S., 1992, Aggregation and scaling of spatially-variable hydrological processes—Local, catchment-scale and macroscale models of water and energy balance: Princeton, N.J., Princeton University, dissertation, 207 p.

Famiglietti, J.S., and Wood, E.F., 1991, Evapotranspiration and runoff from large land areas—Land surface hydrology for atmospheric general circulation models: Surveys in Geophysics, v. 12, nos. 1–3, p. 179–204.

Farmer, W.H., Archfield, S.A., Over, T.M., Hay, L.E., LaFontaine, J.H., and Kiang, J.E., 2015, A comparison of methods to predict historical daily streamflow time series in the southeastern United States: U.S. Geological Survey Scientific Investigations Report 2014–5231, 77 p, accessed September 16, 2015, at http://dx.doi.org/10.3133/sir20145231.

Forster, P.M., Andrews, Timothy, Good, Peter, Gregory, J.M., Jackson, L.S., and Zelinka, Mark, 2013, Evaluating adjusted forcing and model spread for historical and future scenarios in the CMIP5 generation of climate models: Journal of Geophysical Research: Atmospheres, v. 118, no. 3, p. 1139–1150.

Frumhoff, P.C., McCarthy, J.J., Melillo, J.M., Moser, S.C., and Wuebbles, D.J., 2007, Confronting climate change in the U.S. Northeast—Science, impacts, and solutions: Cambridge, Mass., Northeast Climate Impacts Assessment report, 146 p.

Fry, J.A., Xian, George, Jin, Suming, Dewitz, J.A., Homer, C.G., Yang, Limin, Barnes, C.A., Herold, N.D., and Wickham, J.D., 2011, Completion of the 2006 National Land Cover Database for the conterminous United States: Photogrammetric Engineering and Remote Sensing, v. 77, no. 9, p. 858–864.

Gent, P.R., Danabasoglu, Gokhan, Donner, L.J., Holland, M.M., Hunke, E.C., Jayne, S.R., Lawrence, D.M., Neale, R.B., Rasch, P.J., Vertenstein, Mariana, Worley, P.H., Yang, Z.-L., and Zhang, Minghua, 2011, The Community Climate System Model version 4: Journal of Climate, v. 24, no. 19, p. 4973–4991.

Gesch, Dean, Oimoen, Michael, Greenlee, Susan, Nelson, Charles, Steuck, Michael, and Tyler, Dean, 2002, The National Elevation Dataset: Photogrammetric Engineering and Remote Sensing, v. 68, no. 1, accessed September 15, 2009, at http://ned.usgs.gov/.

Hamon, W.R., 1963, Estimating potential evapotranspiration: Transactions of the American Society of Civil Engineers, v. 128, no. 1, p. 324–337.

Homeland Security Infrastructure Program, 2012, HSIP NAVTEQ State Release: U.S. Department of Homeland Security Infrastructure Program, accessed April 24, 2015 at www.hifldwg.org.

Hornberger, G.M., Beven, K.J., Cosby, B.J., and Sappington, D.E., 1985, Shenandoah Watershed Study—Calibration of a topography-based, variable contributing area hydrological model to a small forested catchment: Water Resources Research, v. 21, no. 12, p. 1841–1850.

Hutson, S.S., Linsey, K.S., Ludlow, R.A., Reyes, B., and Shourds, J.L., 2015, Estimated use of water in the Delaware River Basin in Delaware, New Jersey, New York, and Pennsylvania, 2010: U.S. Geological Survey Scientific Investigations Report 2015–5142, in press.

Hydrologics, 2002, Modeling the Delaware River Basin with OASIS, (Available upon request from the Delaware River Basin Commission, Email contact@drbc.nj.gov)

Ijjász-Vásquez, E.J., Bras, R.L., and Moglen, G.E., 1992, Sensitivity of a basin evolution model to the nature of runoff production and to initial conditions: Water Resources Research, v. 28, no. 10, p. 2733–2741.

Jin, Suming, Yang, Limin, Danielson, Patrick, Homer, Collin, Fry, Joyce, and Xian, George, 2013, A comprehensive change detection method for updating the National Land Cover Database to circa 2011: Remote Sensing of Environment, v. 132, p. 159–175, accessed April 11, 2013, at http://www.mrlc.gov/nlcd11_data.php.

Kennen, J.G., Kauffman, L.J., Ayers, M.A., Wolock, D.M., and Colarullo, S.J., 2008, Use of an integrated flow model to estimate ecologically relevant hydrologic characteristics at stream biomonitoring sites: Ecological Modelling, v. 211, nos. 1–2, p. 57–76.

Kirkby, Mike, 1986, A runoff simulation model based on hillslope topography, *in* Gupta, V.K., Rodríguez-Iturbe, Ignacio, and Wood, E.F., eds., Scale problems in hydrology—Runoff generation and basin response: Dordrecht, The Netherlands, D. Reidel Publishing Company, p. 39–56.

Mast, M.A., and Turk, J.T., 1999, Environmental characteristics and water quality of hydrologic benchmark stations in the eastern United States, 1963–95: U.S. Geological Survey Circular 1173–A, 158 p.

Metcalfe, Peter, Beven, K.J., and Freer, J.E., 2014, dynatopmodel—Implementation of the Dynamic TOPMODEL hydrological model (ver. 1.0): The Comprehensive R Archive Network Web page, accessed February 19, 2015, at https://cran.r-project.org/web/packages/dynatopmodel/index.html.

Milly, P.C.D., and Dunne, K.A., 2011, On the hydrologic adjustment of climate-model projections—The potential pitfall of potential evapotranspiration: Earth Interactions, v. 15, no. 1, p. 1–14.

Nash, J.E., and Sutcliffe, J.V., 1970, River flow forecasting through conceptual models; Part I—A discussion of principles: Journal of Hydrology, v. 10, no. 3, p. 282–290.

National Weather Service [NWS], 2012, National Operational Hydrologic Remote Sensing Center Interactive snow information: National Oceanic and Atmospheric Administration database, accessed January 25, 2013, at http://www.nohrsc.noaa.gov/interactive/html/.

Nazarenko, Larissa, Schmidt, G.A., Miller, R.L., Tausnev, N.L., Kelley, Maxwell, Ruedy, R.A., Russell, G.L., Aleinov, Igor, Bauer, M.P., Bauer, S.E., Bleck, Rainer, Canuto, V.M., Cheng, Yen-Ben, Clune, T.L., Del Genio, A.D., Faluvegi, G.S., Hansen, J.E., Healy, R.J., Kiang, N.Y., Koch, D.M., Lacis, A.A., LeGrande, A.N., Lerner, J., Lo, K.K., Menon, Surabi, Oinas, Valdar, Perlwitz, J.P., Puma, M.J., Rind, D.H., Romanou, Anastasia, Sato, Makiko, Shindell, D.T., Sun, Shan, Tsigaridis, Konstantinos, Unger, Nadine, Voulgarakis, Apostolos, Yao, M.S., and Zhang, Jinlun, 2015, Future climate change under RCP emission scenarios with GISS ModelE2: Journal of Advances in Modeling Earth Systems, v. 7, no. 1, p. 244–267.

New Jersey Department of Environmental Protection [NJDEP], 2007, New Jersey land use/land cover dataset: New Jersey Department of Environmental Protection dataset, accessed October 12, 2013, at http://www.nj.gov/dep/gis/lulc07shp.html.

Pellenq, Jennifer, Kalma, Jetse, Boulet, Gilles, Saulnier, G.-M., Wooldridge, Scott, Kerr, Yann, and Chehbouni, Abdelghani, 2003, A disaggregation scheme for soil moisture based on topography and soil depth: Journal of Hydrology, v. 276, no. 1–4, p. 112–127.

Priestley, C.H.B., and Taylor, R.J., 1972, On the assessment of surface heat flux and evaporation using large-scale parameters: Monthly Weather Review, v. 100, no. 2, p. 81–92.

Quinn, P.F., Beven, K.J., and Lamb, R., 1997, The ln(a/tanb) index-How to calculate it and how to use it within the TOPMODEL framework, *in* Beven, K.J., ed., Distributed hydrological modelling—Applications of the TOPMODEL concept: Chichester, England, Wiley, p. 31–52.

Robson, Alice, Beven, K.J., and Neal, Colin, 1992, Towards identifying sources of subsurface flow—A comparison of components identified by a physically based runoff model and those determined by chemical mixing techniques: Hydrological Processes, v. 6, no. 2, p. 199–214.

Romanowicz, Renata, 1997, A MATLAB implementation of TOPMODEL: Hydrological Processes, v. 11, no. 9, p. 1115–1129.

Senay, G.B., Bohms, Stefanie, Singh, R.K., Gowda, P.H., Velpuri, N.M., Alemu, Henok, and Verdin, J.P., 2013, Operational evapotranspiration mapping using remote sensing and weather datasets—A new parameterization for the SSEB approach: Journal of the American Water Resources Association, v. 49, no. 3, p. 577–591.

Sivapalan, Murugesu, Beven, K.J., and Wood, E.F., 1987, On hydrologic similarity—2. A scaled model of storm runoff production: Water Resources Research, v. 23, no. 12, p. 2266–2278.

Sivapalan, Murugesu, Wood, E.F., and Beven, K.J., 1990, On hydrologic similarity—3. A dimensionless flood frequency model using a generalized geomorphologic unit hydrograph and partial area runoff generation: Water Resources Research, v. 26, no. 1, p. 43–58.

Soil Survey Staff [NRCS], 1993, Soil survey manual (3d ed.): U.S. Department of Agriculture, Soil Conservation Service, Handbook 18, 437 p.

Soil Survey Staff [NRCS], 2012, Web soil survey: U.S. Department of Agriculture, Natural Resources Conservation Service database, accessed May 8, 2012, at http://websoilsurvey.nrcs.usda.gov/.

Soil Survey Staff [NRCS], 2014, Web soil survey—gSSURGO: U.S. Department of Agriculture, Natural Resources Conservation Service database, accessed August 13, 2014, at http://websoilsurvey.nrcs.usda.gov/.

Taylor, K.E., Stouffer, R.J., and Meehl, G.A., 2011, An overview of CMIP5 and the experiment design: Bulletin of the American Meteorological Society, v. 93, no. 4, p. 485–498.

Teng, Jin, Vaze, Jai, Chiew, F.H.S., Wang, Biao, and Perraud, J.-M., 2011, Estimating the relative uncertainties sourced from GCMs and hydrological models in modeling climate change impact on runoff: Journal of Hydrometeorology, v. 13, no. 1, p. 122–139.

Thompson, J.L., and Archfield, S.A., 2014, EflowStats [R package]: GitHub USGS–R repository, access October 22, 2014, at https://github.com/USGS-R/EflowStats.

Thornton, P.E., Thornton, M.M., Mayer, B.W., Wilhelmi, Nathan, Wei, Yaxing, and Cook, R.B., 2012, Daymet—Daily surface weather on a 1-km grid for North America, 1980–2012:Oak Ridge, Tenn., Oak Ridge National Laboratory Distributed Active Archive Center, accessed March 14, 2013, at http://dx.doi.org/10.3334/ORNLDAAC/1219.

U.S. Army Corps of Engineers [USACE], 1998, Engineering and design runoff from snowmelt: U.S. Army Corps of Engineers Engineer Manual 1110–2–1406.

U.S. Census Bureau, 2011, TIGER/Line shapefiles—Counties, census blocks: U.S. Census Bureau database, accessed September 21, 2013, at http://www.census.gov/geo/maps-data/data/tiger-line.html.

U.S. Census Bureau, 2012, 2010 Census summary file 1—Technical documentation: U.S. Census Bureau SF1/10–4(RV), chapters separately paged, accessed July 7, 2013, at http://factfinder.census.gov/faces/nav/jsf/pages/index.xhtml.

U.S. Census Bureau, 2013, Longitudinal employer-household dynamics—Origin-destination employment statistics: U.S. Census Bureau database, accessed August 11, 2013, at http://lehd.did.census.gov/data/.

U.S. Department of Agriculture [USDA], 1986, Urban hydrology for small watersheds: U.S. Department of Agriculture, Natural Resources Conservation Service Technical Release 55.

U.S. Environmental Protection Agency [EPA], 2009, Integrated Climate and Land Use Scenarios v.1.3.2 Population Forecasts (2005–2100): U.S. Environmental Protection Agency EPA/600/R–09/143F, 24 p., accessed September 21, 2013, at http://cfpub.epa.gov/ncea/global/recordisplay.cfm?deid=257306.

U.S. Geological Survey [USGS] Gap Analysis Program [GAP], 2012, Protected Areas Database of the United States (PADUS) version 1.3: U.S. Geological Survey PAD–US metadata, accessed March 3, 2014, at http://gapanalysis.usgs.gov/padus/data/metadata/.

U.S. Geological Survey [USGS], U.S. Department of Agriculture, and Natural Resources Conservation Service, 2009, Federal guidelines, requirements, and procedures for the national Watershed Boundary Dataset: U.S. Geological Survey Techniques and Methods, book 11, chap. A3, 55 p, shapefile accessed April 4, 2009, at https://gdg.sc.egov.usda.gov/.

U.S. Supreme Court, 1954, State of New Jersey, Complainant, v. State of New York and City of New York, Defendants, Commonwealth of Pennsylvania and State of Delaware, in States, S.C.o.t.U., No. 5, Original—October Term, 1950, accessed September 19, 2015, at http://www.nj.gov/drbc/library/documents/watercode.pdf.

U.S. Supreme Court, 1982, Interstate water management recommendations of the Parties to the U.S. Supreme Court Decree of 1954 to the Delaware River Basin Commission pursuant to Commission Resolution 78-20, in U. S. Supreme Court, p. 41, accessed September 19, 2015, at http://www.nj.gov/drbc/library/documents/regs/GoodFaithRec.pdf.

van Vuuren, D.P., Edmonds, J.A., Kainuma, Mikiko, Riahi, Keywan, and Weyant, John, 2011, A special issue on the RCPs: Climatic Change, v. 109, nos. 1–2, p. 1–4.

Vitvar, Tomas, Burns, D.A., Lawrence, G.B., McDonnell, J.J., and Wolock, D.M., 2002, Estimation of baseflow residence times in watersheds from the runoff hydrograph recession—Method and application in the Neversink watershed, Catskill Mountains, New York: Hydrological Processes, v. 16, no. 9, p. 1871–1877.

von Salzen, Knut, Scinocca, J.F., McFarlane, N.A., Li, Jiangnan, Cole, J.N.S., Plummer, David, Verseghy, Diana, Reader, M.C., Ma, Xiaoyan, Lazare, Michael, and Solheim, Larry, 2013, The Canadian fourth generation atmospheric global climate model (CanAM4); Part I—Representation of physical processes: Atmosphere—Ocean, v. 51, no. 1, p. 104–125.

Williamson, T.N., Lee, B.D., Schoeneberger, P.J., McCauley, W.M., Indorante, S.J., and Owens, P.R., 2014, Simulating soil-water movement through loess-veneered landscapes using nonconsilient saturated hydraulic conductivity measurements: Soil Science Society of America Journal, v. 78, no. 4, p. 1320–1331.

Williamson, T.N., Odom, K.R., Newson, J.K., Downs, A.C., Nelson Jr., H.L., Cinotto, P.J., and Ayers, M.A., 2009, The Water Availability Tool for Environmental Resources (WATER)—A water-budget modeling approach for managing water-supply resources in Kentucky—Phase I—Data processing, model development, and application to non-karst areas: U.S. Geological Survey Scientific Investigations Report 2009–5248, 34 p.

Williamson, T.N., Taylor, C.J., and Newson, J.K., 2013, Significance of exchanging SSURGO and STATSGO data when modeling hydrology in diverse physiographic terranes: Soil Science Society of America Journal, v. 77, no. 3, p. 877–889.

Wolock, D.M., 1988, Topographic and soil hydraulic control of flow paths and soil contact time—Effects on surface water acidification: Charlottesville, Va., University of Virginia, dissertation, 188 p.

Wolock, D.M., 1993, Simulating the variable-source-area concept of streamflow generation with the watershed model TOPMODEL: U.S. Geological Survey Water-Resources Investigations Report 93–4124, 33 p.

Wolock, D.M., 2003, Infiltration-excess overland flow estimated by TOPMODEL for the conterminous United States: U.S. Geological Survey Open-File Report 03–310, digital dataset, accessed November 12, 2012, at http://water.usgs.gov/lookup/getspatial?ieof48.

Wolock, D.M., and Hornberger, G.M., 1991, Hydrological effects of changes in levels of atmospheric carbon dioxide: Journal of Forecasting, v. 10, nos. 1–2, p. 105–116.

Wolock, D.M., Hornberger, G.M., and Musgrove, T.J., 1990, Topographic effects on flow path and surface water chemistry of the Llyn Brianne catchments in Wales: Journal of Hydrology, v. 115, nos. 1–4, p. 243–259.

Wolock, D.M., and McCabe, G.J., 1999, Explaining spatial variability in mean annual runoff in the conterminous United States: Climate Research, v. 11, no. 2, p. 149–159.

Wolock, D.M., and McCabe, G.J., 1995, Comparison of single and multiple flow direction algorithms for computing topographic parameters in TOPMODEL: Water Resources Research, v. 31, no. 5, p. 1315–1324.

Wood, E.F., Sivapalan, Murugesu, and Beven, K.J., 1990, Similarity and scale in catchment storm response: Reviews of Geophysics, v. 28, no. 1, p. 1–18.

Wood, E.F., Sivapalan, Murugesu, Beven, K.J., and Band, L.E., 1988, Effects of spatial variability and scale with implications to hydrologic modeling: Journal of Hydrology, v. 102, nos. 1–4, p. 29–47.

ISSN 2328-0328 (online)
http://dx.doi.org/10.3133/sir20155143